Accepted Manuscript

2,3-Diarylpropenoic acids as selective non-steroidal inhibitors of type-5 17β-hydroxysteroid dehydrogenase (AKR1C3)

Martin Gazvoda, Nataša Beranič, Samo Turk, Bojan Burja, Marijan Kočevar, Tea Lanišnik Rižner, Stanislav Gobec, Slovenko Polanc

PII: S0223-5234(12)00767-2

DOI: 10.1016/j.ejmech.2012.12.045

Reference: EJMECH 5916

To appear in: *European Journal of Medicinal Chemistry*

Received Date: 14 September 2012

Revised Date: 24 December 2012

Accepted Date: 26 December 2012

Please cite this article as: M. Gazvoda, N. Beranič, S. Turk, B. Burja, M. Kočevar, T.L. Rižner, S. Gobec, S. Polanc, 2,3-Diarylpropenoic acids as selective non-steroidal inhibitors of type-5 17β-hydroxysteroid dehydrogenase (AKR1C3), *European Journal of Medicinal Chemistry* (2013), doi: 10.1016/j.ejmech.2012.12.045.

GRAPHICAL ABSTRACT

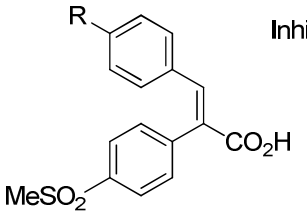

Inhibition of AKR1C3 (IC_{50}):

R = Me	13.4 μM
R = Et	13.6 μM
R = Br	4.9 μM
R = MeS	5.8 μM

Methyl and ethyl substituted acids are the most selective inhibitors of AKR1C3.

2,3-Diarylpropenoic acids as selective non-steroidal inhibitors of type-5 17β-hydroxysteroid dehydrogenase (AKR1C3)

Martin Gazvoda[a,&], Nataša Beranič[b,&], Samo Turk[c], Bojan Burja[a], Marijan Kočevar[a], Tea Lanišnik Rižner,[b] Stanislav Gobec**[,c], Slovenko Polanc*[,a]

[a]*Faculty of Chemistry and Chemical Technology, University of Ljubljana, Aškerčeva 5, SI-1000, Ljubljana, Slovenia*

[b]*Institute of Biochemistry, Faculty of Medicine, University of Ljubljana, Vrazov trg 2, SI-1000, Ljubljana, Slovenia*

[c]*Faculty of Pharmacy, University of Ljubljana, Aškerčeva 7, SI-1000, Ljubljana, Slovenia*

G R A P H I C A L A B S T R A C T

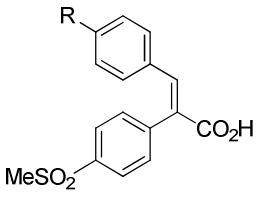

Abbreviations: DMF, *N*,*N*-dimethylformamide; DMSO, dimethyl sulfoxide; ESI, electrospray ionization; HPLC, high-performance liquid chromatography; HRMS, high-resolution mass spectrometry; IR, infrared; LC-MS liquid chromatography-mass spectrometry; NADPH, reduced nicotinamide adenine dinucleotide phosphate; NMR, nuclear magnetic resonance; NSAID, non-steroidal anti-inflammatory drug.

[&] Both authors contributed equally to the manuscript.

* Corresponding author. Tel.: +386-1-24-19-236; fax: +386-1-24-19-220.

** Corresponding author. Tel.: +386-1-47-69-585; fax: +386-1-42-58-031.

E-mail addresses: slovenko.polanc@fkkt.uni-lj.si (S. Polanc), stanislav.gobec@ffa.uni-lj.si (S. Gobec).

A B S T R A C T

The aldo-keto reductase AKR1C3 is an important target for the development of new drugs. Selective inhibitors of this enzyme are needed because they should not inhibit other, structurally closely related AKR1C isoforms. A comprehensive series of 2,3-diarylpropenoic acids was synthesized and evaluated for the inhibition of AKR1C1–AKR1C3. We found that the 4-methylsulfonylphenyl substituent at position 2 of these acids is required to exhibit the selective inhibition of AKR1C3. The best results were obtained for the compounds that fulfill the above requirement and possess a 4-bromophenyl, 4-methylthiophenyl, 4-methylphenyl or 4-ethylphenyl substituent at position 3 of the substituted propenoic acids (i.e., acids **28**, **29**, **37**, and **39**, respectively). These compounds represent an important step towards the development of drug candidates for a treatment of the hormone-dependent and hormone-independent forms of prostate and breast cancers.

Keywords: Aldo-keto reductase; AKR1C3; Selective inhibitors; 2,3-Diarylpropenoic acids; Cancer

1. Introduction

The enzymes AKR1C1–AKR1C4, members of the aldo-keto reductase superfamily, catalyze the interconversions of 3-, 17- and 20-ketosteroids with the corresponding 3α/β-, 17β-, 20α-hydroxysteroids to varying extents, using NADPH as a cofactor [1,2]. In this way they can control the ligand occupancy and *trans*-activation of androgen, estrogen and progesterone receptors by modulating the concentrations of the active steroids [3]. The AKR1C enzymes are also involved in the prostaglandin and neurosteroid production and inactivation, and in the metabolism of xenobiotics [2].

Among the AKR1C enzymes, AKR1C3 preferentially acts as a 17-ketosteroid reductase and converts a weak androgen 4-androstene-3,17-dione to a potent androgen testosterone and estrone to a potent estrogen 17β-estradiol. As a 20-ketosteroid reductase, AKR1C3 inactivates progesterone by forming its metabolite 20α-hydroxyprogesterone, which has a lower affinity towards the progesterone receptor [1,4]. AKR1C3 also acts as a 3-ketosteroid reductase by converting 5α-dihydrotestosterone into an estrogen receptor β ligand 3β-androstandiol, and inactive androgen 3α-androstandiol [1]. Catalyzing these reactions AKR1C3 represents an important target enzyme for the development of potential drugs for a treatment of the hormone-dependent forms of cancer. Finally, AKR1C3 catalyzes the reduction of prostaglandin H2 (PGH2) into PGF2α, and PGD2 into 11β-PGF2, thereby diverting the

biosynthesis of prostanoids away from the antiproliferative J-series [2]. This makes AKR1C3 an interesting target enzyme also for the development of the hormone-independent forms of cancer.

The products of AKR1C3-catalyzed reactions stimulate tumor growth, so an imbalance in the AKR1C3 expression and action can be related to the different hormone-dependent and hormone-independent cancers like breast [5], prostate [6], endometrial [7], and also other diseases, such as endometriosis [8], benign prostatic hyperplasia and dysmenorrhea [9,10]. AKR1C3 thus represents an interesting therapeutic target for the development of new drugs. Since AKR1C3 shares at least an 84% sequence homology and overlapping catalytic properties with other human members of the AKR1C superfamily (AKR1C1, AKR1C2 and AKR1C4) that are, with the exception of the liver-specific AKR1C4, expressed in different tissues [1], selective AKR1C3 inhibition is crucial and remains a great challenge. To date several structurally different classes of compounds have been reported to possess AKR1C3-inhibitory activity. The structural analogues of AKR1C3 substrates with a steroidal backbone, such as progestins [11] and estrogen lactones [12], have been shown to inhibit AKR1C3 in the low-μM or even the low-nM range, respectively. Inhibitors of AKR1C3 also comprise other classes of compounds, like cyclopentane derivatives [13], benzodiazepines [14], flavonoids [15], cinnamic acid derivatives [16] jasmonates [17] or NSAIDs [18]. All these compounds inhibit AKR1C3 with μM IC_{50} values, but most of these inhibitors have low selectivity over AKR1C3. To date only a few compounds that act as selective AKR1C3 inhibitors have been reported (e.g., an indole derivative known as CBM, and an indomethacin analogue that belongs to the group of NSAIDs). Unfortunately, CBM possesses poor bioavailability relative to its potency [10], so the search for a selective AKR1C3 inhibitor continues.

From the above facts it is evident that the desired inhibitor of AKR1C3 should not inhibit the closely related isoforms AKR1C1 and AKR1C2, which play distinct roles in the metabolism of steroidal hormones. Recently described *N*-phenylaminobenzoates were found to fulfill this requirement and can serve as potent and selective inhibitors of AKR1C3 [19]. On the other hand, the already-mentioned cinnamic acid and derivatives are also promising inhibitors of AKR1C3 [16].

Here we report on the effectiveness and the selectivity of inhibition of AKR1C3 by the related 2,3-diarylpropenoic acids (α-arylcinnamic acids, Table 1). Although a half of the examined compounds have been previously described in the literature, their inhibition of AKR1C3 and other isoforms has not been studied so far. These acids have been used in our study, together

with a set of new compounds, to get the information concerning an effect of the substituents, attached to the aromatic rings, on AKR1C3 selectivity and inhibitory activity.

[Table 1]

2. Results and discussion

2.1. Design of new AKR1C3 inhibitors based on a cinnamic acid scaffold

In 2006, some of us discovered that cinnamic acid and several of its simple, substituted derivatives inhibited AKR1C3 with micromolar IC_{50} values [16a]. Among them, α-methylcinnamic acid was the most promising inhibitor. This prompted us to design the synthesis of a series of cinnamic acids with bulky aryl substituents on the position α (α-arylcinnamic acids) and to evaluate their AKR1C1–AKR1C3 inhibitory activities (Figure 1).

[Fig. 1]

2.2. Chemistry

Several acids were synthesized as described before (**1** [20], **2** [21], **3** [21], **5** [21], **6** [21], **7** [21], **8** [21], **9** [21], **10** [21], **11** [21], **12** [21], **16** [22] and **26** [22]). Most of them were recently applied by us as a precursor to pyrazolo-fused combretastatins [21]. Some acids have also been mentioned in the literature (**13** [23], **15** [24], **19** [25], **20** [24], **30** [26], **31** [25], **36** [27], and **40** [28]), but the synthesis and characterization details were not available. For this reason they were prepared following our general synthesis and all the missing data are provided (see Supporting information). The latter acids as well as the new ones were available with the Perkin reaction between substituted benzaldehydes and properly functionalized arylacetic acids in acetic anhydride using either potassium acetate or triethylamine as a base that led to the desired 2,3-diarylpropenoic acids as the final products (Scheme 1). Reaction conditions were optimized in all cases. The experiments indicated that the yield of the isolated product depend mainly on the nature of an aromatic aldehyde employed in a particular reaction. Namely, benzaldehydes bearing electron withdrawing groups (e.g., halogen, trifluoromethyl, methylsulfonyl) led to 2,3-diarylpropenoic acids **17**, **18**, **22**, **25**, **27**, **35**−**38** in higher yields (63−89%) than those possessing electron donating substituents (e.g., alkyl, methoxy, hydroxy, methylthio) that gave the acids **28**−**34** and **39** in 21−76% yield. Similar results were reported for the synthesis of various cinnamic acids from substituted benzaldehydes and acetic anhydride [29].

[Scheme 1]

The synthesis of acetoxy-substituted acid **4** required an acetylation of the initially formed (2*E*)-3-(3-hydroxyphenyl)-2-(3,4,5-trimethoxyphenyl)prop-2-enoic acid applying acetic anhydride in the presence of catalytic amounts of 4-dimethylaminopyridine in DMF as a solvent. The methylsulfonyl- substituted acids **21**, **24**, and **40** were prepared from their methylthio analogues **20**, **23** and **39** using the appropriate reaction conditions to keep an olefinic C=C bond intact. The best results for such selective oxidation of the sulfur atom were obtained employing hydrogen peroxide in acetic acid (Scheme 2). Furthermore, the acid **42** resulted from the Suzuki coupling of **37** with 4-(methylthio)phenylboronic acid (Scheme 3).

[Scheme 2]

[Scheme 3]

2.3. Biological Activity

The compounds shown in Table 1 were assayed for the inhibition of the enzymes AKR1C1–AKR1C3. These enzymes catalyze the oxidation of an artificial substrate 1-acenaphthenol with NAD^+ as a coenzyme, in the presence and absence of individual compounds. The enzymatic activity was followed spectrophotometrically (Table 2). The results are given as a percentage of the inhibition of the enzyme in the presence of 100 µM of each acid. For the compounds that showed more than 50% inhibition the IC_{50} values were determined. Medroxyprogesterone acetate, previously described inhibitor of AKR1C enzymes [14], was assayed on our test as a reference and a positive control. The IC_{50} values were 1.8 µM (AKR1C1), 4.1 µM (AKR1C2), and 0.3 µM (AKR1C3), respectively.

[Table 2]

A non-substituted 2,3-diphenylpropenoic acid (**1**) inhibits AKR1C1. Several acids with two or more methoxy groups in the molecule are either not active (**2**–**5**, **7**–**12**) or slightly active against AKR1C2 or AKR1C3 (**6**, **13**, **14**). We noticed that the introduction of the sulfur-containing substituent increased the inhibitory activity. Thus, out of the four acids **15**–**18**, three of them inhibit at least two enzymes. The acid **19** having the $MeSO_2$ substituent on the

fragment Ar^1 (i.e., at the position adjacent to the carboxylic functionality) revealed the selective inhibition of AKR1C3. In addition, **20** and **21** inhibit all three enzymes, but the acid **22** is a selective inhibitor of AKR1C3. These results indicate the influence of the sulfur-containing group. Comparing the activity of the acids **21** and **22** it is evident that the acid **22** containing the 4-$MeSO_2$ group is a selective inhibitor of AKR1C3 but **21,** possessing the 4-chloro substituent, is not. So, they differ only in the presence of the chlorine or the $MeSO_2$ functionalities. Similar results were obtained in the case of the acids **23**–**27**. Namely, the molecules with a sulfur substituent as a part of the Ar^2 moiety are not selective inhibitors (**23**, **24** and **26**), while the acids possessing the $MeSO_2$ group at the *para* position of the Ar^1 inhibit AKR1C3 selectively (**25** and **27**). Having the above results in hand we focused exclusively on the activity of the 2-(4-methylsulfonyl)phenylpropenoic acids **28**–**39** that differ only in the Ar^2 moiety. Most of them are indeed selective inhibitors of AKR1C3, with the exception of the non-active **31**, **32**, and **34,** as well as **36** that is not a selective inhibitor. The most efficient and selective inhibitors are the 4-bromo-substituted acid **37** and 4-methylthio analogue **39**. The structure of the latter compound was further modified. The introduction of the methylsulfonyl functionality in the place of the methylthio group leads to a considerable drop of activity (an acid **40**), although the selectivity is retained. On the other hand, **41**, bearing the acetylaminosulfonyl moiety at the *para* position of the Ar^2, is not active at all. The same is true if the *para*-phenylen linker is introduced to connect the methylthio group and the benzene ring of Ar^2 (an acid **42**). It is also interesting to note that acids **28** and **29**, although they exhibit a lower activity against AKR1C3 compared to the above-mentioned **37** and **39**, are the most selective inhibitors of this enzyme. Namely, they practically do not inhibit AKR1C1 and AKR1C2 at a 100 μM concentration.

Several important conclusions can be drawn from these results. Firstly, the 4-$MeSO_2$ group on Ar^1 seems to be crucial for AKR1C3 selectivity as shown by the activities of the compounds **19**, **22**, **25**, **27**–**30**, **33** and **35**–**40** with only compound **36** possessing also a weak AKR1C2 activity. This is consistent with the docking study (see below) predicting that $MeSO_2$ functionality forms interactions with the SP1 sub-pocket, and with previous studies which reported that the binding to the SP1 sub-pocket was responsible for the isoform selectivity [10]. Secondly, a group on Ar^2 seems to regulate the activity. The nature of the substituents and their positions are of course important. Here, the bulky hydrophobic substituents seem to be the most appropriate. This can be concluded from a series of halogenated analogs. Namely, the activity is increased with the size of the substituent and is also dependent on a position of the substituent on the aromatic ring. Thus, the fluorine bearing acids **27** and **35** have

inhibitory activities of 43.1 and 38.9 μM, respectively. Furthermore, the chlorophenyl acids **22** and **25** possess the activities of 10.8 and 16.8 μM, respectively, and finally with the bromo analogs **36** and **37**, which are the most active and have activities of 13.6 and 4.9 μM, respectively. An enzyme inhibitory potency is therefore increased with the bulk of the substituent and is generally higher in the case of the *para* substituted analogues. A positive influence of the *para* substituent is particularly pronounced with its size. Thus, both fluorinated analogs possess almost the same activities, the *para* substituted chloro analog has 50% better activity as the *meta* one, while the *para* substituted bromo acid has almost 3-fold better activity than the *meta* compound. In addition, the need for a lipophilic substituent is indicated by a good activity of the acids **28**, **29**, **38** and **39** containing 4-Me, 4-Et, 4-CF_3 or 4-MeS functionality attached to the Ar^2 ring. On the other hand, and the lack of activity obtained for the compounds **31**, **32**, and **34**, or weak activity in the case of **40**, seems to be attributed to the more hydrophilic substituents on the Ar^2 ring (4-OH, 3-OH, 3,4,5-OMe and $MeSO_2$).

2.4. Molecular docking

To gain an additional insight into the binding mode and selectivity of the 2,3-diarylpropenoic acids, the compounds with the best AKR1C1 (compound **1**) or AKR1C3 (compounds **20**, **22**, **28**, **29**, **36**, **37**, **39**) inhibitory activities were docked to the crystal structures of both isoforms. For the docking, the AKR1C1 crystal structure with co-crystallized 3,5-dichlorosalicylic acid (PDB code 3C3U) [30] and the AKR1C3 crystal structure with co-crystallized indomethacin (PDB code 1S2A) [31] were used.

The docking results are in good correlation with the results of the inhibition assays. In the case of the AKR1C1 docking, compound **1** has the highest score, closely followed by compound **20**. In both cases the Ar^1 is aligned with the co-crystallized 3,5-dichlorosalicylic acid, with Ar^2 extending into the steroid-binding channel. The Ar^1 containing a bulky $MeSO_2$ substituent are unfavorable since they prevent the binding of Ar^1 in the same way as the 3,5-dichlorosalicylic acid, explaining the lack of AKR1C1 activity in those compounds (see Supporting information).

In the case of AKR1C3, the docked poses of the compounds **22**, **28**, **29**, **36**, **37** and **39** occupy a similar position of the active site as the co-crystallized indomethacin, with the Ar^1 overlapping with the *p*-chlorobenzoyl moiety of the indomethacin and the Ar^2 overlapping with an indole part of the indomethacin. A typical docking pose is presented in Figure 2 (docking pose for the compound **37**). Due to the nature of AKR1C3, which has a large

number of aromatic residues in a steroid-binding channel, the dominating interactions are predicted to be pi interactions. Ar^1 forms pi interactions with the Phe306 of the SP1 sub-pocket and the Trp227 of the SP2 sub-pocket, while the Ar^2 forms pi interactions with the Phe306 of the SP1. Additional pi interactions are also possible between the propenoic acid double bond and Tyr24, a part of the SP3 sub-pocket. The $MeSO_2$ group on the *para* position of the Ar^1 seems to be crucial for selectivity and forms important H-bonds with the amino acid residues Ser118 and Asn167 of the SP1 sub-pocket. The differences in the SP1 sub-pockets between the AKR1C isoforms have previously been noted and suggested to be exploited in the design of AKR1C3 selective inhibitors [10].

[Fig. 2]

3. Conclusions

The aldo-keto reductases AKR1C1–AKR1C3 play an important role in the production and inactivation of neurosteroids and prostaglandins as well as in the metabolism of xenobiotics and lipid aldehydes. They can regulate the occupancy and *trans*-activation of the androgen, estrogen and progesterone receptors. These facts make them important drug targets for the treatment of the hormone-dependent and hormone-independent forms of cancer and other diseases. Several 2,3-diarylpropenoic acids were synthesized by the Perkin reaction between the substituted benzaldehydes and the properly functionalized arylacetic acids. They were evaluated as inhibitors of AKR1C1–AKR1C3. A modification of the structure revealed that the 4-methylsulfonylphenyl substituent at the position 2 of the 2,3-diarylpropenoic acid is an appropriate one to obtain a selective inhibition of AKR1C3. We found that the compounds **37** and **39** are the best inhibitors of AKR1C3 and also show very good selectivity. On the other hand, their 4-methylphenyl and 4-ethylphenyl analogues (**28** and **29**, respectively), which exhibit a slightly lower activity against AKR1C3, are the most selective ones. Namely, they practically do not inhibit AKR1C1 and AKR1C2 at a 100 μM concentration. Our data suggest that 2,3-diarylpropenoic acids represent a new class of selective inhibitors of AKR1C3 and may serve as a good starting point for the development of new antitumor agents for the treatment of the hormone-dependent and hormone-independent forms of prostate and breast cancers.

4. Experimental protocols

4.1. Chemistry

Starting materials for the synthesis of the examined compounds were used as obtained from the commercial source (Aldrich). Melting points were determined on a Kofler micro hot stage and are uncorrected. NMR spectra were recorded at 29 °C with a Bruker Avance DPX 300 spectrometer (^{1}H NMR spectra at 300 MHz; ^{13}C NMR spectra at 75.5 MHz) and with a Bruker Avance III spectrometer (^{1}H NMR spectra at 500 MHz; ^{13}C NMR spectra at 125.8 MHz). Proton spectra are referenced to TMS as an internal standard; the carbon shifts are given against the central line of the solvent signal (DMSO-d_6 at δ = 39.5 ppm; $CDCl_3$ at δ = 77.1 ppm). IR spectra were obtained with a Bio-Rad FTS 3000MX (KBr pellets) and a Perkin–Elmer Spectrum 100, equipped with a Specac Golden Gate Diamond ATR as a solid sample support. MS spectra were recorded with a VG-Analytical AutoSpec Q instrument and an Agilent 62224 Accurate Mass TOF LC/MS spectrometer. Elemental analyses (C, H, N) were performed with Perkin Elmer 2400 Series II CHNS/O Analyzer. TLC was carried out on Fluka silica-gel TLC-cards.

A purity of all tested compounds was checked by HPLC (see Supporting information), ^{1}H NMR and ^{13}C NMR spectroscopy as well as with elemental microanalysis. The figures obtained for the C, H, N analyses were always within ±0.35% of the calculated values.

4.1.1. General procedure for the synthesis of acids

Potassium acetate (982 mg, 10 mmol) or triethylamine (1.5 mL, 10.75 mmol; for the synthesis of **13**, **14**, **15**, **18**, **20**, **22**, **23**, and **25**) was added to a stirred mixture of the appropriate arylacetic acid (7.5 mmol), aromatic aldehyde (7.5 mmol) and acetic anhydride (3 mL, 32 mmol). The reaction mixture was stirred at 100–140 °C for 3.5–70 h. Then it was cooled to rt, water was added (40 mL) and the mixture was treated with a solution of 10 M NaOH until pH 12 was reached, followed by conc. HCl (to pH 1). The resulting mixture was extracted with CH_2Cl_2 (3 x 80 mL). Organic phases were extracted with 2 M NaOH (3 x 80 mL) and water (80 mL). The combined aqueous solutions were washed with CH_2Cl_2 (100 mL) to remove the impurities and traces of starting materials, then acidified with conc. HCl (until pH was 1), and finally extracted with CH_2Cl_2 (4 x 50 mL). The methylene chloride phase was washed with brine (100 mL), dried over anhydrous sodium sulfate, evaporated to dryness and the residue was crystallized from a suitable solvent.

4.1.1.1 (2*E*)-3-(3,4-Dimetoxyphenyl)-2-(naphthalen-2-yl)prop-2-enoic acid (14). Reaction time: 48 h; temperature: 100 °C; yield 22%; mp 220–222 °C (EtOAc); IR (KBr) 2955, 1677, 1595, 1512, 1421, 1259, 1143, 1026 cm^{-1}; ^{1}H NMR (DMSO-d_6) δ 3.07 (3H, s), 3.66 (3H, s), 6.50 (1H, d, J = 1.5 Hz), 6.73−6.81 (2H, m), 7.36 (1H, dd, J_1 = 1.5 Hz, J_2 = 8.4 Hz),

7.47−7.55 (2H, m), 7.78−7.80 (1H, m), 7.82−7.99 (4H, m), 12.62 (1H, broad s); ^{13}C NMR (DMSO-d_6) δ 54.3, 55.4, 111.3, 112.9, 124.7, 126.2, 126.9, 127.5, 127.7, 128.00, 128.04, 128.2, 130.6, 132.2, 133.2, 134.5, 139.5, 147.9, 149.8, 168.6; MS (ESI–) *m/z* 333 ([M - H]$^-$, 22); HRMS for $C_{21}H_{17}O_4$ ([M - H]$^-$): calcd 333.1127; found 333.1130. Anal. for $C_{21}H_{18}O_4$: calcd C, 75.43; H, 5.43; found C, 75.31; H, 5.33.

4.1.1.2 (2*E*)-2-[1,3-Benzodixol-5-yl]-3-[4-(methylsulfonyl)phenyl]prop-2-enoic acid (17). Reaction time: 19 h; temperature: 100 °C; yield 89%; mp 231–232 °C (EtOAc); IR 3021, 2925, 1677, 1618, 1592, 1493, 1441, 1308, 1239, 1146 cm^{-1}; ^{1}H NMR (DMSO-d_6) δ 3.19 (3H, s), 6.05 (2H, s), 6.58 (1H, dd, J_1 = 7.9 Hz, J_2 = 1.6 Hz), 6.77 (1H, d, J = 1.6 Hz), 6.89 (1H, d, J = 7.9 Hz), 7.35 (2H, d, J = 8.4 Hz), 7.74 (1H, s), 7.77 (2H, d, J = 8.4 Hz), 12.94 (1H, broad s); ^{13}C NMR (DMSO-d_6) δ 43.1, 101.1, 108.5, 109.9, 123.0, 126.8, 128.9, 130.6, 135.9, 136.8, 139.8, 140.3, 146.9, 147.4, 168.0; MS (ESI+) *m/z* 347 ([M + H]$^+$); HRMS for $C_{17}H_{15}O_6S$ ([M + H]$^+$): calcd 347.0584; found 347.0576. Anal. for $C_{17}H_{14}O_6S$: calcd C, 58.95; H, 4.07; found C, 58.66; H, 3.96.

4.1.1.3 (2*E*)-3-[4-(Acetylsulfamoyl)phenyl]-2-phenylprop-2-enoic acid (18). Reaction time: 3.5 h; temperature: 100 °C; yield 63%; mp 238–241 °C (H_2O); IR 3259, 2988, 2901, 1731, 1722, 1659, 1594, 1423, 1348, 1273 cm^{-1}; ^{1}H NMR (DMSO-d_6) δ 1.90 (3H, s), 7.16−7.20 (2H, m), 7.25 (2H, d, J = 8.4 Hz), 7.36−7.42 (3H, m), 7.69 (2H, d, J = 8.4 Hz), 7.81 (1H, s), 12.07 (1H, broad s), 13.1 (1H, broad s); ^{13}C NMR (DMSO-d_6) δ 23.3, 127.3, 128.0, 128.6, 129.4, 130.4, 135.5, 136.4, 137.0, 138.9, 139.7, 168.0, 168.9; MS (ESI–) *m/z* 346 ([M + H]$^+$, 100 %); Anal. for $C_{17}H_{15}NO_5S$: C, 59.12; H, 4.38; N, 4.06; found C, 59.36; H, 4.35; N, 3.97.

4.1.1.4 (2*E*)-3-(4-Chlorophenyl)-2-[4-(methylsulfonyl)phenyl]prop-2-enoic acid (22). Reaction time: 70 h; temperature: 140 °C; yield 63%; mp 263–264 °C (EtOAc); IR 2970, 2879, 1667, 1610, 1592, 1564, 1492, 1414, 1393, 1311 cm^{-1}; ^{1}H NMR (DMSO-d_6) δ 3.27 (3H, s), 7.07 (2H, d, J = 8.8 Hz), 7.32 (2H, d, J = 8.8 Hz), 7.46 (2H, d, J = 8.5 Hz), 7.86 (1H, s), 7.93 (2H, d, J = 8.5 Hz), 13.05 (1H, broad s); ^{13}C NMR (DMSO-d_6) δ 43.5, 127.2, 128.6, 130.7, 131.8, 132.6, 132.9, 133.9, 138.9, 140.0, 141.4, 167.5; MS (ESI+) *m/z* 354 ([M + NH_4]$^+$); HRMS for $C_{16}H_{14}ClO_4S$ ([M + H]$^+$): calcd 337.0296; found 337.0288. Anal. for $C_{16}H_{13}ClO_4S$: calcd C, 57.06; H, 3.89; found C, 56.96; H, 3.74.

4.1.1.5 (2*E*)-2-(3-Chlorophenyl)-3-[4-(methylsulfanyl)phenyl]prop-2-enoic acid (23). Reaction time: 6 h; temperature: 100 °C; yield 49%; mp 213–215 °C (EtOAc/*n*-heptane); IR (KBr) 3418, 1668, 1609, 1589, 1426, 1287, 1272, 1191 cm^{-1}; ^{1}H NMR (DMSO-d_6) δ 2.42 (3H, s), 7.00 and 7.09 (4H, AA′BB′, J = 8.7 Hz), 7.11−7.18 (1H, m), 7.27 (1H, broad s), 7.38−7.46 (2H, m), 7.77 (1H, s), 12.77 (1H, broad s); ^{13}C NMR (DMSO-d_6) δ 14.0, 125.1,

127.6, 128.3, 129.3, 130.2, 130.4, 130.6, 130.8, 133.1, 138.7, 139.3, 140.6, 167.8; MS (ESI–) m/z 303.0 ([M – H]$^-$); HRMS for $C_{16}H_{12}ClO_2S$ ([M – H]$^-$): calcd 303.0247; found 303.0253. Anal. for $C_{16}H_{13}ClO_2S$: calcd C, 63.05; H, 4.30; found C, 53.23; H, 4.23.

4.1.1.6 (2*E*)-3-(3-Chlorophenyl)-2-[4-(methylsulfonyl)phenyl]prop-2-enoic acid (25). Reaction time: 41 h; temperature: 100 °C; yield 68%; mp 210–212 °C (EtOAc); IR 2979, 2942, 1674, 1618, 1560, 1478, 1424, 1288, 1211, 1144 cm^{-1}; ^{1}H NMR (DMSO-d_6) δ 3.25 (3H, s), 6.98 (1H, d, J = 8.0 Hz), 7.08−7.10 (1H, m), 7.25 (1H, t, J = 7.8 Hz), 7.33 (1H, dd, J_1 = 8.0 Hz, J_2 = 1.5 Hz), 7.47 (2H, d, J = 8.3 Hz), 7.85 (1H, s), 7.94 (2H, d, J = 8.3 Hz), 13.11 (1H, broad s); ^{13}C NMR (DMSO-d_6) δ 43.5, 127.2, 128.6, 129.0, 129.7, 130.2, 130.7, 133.1, 133.5, 136.2, 138.6, 140.1, 141.4, 167.3; MS (ESI+) *m*/*z* 354 ([M + NH]$^+$); HRMS for $C_{16}H_{14}ClO_4S$ ([M + H]$^+$): calcd 337.0296; found 337.0285. Anal. for $C_{16}H_{13}ClO_4S$: calcd C, 57.06; H, 3.89; found C, 57.21; H, 3.96.

4.1.1.7 (2*E*)-3-(4-Fluorophenyl)-2-[4-(methylsulfonyl)phenyl]prop-2-enoic acid (27). Reaction time: 48 h; temperature: 140 °C; yield 65%; mp 224–226 °C (EtOAc/*n*-hexane); IR 3024, 1667, 1599, 1586, 1508, 1414, 1392, 1304, 1264, 1147 cm^{-1}; ^{1}H NMR (DMSO-d_6) δ 3.26 (3H, s), 7.08−7.13 (4H, m), 7.46 (2H, d, J = 8.4 Hz), 7.86 (1H, s), 7.93 (2H, d, J = 8.4 Hz), 12.94 (1H, broad s); ^{13}C NMR (DMSO-d_6) δ 43.5, 115.6 (d, J = 21.8 Hz), 127.2, 130.5 (d, J = 3.2 Hz), 130.7, 131.7, 132.5 (d, J = 8.6 Hz), 139.1, 140.0, 141.7, 162.3 (d, J = 249.0 Hz), 167.6; MS (ESI+) *m*/*z* 338 ([M + NH$_4$]$^+$); HRMS for $C_{16}H_{14}FO_4S$ ([M + H]$^+$): calcd 321.0591; found 321.0596. Anal. for $C_{16}H_{13}FO_4S$: calcd C, 59.99; H, 4.09; found C, 59.74; H, 3.98.

4.1.1.8 (2*E*)-3-(4-Methylphenyl)-2-[4-(methylsulfonyl)phenyl]prop-2-enoic acid (28). Reaction time: 22 h; temperature: 120 °C; yield 59%; mp 256–258 °C (EtOAc); IR 2976, 2927, 1684, 1602, 1593, 1563, 1510, 1420, 1275, 1148 cm^{-1}; ^{1}H NMR (DMSO-d_6) δ 2.22 (3H, s), 3.26 (3H, s), 6.93 (2H, d, J = 8.3 Hz), 7.03 (2H, d, J = 8.3 Hz), 7.45 (2H, d, J = 8.3 Hz), 7.84 (1H, s), 7.93 (2H, d, J = 8.3 Hz), 12.92 (1H, broad s); ^{13}C NMR (DMSO-d_6) δ 20.9, 43.6, 127.2, 129.2, 130.3, 130.8, 130.9, 131.1, 139.4, 139.8, 140.3, 142.2, 167.8; MS (ESI+) *m*/*z* 317 ([M + H]$^+$); HRMS for $C_{17}H_{16}O_4S$ ([M + H]$^+$): calcd 317.0842; found 317.0837. Anal. for $C_{17}H_{16}O_4S$: calcd C, 64.54; H, 5.10; found C, 64.52.; H, 5.13.

4.1.1.9 (2*E*)-3-(4-Ethylphenyl)-2-[4-(methylsulfonyl)phenyl]prop-2-enoic acid (29). Reaction time: 20 h; temperature: 120 °C; yield 59%; mp 227–229 °C (EtOAc); IR 3026, 2961, 2868, 1687, 1617, 1603, 1592, 1419, 1274, 1141 cm^{-1}; ^{1}H NMR (DMSO-d_6) δ 1.10 (3H, t, J = 7.8 Hz), 2.52 (2H, q, J = 7.8 Hz), 6.96 (2H, d, J = 8.5 Hz), 7.08 (2H, d, J = 8.5 Hz), 7.46 (2H, d, J = 8.3 Hz), 7.83 (1H, s), 7.93 (2H, d, J = 8.3 Hz), 12.88 (1H, broad s); ^{13}C NMR

(DMSO-d_6) δ 15.1, 27.9, 43.5, 127.2, 128.0, 130.4, 130.7, 130.9, 131.3, 139.9, 140.2, 142.2, 145.6, 167.8; MS (ESI+) *m*/*z* 331 ([M + H]$^+$); HRMS for $C_{18}H_{19}O_4S$ ([M + H]$^+$): calcd 331.0999; found 331.0993. Anal. for $C_{18}H_{18}O_4S$: calcd C, 65.43; H, 5.49; found C, 65.24; H, 5.46.

4.1.1.10 (2*E*)-3-(3-Hydroxyphenyl)-2-[4-(methylsulfonyl)phenyl]prop-2-enoic acid (32). Reaction time: 23 h; temperature: 120 °C; yield 64%; mp 236–238 °C (H_2O/EtOH); IR 3371, 2988, 2901, 1667, 1578, 1470, 1394, 1266, 1137, 1066 cm^{-1}; ^{1}H NMR (DMSO-d_6) δ 3.25 (3H, s), 6.42−6.44 (1H, m), 6.48 (1H, d, *J* = 7.5 Hz), 6.65−6.69 (1H, m), 7.02 (1H, t, *J* = 8.0 Hz), 7.45 (2H, d, *J* = 8.5 Hz), 7.75 (1H, s), 7.92 (2H, d, *J* = 8.5 Hz), 9.48 (1H, broad s), 12.94 (1H, broad s); ^{13}C NMR (DMSO-d_6) δ 43.6, 116.6, 116.8, 121.3, 127.1, 129.5, 130.7, 131.8, 135.1, 139.8, 140.4, 142.0, 157.2, 167.8; MS *m*/*z* 336 ([M + NH_4]$^+$); HRMS for $C_{16}H_{15}O_5S$ ([M + H]$^+$): calcd 319.0635; found 319.0637. Anal. for $C_{16}H_{14}O_5S$: calcd C, 60.37; H, 4.43; found C, 60.12; H, 4.33.

4.1.1.11 (2*E*)-3-(3,4-Dihydroxyphenyl)-2-[4-(methylsulfonyl)phenyl]prop-2-enoic acid (33). Reaction time: 50 h; temperature: 120 °C; yield 44%; mp 229–231 °C (H_2O/EtOH); IR 3429, 2937, 1663, 1598, 1524, 1443, 1425, 1262, 1172, 1133 cm^{-1}; ^{1}H NMR (DMSO-d_6) δ 3.26 (3H, s), 6.39 (1H, d, *J* = 2.0 Hz), 6.44 (1H, dd, J_1 = 8.0 Hz, J_2 = 2.0 Hz), 6.59 (1H, d, *J* = 8.0 Hz), 7.44 (2H, d, *J* = 8.5 Hz) 7.67 (1H, s), 7.93 (2H, d, *J* = 8.5 Hz), 8.98 (1H, broad s), 9.50 (1H, broad s), 12.61 (1H, broad s); ^{13}C NMR (DMSO-d_6) δ 43.6, 115.4, 117.4, 123.6, 125.1, 127.2, 127.9, 130.8, 139.6, 140.8, 142.6, 145.0, 147.5, 168.1; MS (ESI+) *m*/*z* 335 ([M + H]$^+$); HRMS for $C_{16}H_{15}O_6S$ ([M + H]$^+$): calcd 335.0584; found 335.0579. Anal. for $C_{16}H_{14}O_6S$: calcd C, 57.48; H, 4.22; found C, 57.41; H, 4.08.

4.1.1.12 (2*E*)-2-[4-(Methylsulfonyl)phenyl]-3-(3,4,5-trimethoxyphenyl)prop-2-enoic acid (34). Reaction time: 19.5 h; temperature: 130 °C; yield 76%; mp 218–220 °C (EtOH); IR 2988, 2842, 1677, 1604, 1578, 1505, 1451, 1417, 1308, 1252 cm^{-1}; ^{1}H NMR (DMSO-d_6) δ 3.24 (3H, s), 3.44 (6H, s), 3.61 (3H, s), 6.35 (2H, s), 7.51 (2H, d, *J* = 8.5 Hz), 7.80 (1H, s), 7.99 (2H, d, *J* = 8.5 Hz), 12.88 (1H, broad s); ^{13}C NMR (DMSO-d_6) δ 43.3, 55.3, 60.1, 108.1, 127.4, 129.0, 130.8, 130.9, 138.5, 140.0, 140.2, 142.5, 152.4, 167.6; MS (ESI+) *m*/*z* 393 ([M + H]$^+$); HRMS for $C_{19}H_{21}O_7S$ ([M + H]$^+$): calcd 393.1003; found 393.1004. Anal. for $C_{19}H_{20}O_7S$: calcd C, 58.15; H, 5.14; found C, 58.31; H, 5.21.

4.1.1.13 (2*E*)-3-(3-Fluorophenyl)-2-[4-(methylsulfonyl)phenyl]prop-2-enoic acid (35). Reaction time: 19 h; temperature: 100 °C; yield 75%; mp 201–203 °C (EtOAc); IR 3187, 3002, 1705, 1624, 1582, 1481, 1447, 1393, 1275, 1134 cm^{-1}; ^{1}H NMR (DMSO-d_6) δ 3.26 (3H, s), 6.84−6.89 (2H, m), 7.12 (1H, dt, J_1 = 8.5 Hz, J_2 = 2.5 Hz), 7.25−7.30 (1H, m), 7.47

(2H, d, *J* = 8.5 Hz), 7.86 (1H, s), 7.94 (2H, d, *J* = 8.5 Hz), 13.10 (1H, broad s); ^{13}C NMR (DMSO-d_6) δ 43.5, 116.1 (d, *J* = 21.3 Hz), 116.5 (d, *J* = 22.4 Hz), 126.3 (d, *J* = 2.6 Hz), 127.2, 130.5 (d, *J* = 8.4 Hz), 130.7, 133.4, 136.4 (d, *J* = 8.1 Hz), 138.7, 140.1, 141.5, 161.7 (d, *J* = 244.2 Hz), 167.4; MS ESI–) *m*/*z* 319 ([M - H]$^-$); HRMS for $C_{16}H_{12}FO_4S$ ([M - H]$^-$): calcd 319.0446; found 319.0447. Anal. for $C_{16}H_{13}FO_4S$: calcd C, 59.99; H, 4.09; found C, 59.70; H, 3.82.

4.1.1.14 (2*E*)-3-(4-Bromophenyl)-2-[4-(methylsulfonyl)phenyl]prop-2-enoic acid (37). Reaction time: 19.5 h; temperature: 120 °C; yield 68%; mp 261–262 °C (H_2O); IR 2971, 1672, 1609, 1583, 1489, 1406, 1311, 1274, 1259, 1147 cm^{-1}; ^{1}H NMR (DMSO-d_6) δ 3.27 (3H, s), 6.99 (2H, d, *J* = 8.5 Hz), 7.44–7.48 (4H, m), 7.46 (2H, d, *J* = 8.3 Hz), 7.83 (1H, s), 7.93 (2H, d, *J* = 8.3 Hz), 13.03 (1H, broad s); ^{13}C NMR (DMSO-d_6) δ 43.5, 122.8, 127.2, 130.7, 131.5, 132.0, 132.7, 133.2, 139.0, 140.0, 131.4, 167.5; MS (ESI+) *m*/*z* 381 ([M + H]$^+$); HRMS for $C_{16}H_{14}BrO_4S$ ([M + H]$^+$): calcd 380.9791; found 380.9791. Anal. for $C_{16}H_{13}BrO_4S$: calcd C, 50.41; H, 3.44; found C, 50.26; H, 3.19.

4.1.1.15 (2*E*)-2-[4-(Methylsulfonyl)phenyl]-3-[4-(trifluoromethyl)phenyl]prop-2-enoic acid (38). Reaction time: 18.5 h; temperature: 120 °C; yield 66%; mp 218–221 °C (EtOAc); IR 2988, 1682, 1620, 1595, 1416, 1394, 1323, 1307, 1271, 1148 cm^{-1}; ^{1}H NMR (DMSO-d_6) δ 3.26 (3H, s), 7.26 (2H, d, *J* = 8.5 Hz), 7.48 (2H, d, *J* = 8.3 Hz), 7.61 (2H, d, *J* = 8.5 Hz), 7.93–7.95 (3H, m), 13.20 (1H, broad s); ^{13}C NMR (DMSO-d_6) δ 43.5, 123.9 (q, *J* = 272.7 Hz), 125.3 (q, *J* = 3.7 Hz), 127.2, 129.0 (q, *J* = 32.0 Hz), 130.69, 130.71, 134.4, 138.2 (q, *J* = 1.0 Hz), 138.6, 140.1, 141.1, 167.3; MS (ESI+) *m*/*z* 388 ([M + NH_4]$^+$); HRMS for $C_{17}H_{14}F_3O_4S$ ([M + H]$^+$): calcd 371.0559; found 371.0559. Anal. for $C_{17}H_{13}F_3O_4S$: calcd C, 55.13; H, 3.54; found C, 55.15; H, 3.43.

4.1.1.16 (2*E*)-3-[4-(Methylsulfanyl)phenyl]-2-[4-(methylsulfonyl)phenyl]prop-2-enoic acid (39). Reaction time: 20 h; temperature: 120 °C; yield 53%; mp 238–240 °C (EtOAc/*n*-heptane); IR (KBr) 3416, 2927, 1665, 1586, 1410, 1309, 1251, 1190, 1146, 1088 cm^{-1}; ^{1}H NMR (DMSO-d_6) δ 2.42 (3H, s), 3.26 (3H, s), 6.98 (2H, d, *J* = 8.7 Hz), 7.10 (2H, d, *J* = 8.7 Hz), 7.47 (2H, d, *J* = 8.4 Hz), 7.81 (1H, s), 7.94 (2H, d, *J* = 8.4 Hz), 12.83 (1H, broad s); ^{13}C NMR (DMSO-d_6) δ 14.0, 43.5, 125.1, 127.2, 130.0, 130.68, 130.69, 130.72, 139.7, 139.9, 140.8, 142.1, 167.7; MS (ESI+) *m*/*z* 349 ([M + H]$^+$); HRMS for $C_{17}H_{17}O_4S_2$ ([M + H]$^+$): calcd 349.0568; found 349.0555. Anal. for $C_{17}H_{16}O_4S_2$: calcd C, 58.60; H, 4.63; found C, 58.83; H, 4.79.

4.1.1.17 (2*E*)-3-[4-(Acetylsulfamoyl)phenyl]-2-[4-(methylsulfonyl)phenyl]prop-2-enoic acid (41). Reaction time: 4.5 h; temperature: 110 °C; yield 25% (column chromatography);

mp 177.5–179.0 °C (H_2O/EtOH); IR 3342, 2988, 2901, 1721, 1689, 1607, 1470, 1406, 1287, 1145 cm^{-1}; ^1H NMR (DMSO-d_6) δ 1.91 (3H, s), 3.27 (3H, s), 7.28 (2H, d, J = 8.5 Hz), 7.47 (7H, d, J = 8.5 Hz), 7.74 (2H, d, J = 8.5 Hz), 7.92 (1H, s) 7.93 (2H, d, J = 8.5 Hz), 12.12 (1H, broad s), 13.20 (1H, broad s); ^{13}C NMR (DMSO-d_6) δ 23.2, 43.5, 127.2, 127.5, 130.5, 130.6, 134.7, 138.3, 139.0, 139.2, 140.2, 140.9, 167.3, 168.9; MS (ESI+) m/z 424 ($[M + H]^+$); HRMS for $C_{18}H_{18}NO_7S_2$ ($[M + H]^+$): calcd 424.0519; found 424.0515. Anal. for $C_{18}H_{17}NO_7S_2$ x $^2/_3$ H_2O: calcd C, 49.65; H, 4.24; N, 3.22; found C, 49.34.; H, 4.08.; N, 3.18.

4.1.2. Synthesis of (2*E*)-3-(3-acetoxyphenyl)-2-(3,4,5-trimethoxyphenyl)prop-2-enoic acid (4). Applying a general method described above, (2*E*)-3-(3-hydroxyphenyl)-2-(3,4,5-trimethoxyphenyl)prop-2-enoic acid was obtained from 3-hydroxybenzaldehyde and (3,4,5-trimethoxyphenyl)acetic acid using triethylamine as a base; reaction time: 45 h; temperature: 100 °C; yield 42%; mp 220−225 °C (EtOAc); IR (KBr) 3447, 2941, 1678, 1587, 1413, 1310, 1271, 1127 cm^{-1}; ^1H NMR (DMSO-d_6) δ 3.68 (6H, s), 3.71 (3H, s), 6.46 (2H, s), 6.53−6.59 (2H, m), 6.67−6.70 (1H, m), 7.02−7.05 (1H, m), 7.64 (1H, s), 9.40 (1H, s), 12.60 (1H, broad s); ^{13}C NMR (DMSO-d_6) δ 56.0, 60.1, 106.9, 116.3, 116.9, 121.3, 129.2, 131.7, 133.0, 135.7, 137.1, 139.1, 153.0, 157.1, 168.4; MS (ESI–) m/z 329 ($[M - H]^-$, 68); HRMS for $C_{18}H_{17}O_6$: calcd 329.1025; found 329.1028. Anal. for $C_{18}H_{18}O_6$: calcd C, 65.45; H, 5.49; found C, 65.33; H, 5.51.

To the solution of (2*E*)-3-(3-hydroxyphenyl)-2-(3,4,5-trimethoxyphenyl)prop-2-enoic acid (3.96 g, 12 mmol) in DMF (12 mL) were added 4-dimethylaminopyridine (30 mg, 0.245 mmol) and acetic anhydride (1.73 mL, 18 mmol). The reaction mixture was stirred at rt for 48 h, treated with water (36 mL) and extracted with EtOAc:THF 3:1 (3 x 60 mL). The combined organic phases were washed with 5% HCl, dried over anhydrous sodium sulfate and evaporated to dryness to give the acid **4**. Yield 64%; mp 186.9−189.7 °C (EtOAc); IR 2946, 1683, 1582, 1412, 1289, 1240, 1211, 1128 cm^{-1}; ^1H NMR (DMSO-d_6) δ 2.18 (3H, s), 3.67 (6H, s), 3.71 (3H, s), 6.46 (2H, s), 6.77−6.79 (1H, m), 7.01−7.05 (2H, m), 7.26−7.31 (1H, m), 7.72 (1H, s), 12.73 (1H, broad s); ^{13}C NMR (DMSO-d_6) δ 20.6, 55.9, 60.1, 106.8, 122.5, 123.1, 127.7, 129.3, 131.3, 134.3, 135.9, 137.3, 137.7, 150.2, 153.1, 168.1, 168.8; MS (ESI–) m/z 371 ($[M - H]^-$, 10); HRMS for $C_{20}H_{19}O_7$ ($[M - H]^-$): calcd 371.1131; found 371.1123. Anal. for $C_{20}H_{20}O_7$: calcd C, 64.51; H, 5.41; found C, 64.34; H, 5.39.

4.1.3. Oxidation of the methylthio moiety into methylsulfonyl group

Hydrogen peroxide (30%, 30 mmol, 3.1 mL) was added to a stirred suspension of the propenoic acid **20** or **23** (6 mmol) in acetic acid (60 mL) at 0 °C and the reaction mixture was stirred at rt for 48 h. Then, it was poured into cold water (300 mL) and the precipitate was filtered off to give the product **21** or **24**.

4.1.3.1. (2*E*)-2-(4-Chlorophenyl)-3-[4-(methylsulfonyl)phenyl]prop-2-enoic acid (21). Yield 73%; mp 231−234 °C (AcOH/H_2O); IR (KBr) 3414, 2928, 1688, 1433, 1312, 1303, 1271, 1152 cm^{-1}; ^1H NMR (DMSO-d_6) δ 3.19 (3H, s), 7.22 and 7.44 (4H, AA'XX', J = 8.4 Hz), 7.33 and 7.79 (4H, AA'XX', J = 8.4 Hz), 7.88 (1H, s), 13.03 (1H, broad s); ^{13}C NMR (DMSO-d_6) δ 43.2, 126.8, 128.6, 130.6, 131.5, 132.8, 134.3, 135.1, 137.6, 139.4, 140.5, 167.6; MS (ESI–) *m/z* 335.0 ([M - H]$^-$, 30); HRMS for $C_{16}H_{12}ClO_4S$ ([M - H]$^-$): calcd 335.0145; found 335.0150. Anal. for $C_{16}H_{13}ClO_4S$: calcd C, 57.06; H, 3.89; found C, 57.32; H, 3.66.

4.1.3.2. (2*E*)-2-(3-Chlorophenyl)-3-[4-(methylsulfonyl)phenyl]prop-2-enoic acid (24). Yield 74%; mp 205–207 °C (AcOH/H_2O); IR (KBr) 3418, 1668, 1609, 1589, 1426, 1287, 1272, 1191 cm^{-1}; ^1H NMR (DMSO-d_6) δ 3.19 (3H, s), 7.12−7.16 (1H, m), 7.30−7.47 (5H, m), 7.77−7.80 (2H, m), 7.89 (1H, s), 13.06 (1H, broad s); ^{13}C NMR (DMSO-d_6) δ 43.2, 126.8, 128.0, 128.3, 129.3, 130.4, 130.7, 133.1, 134.8, 137.6, 137.9, 139.3, 140.6, 167.4; MS (ESI–) *m/z* 335.0 ([M - H]$^-$); HRMS for $C_{16}H_{12}ClO_4S$ ([M - H]$^-$): calcd 335.0145; found 335.0141. Anal. for $C_{16}H_{13}ClO_4S$: calcd C, 57.06; H, 3.89; found C, 57.17; H, 3.76.

4.1.4. Suzuki coupling to obtain (2*E*)-3-[4'-(methylsulfanyl)biphenyl-4-yl]-2-[4-(methylsulfonyl)phenyl]prop-2-enoic acid (42). An aqueous solution of 2 M potassium carbonate (4.0 mL), triphenylphosphine (32 mg, 0.12 mmol) and $Pd(OAc)_2$ (7 mg, 0.03 mmol) were added to a solution of (2*E*)-3-(4-bromophenyl)-2-[4-(methylsulfonyl)-phenyl]prop-2-enoic acid (**37**; 381 mg, 1.0 mmol) and 4-(methylthio)phenylboronic acid (252 mg, 1.5 mmol) in dimethoxyethane (10 mL) under an argon atmosphere. The reaction mixture was heated at 100 °C for 17 h, cooled to rt and the solvent was removed under reduced pressure. Dichloromethane (30 mL) and water (20 mL) were added and the mixture was acidified with 1 M aqueous HCl to pH 3. Layers were separated and the water phase was additionally extracted with dichloromethane (3 x 20 mL). The combined organic layers were washed with brine (2 x 30 mL), dried over anhydrous sodium sulfate and evaporated to dryness giving the acid **42**. Yield 72%; mp 291–293 °C (EtOAc); IR 2988, 2923, 1666, 1590, 1486, 1425, 1396, 1307, 1275, 1150 cm^{-1}; ^1H NMR (DMSO-d_6) δ 2.49 (3H, s), 3.28 (3H, s), 7.13 (2H, d, J = 8.5 Hz), 7.30 (2H, d, J = 8.5 Hz), 7.51 (2H, d, J = 8.3 Hz), 7.56 (2H, d, J =

8.5 Hz), 7.61 (2H, d, *J* = 8.5), 7.90 (1H, s), 7.96 (2H, d, *J* = 8.3 Hz), 12.98 (1H, broad s); ^{13}C NMR (DMSO-d_6) δ 14.5, 43.5, 126.2, 127.0, 127.2, 130.7, 131.0, 131.6, 132.7, 135.2, 138.3, 139.7, 139.9, 140.1, 142.0, 167.7 (one signal missing); MS (ESI+) *m*/*z* 423 ($[M + H]^+$); HRMS for $C_{23}H_{21}O_4S_2$ ($[M + H]^+$): calcd 425.0876; found 425.0876. Anal. for $C_{23}H_{20}O_4S_2$ x 0.5 H_2O: calcd C, 63.72; H, 4.88; found C, 63.56; H, 4.66.

4.2. Molecular docking

A multi-conformer library of 3D structures of the compounds **1**, **20**, **22**, **28**, **29**, **36**, **37** and **39** was prepared with the program Omega (OpenEye Scientific Software Inc.). For the preparation of 3D conformations the default parameters were used, except that the maximum number of conformations per compound was increased to 300. Active sites of AKR1C1 (PDB code 3C3U) [30] and AKR1C3 (PDB code 1S2A) [31] were prepared with the program fred_receptor (OpenEye Scientific Software Inc.). Co-crystallized cofactors were retained in the structures. An active site was in both cases defined as a box around co-crystallized inhibitor, 3,5-dichlorosalicylic acid in the case of AKR1C1 and indomethacin in the case of AKR1C3. A docking protocol was validated by re-docking of co-crystallized inhibitors. Subsequently, the multi-conformer library of the compounds **1**, **20**, **22**, **28**, **29**, **36**, **37** and **39** was docked with FRED [32] in both enzymes using chemgauss3 as a scoring function.

4.3. Inhibition Assays

Recombinant enzymes AKR1C1-AKR1C3 were prepared as described before [33]. These enzymes *in vitro* catalyze the oxidation of the 1-acenaphthenol in the presence of the coenzyme NAD^+ and this reaction was followed spectrophotometrically by measuring the increase in NADH absorbance ($\varepsilon_{\lambda 340}$ = 6220 $M^{-1}.cm^{-1}$) in the presence and absence of each of the compounds. The assays were carried out in a 0.3 mL volume that included a 100 mM phosphate buffer (pH 9.0), 0.005% triton X-114 and 5% DMSO as a co-solvent. A substrate concentration of 30 µM (K_m), 50 µM (K_m) and 100 µM (< K_m) and an enzyme concentration of 0.3 µM, 0.2 µM, and 1.5 µM were used for assays with AKR1C1, AKR1C2 and AKR1C3, respectively, in the presence of 2.3 mM coenzyme. Screening was performed for 100 µM compounds. For the compounds that showed more than 50% inhibition, the IC_{50} values were determined. The measurements were performed on Biotek PowerWave XS microplate readers with initial velocities calculated, and the IC_{50} values were determined graphically from plots of $\log_{10}$ [inhibitor concentration] versus % inhibition, using GraphPad Prism Version 4.00

(GraphPad Software, Inc.). Ki values were then calculated using the Cheng-Prusoff equation for competitive inhibition.

Acknowledgements

Slovenian Research Agency is gratefully acknowledged for the financial support (projects P1-0230, J3-4135). We thank Dr. Bogdan Kralj and Dr. Dušan Žigon (Mass Spectrometry Centre, Jožef Stefan Institute, Ljubljana, Slovenia) for recording the mass spectra. This work was supported with the infrastructure of the EN-FIST Centre of Excellence, Dunajska 156, SI-1000 Ljubljana, Slovenia. We thank OpenEye Scientific Software, Inc. for free academic licenses of their software. The authors thank Dr. Trevor M. Penning (University of Pennsylvania, School of Medicine, Philadelphia, PA, USA) for the pcDNA3-AKR1C1 and pcDNA3-AKR1C2 constructs and Dr. Jerzy Adamski (Helmholtz Zentrum Munchen, Germany) for the pGex-AKR1C3 construct. This study was partially supported by Young Researcher grants to M.G. and N.B. from the Slovenian Research Agency.

Appendix A. Supporting information

Supplementary material associated with this article can be found, in the online version, at http://..... It includes the characterization data of the compounds **13**, **15**, **19**, **20**, **30**, **31**, **36**, and **40** as well as the predicted binding pose of the compound **1** in the AKR1C1 active site and the data about a purity of all tested acids checked by HPLC .

References

[1] T.M. Penning, M.E. Burczynski, J.M. Jez, C.F. Hung, H.K. Lin, H. Ma, M. Moore, N. Palackal, K. Ratnam, Human 3α-hydroxysteroid dehydrogenase isoforms (AKR1C1–AKR1C4) of the aldo-keto reductase superfamily: functional plasticity and tissue distribution reveals roles in the inactivation and formation of male and female sex hormones, Biochem. J. 351 (2000) 67–77.

[2] T.M. Penning, M.C. Byrns, Steroid hormone transforming aldo-keto reductases and cancer, Ann. N. Y. Acad. Sci. 1155 (2009) 33–42.

[3] T.M. Penning, J.E. Drury, Human aldo-keto reductases: function, gene regulation, and single nucleotide polymorphisms, Arch. Biochem. Biophys. 464 (2007) 241–250.

[4] I. Dufort, P. Rheault, X.F. Huang, P. Soucy, V. Luu-The, Characteristics of a highly labile human type 5 17β-hydroxysteroid dehydrogenase, Endocrinology 140 (1999) 568–574.

[5] M.C. Byrns, L. Duan, S.H. Lee, I.A. Blair, T.M. Penning, Aldo-keto reductase 1C3 expression in MCF-7 cells reveals roles in steroid hormone and prostaglandin metabolism that may explain its over-expression in breast cancer, J. Steroid Biochem. Mol. Biol. 118 (2010) 177–187.

[6] R.B. Montgomery, E.A. Mostaghel, R. Vessella, D.L. Hess, T.F. Kalhorn, C.S. Higano, L.D. True, P.S. Nelson, Maintenance of intratumoral androgens in metastatic prostate cancer: a mechanism for castration-resistant tumor growth, Cancer Res. 68 (2008) 4447–4454.

[7] T. Lanišnik-Rižner, T. Šmuc, R. Rupreht, J. Šinkovec, T.M. Penning, AKR1C1 and AKR1C3 may determine progesterone and estrogen ratios in endometrial cancer, Mol. Cell. Endocrinol. 248 (2006) 126–135.

[8] T. Šmuc, N. Hevir, M. Ribič-Pucelj, B. Husen, H. Thole, T.L. Rižner, Disturbed estrogen and progesterone action in ovarian endometriosis, Mol. Cell. Endocrinol. 301 (2009) 59–64.

[9] P. Brožič, S. Turk, T.L. Rižner, S. Gobec, Inhibitors of Aldo-Keto reductases AKR1C1–AKR1C4, Curr. Med. Chem. 18 (2011) 2554–2565.

[10] M.C. Byrns, Y. Jin, M.P. Penning, Inhibitors of type 5 17β-hydroxysteroid dehydrogenase (AKR1C3): Overview and structural insights, J. Steroid Biochem. Mol. Biol. 125 (2011) 95–104.

[11] N. Beranič, S. Gobec, T.L. Rižner, Progestins as inhibitors of the human 20-ketosteroid reductases, AKR1C1 and AKR1C3, Chem. Biol. Interact. 191 (2011) 227–233.

[12] P. Bydal, V. Luu-The, F. Labrie, D. Poirier, Steroidal lactones as inhibitors of 17β-hydroxysteroid dehydrogenase type 5: chemical synthesis, enzyme inhibitory activity, and assessment of estrogenic and androgenic activities, Eur. J. Med. Chem. 44 (2009) 632–644.

[13] B. Štefane, P. Brožič, M. Vehovc, T.L. Rižner, S. Gobec, New cyclopentane derivatives as inhibitors of steroid metabolizing enzymes AKR1C1 and AKR1C3, Eur. J. Med. Chem. 44 (2009) 2563–2571.

[14] Y. Higaki, N. Usami, S. Shintani, S. Ishikura, O. El-Kabbani, A. Hara, Selective and potent inhibitors of human 20α-hydroxysteroid dehydrogenase (AKR1C1) that

metabolizes neurosteroids derived from progesterone, Chem. Biol. Interact. 143–144 (2003) 503–513.

[15] L. Skarydova, L. Zivna, G. Xiong, E. Maser, V. Wsol, AKR1C3 as a potential target for the inhibitory effect of dietary flavonoids, Chem. Biol. Interact. 178 (2009) 138–144.

[16] (a) P. Brožič, B. Golob, N. Gomboc, T. Lanišnik-Rižner, S. Gobec, Cinnamic acids as new inhibitors of 17β-hydroxysteroid dehydrogenase type 5 (AKR1C3), Mol. Cell. Endocrinol. 248 (2006) 233–235;

(b) S. Endo, T. Matsunaga, A. Kanamori, Y. Otsuji, H. Nagai, K. Sundaram, O. El-Kabbani, N. Toyooka, S. Ohta, A. Hara, Selective inhibition of human type-5 17β-hydroxysteroid dehydrogenase (AKR1C3) by baccharin, a component of brazilian propolis, J. Nat. Prod. 75 (2012) 716−721.

[17] N.J. Davies, R.E. Hayden, P.J. Simpson, J. Birtwistle, K. Mayer, J.P. Ride, C.M. Bunce, AKR1C isoforms represent a novel cellular target for jasmonates alongside their mitochondrial-mediated effects, Cancer Res. 69 (2009) 4769–4775.

[18] M.C. Byrns, S. Steckelbroeck, T.M. Penning, An indomethacin analogue, N-(4-chlorobenzoyl)-melatonin, is a selective inhibitor of aldo-keto reductase 1C3 (type 2 3α-HSD, type 5 17β-HSD, and prostaglandin F synthase), a potential target for the treatment of hormone dependent and hormone independent malignancies, Biochem. Pharmacol. 75 (2008) 484–493.

[19] (a) A.O. Adeniji, B.M. Twenter, M.C. Byrns, Y. Jin, J.D. Winkler, T.M. Penning, Discovery of substituted 3-(phenylamino)benzoic acids as potent and selective inhibitors of type 5 17β-hydroxysteroid dehydrogenase (AKR1C3), Bioorg. Med. Chem. Lett. 21 (2011) 1464–1468;

(b) A.O. Adeniji, B.M. Twenter, M.C. Byrns, Y. Jin, M. Chen, J.D. Winkler, T.M. Penning, Development of potent and selective inhibitors of aldo−keto reductase 1C3 (type 5 17β-hydroxysteroid dehydrogenase) based on N-phenyl-aminobenzoates and their structure−activity relationships, J. Med. Chem. 55 (2012) 2311–2323.

[20] S. Li, W. Yuan, S. Ma, Highly regio- and stereoselective three-component nickel-catalyzed syn-hydrocarboxylation of alkynes with diethyl zinc and carbon dioxide, Angew. Chem. Int. Ed. 50 (2011) 2578–2582.

[21] B. Burja, T. Čimbora-Zovko, S. Tomić, T. Jelušić, M. Kočevar, S. Polanc, M. Osmak, Pyrazolone-fused combretastatins and their precursors: synthesis, cytotoxicity, antitubulin activity and molecular modeling studies, Bioorg. Med. Chem. 18 (2010) 2375–2387.

[22] A. Moreau, O.-H. Chen, P.N.P. Rao, E.E. Knaus, Design, synthesis, and biological evaluation of (E)-3-(4-methanesulfonylphenyl)-2-(aryl)acrylic acids as dual inhibitors of cyclooxygenases and lipoxygenases, Bioorg. Med. Chem. 14 (2006) 7716–7727.

[23] C. Zhu, Y. Zhang, G. Cao, S. Peng, W. Wang, J. Zheng, Studies on the nonsteroidal antifertility agents. II. Synthesis and antifertility activity of some p-coumaric acid derivatives, Nanjing Yaoxueyuan Xuebao (1982) 50−56. Chem. Abstr. 99 (1983) 212230.

[24] J. J. Talley, J. S. Carter, P. W. Collins, S.W. Kramer, T. D. Penning, D.J. Rogier Jr., R.S. Rogers, Substituted thiazoles for the treatment of inflammation, WO 9603392 A1; Chem. Abstr. 125 (1996) 33628.

[25] J.-L. Mao, X.-K. Ran, J.-Z. Tian, B. Jiao, H.-L. Zhou, L. Chen, Z.-G. Wang, Design, synthesis and biological evaluation of novel 4-hydroxybenzeneacrylic acid derivatives, Bioorg. Med. Chem. Lett. 21 (2011) 1549–1553.

[26] X. Ran, J. Mao, H. Pang, L. Chen, B. Jiao, Preparation of 3-phenyl-2-(4-mesylphenyl)acrylates as cyclooxygenase-2 inhibitors for treatment of inflammation and pain, Faming Zhuanli Shenqing Gongkai Shuomingshu, Patent CN 1762994 (April 26, 2006); Chem. Abstr. 145 (2006) 62680.

[27] D. Macdonald, A. Mastracchio, H. Perrier, D. Dube, M. Gallant, C. Li, L.A. Trimble, S. Day, N. Chauret, D.A. Nicoll-Griffith, J.M. Silva, Z. Huang, F. Laliberte, S. Liu, D. Ethier, D. Pon, E. Muise, L. Boulet, C.C. Chan, A. Styhler, S. Charleson, J. Mancini, P. Masson, D. Claveau, D. Nicholson, M. Turner, R.N. Young, Y. Girard, Discovery of a substituted 8-arylquinoline series of PDE4 inhibitors: structure-activity relationship, optimization, and identification of a highly potent, well tolerated, PDE4 inhibitor, Bioorg. Med. Chem. Lett. 15 (2005) 5241–5246.

[28] F. Wang, S. Li, W. Feng, Anti-inflammatory structure-activity relationships of a new series of open-loop COX-2 inhibitors derived from rofecoxib, Beijing Huagong Daxue Xuebao, Ziran Kexueban 31 (2004) 84–87, Chem. Abstr. 142 (2005) 385056.

[29] T. Rosen, The Perkin reaction, in: B. Trost, I. Fleming (Eds.), Comprehensive Organic Synthesis, vol. 2, Pergamon Press, Oxford, 1991, pp. 395–408.

[30] U. Dhagat, S. Endo, R. Sumii, A. Hara, O. El-Kabbani, Selectivity determinants of inhibitor binding to human 20α-hydroxysteroid dehydrogenase: crystal structure of the enzyme in ternary complex with coenzyme and the potent inhibitor 3,5-dichlorosalicylic acid, J. Med. Chem. 51 (2008) 4844–4848.

[31] A.L. Lovering, J.P. Ride, C.M. Bunce, J.C. Desmond, S.M. Cummings, S.A. White, Crystal structures of prostaglandin D2 11-ketoreductase (AKR1C3) in complex with the nonsteroidal anti-inflammatory drugs flufenamic acid and indomethacin, Cancer Res. 64 (2004) 1802–1810.

[32] M. McGann, FRED pose prediction and virtual screening accuracy, J. Chem. Inf. Model. 51 (2011) 578–596.

[33] P. Brožič, T. Šmuc, S. Gobec, T. Lanišnik-Rižner, Phytoestrogens as inhibitors of the human progesterone metabolizing enzyme AKR1C1, Mol. Cell. Endocrinol. 259 (2006) 30–42.

List of captions

Fig. 1. Design of 2,3-diarylpropenoic acids.

Fig. 2. Predicted binding pose of the compound **37** (blue) in the AKR1C3 active site (green).

Scheme 1. Synthesis of 2,3-diarylpropenoic acids employing the Perkin reaction.

Scheme 2. Selective oxidation of the methylthio groups of the acids **20**, **23** and **39**.

Scheme 3. Synthesis of the acid **42**.

Table 1. Structures of 2,3-diarylpropenoic acids **1**–**42**.

Table 2. Effect of 2,3-diarylpropenoic acids **1**–**42** on the inhibition of AKR1C1–AKR1C3.

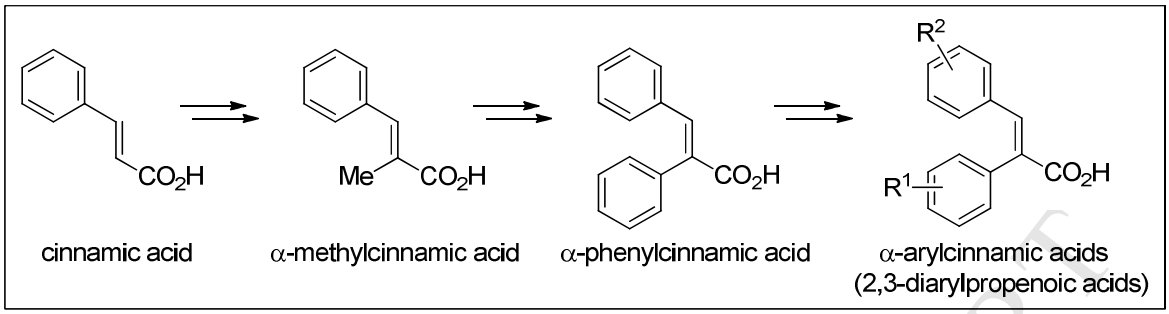

Fig. 1. Design of 2,3-diarylpropenoic acids.

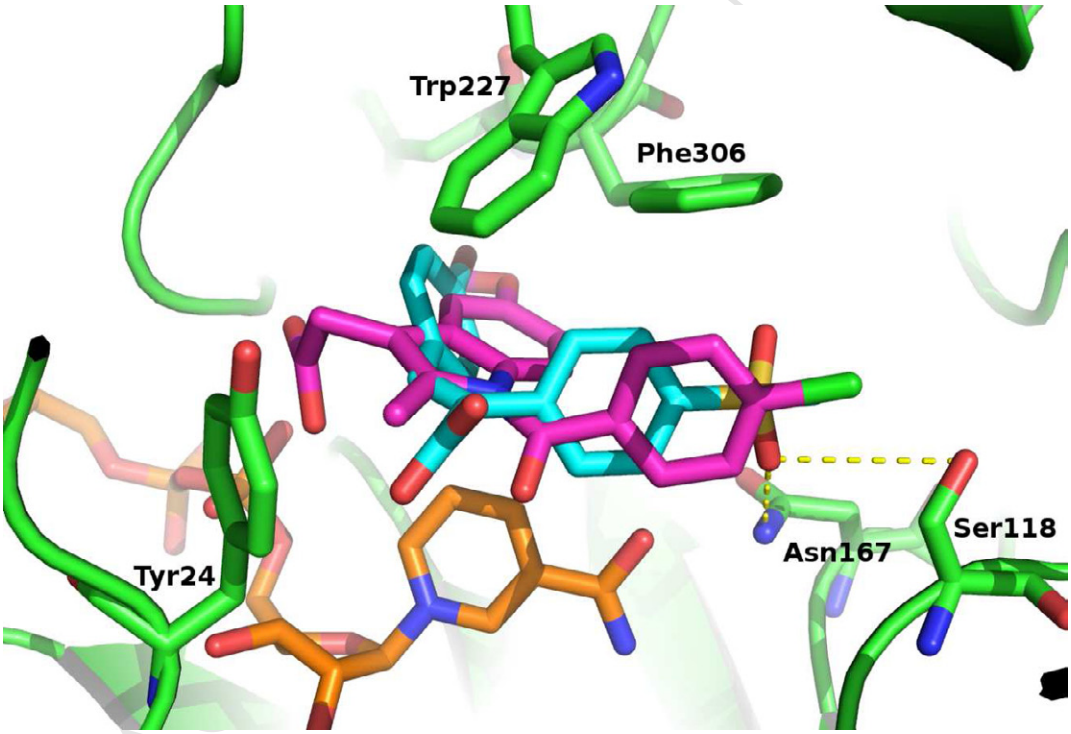

Fig. 2. Predicted binding pose of the compound **37** (blue) in the AKR1C3 active site (green). Only relevant amino acid residues are shown and labeled. The co-crystallized indomethacin is shown as magenta sticks and the cofactor as orange sticks. The H-bonds are shown as yellow dashes.

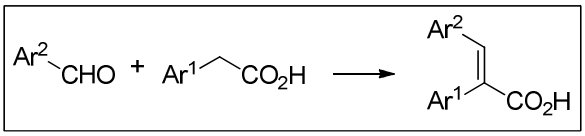

Reagents and conditions: arylacetic acid (7.5 mmol), aromatic aldehyde (7.5 mmol), acetic anhydride (32 mmol), potassium acetate (10 mmol) or triethylamine (10.75 mmol), 100–140 ºC, 3.5–70 h.

Scheme 1. Synthesis of 2,3-diarylpropenoic acids employing the Perkin reaction.

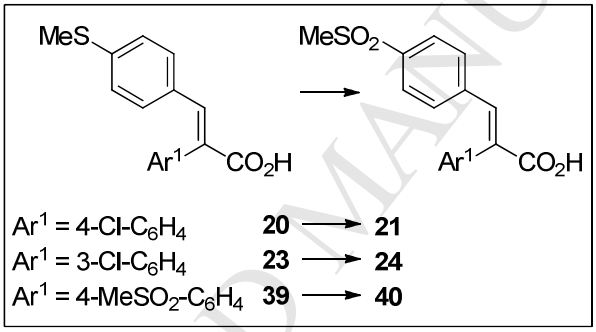

Reagents and conditions: 2,3-diarylpropenoic acid (6 mmol), hydrogen peroxide (30%, 30 mmol, 3.1 mL), acetic acid (60 mL), rt, 48 h.

Scheme 2. Selective oxidation of the methylthio groups of the acids **20**, **23** and **39**.

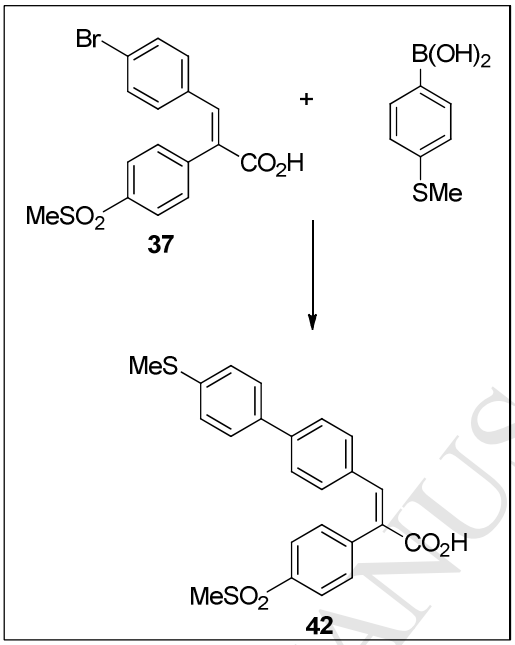

Reagents and conditions: acid **37** (1 mmol), 4-(methylthio)phenylboronic acid (1.5 mmol), potassium carbonate (4 mL of 2 M aqueous solution), Ph_3P (0.12 mmol), $Pd(OAc)_2$ (0.03 mmol), DME (10 mL), argon, 100 ºC, 17 h.

Scheme 3. Synthesis of the acid **42**.

Table 1
Structures of 2,3-diarylpropenoic acids **1**–**42**.

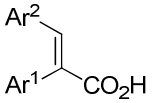

Acid	Ar^1	Ar^2	Acid	Ar^1	Ar^2
1	C_6H_5	C_6H_5	**22**	4-$MeSO_2$-C_6H_4	4-Cl-C_6H_4
2	3,4,5-MeO-C_6H_2	3-OH,4-MeO-C_6H_3	**23**	3-Cl-C_6H_4	4-MeS-C_6H_4
3	3,4,5-MeO-C_6H_2	3-OAc,4-MeO-C_6H_3	**24**	3-Cl-C_6H_4	4-$MeSO_2$-C_6H_4
4	3,4,5-MeO-C_6H_2	3-OAc-C_6H_4	**25**	4-$MeSO_2$-C_6H_4	3-Cl-C_6H_4
5	3,4,5-MeO-C_6H_2	3-F,4-MeO-C_6H_3	**26**	4-F-C_6H_4	4-$MeSO_2$-C_6H_4
6	3,4,5-MeO-C_6H_2	3-F-C_6H_4	**27**	4-$MeSO_2$-C_6H_4	4-F-C_6H_4
7	3,4,5-MeO-C_6H_2	3,4-MeO-C_6H_3	**28**	4-$MeSO_2$-C_6H_4	4-Me-C_6H_4
8	3,4,5-MeO-C_6H_2	4-MeO-C_6H_4	**29**	4-$MeSO_2$-C_6H_4	4-Et-C_6H_4
9	3,4,5-MeO-C_6H_2	1-naphthyl	**30**	4-$MeSO_2$-C_6H_4	4-MeO-C_6H_4
10	3,4,5-MeO-C_6H_2	2-naphthyl	**31**	4-$MeSO_2$-C_6H_4	4-HO-C_6H_4
11	3,4-MeO-C_6H_3	3,4,5-MeO-C_6H_2	**32**	4-$MeSO_2$-C_6H_4	3-HO-C_6H_4
12	3,4-MeO-C_6H_3	2,4,5-MeO-C_6H_2	**33**	4-$MeSO_2$-C_6H_4	3,4-HO-C_6H_3
13	1-naphthyl	3,4-MeO-C_6H_3	**34**	4-$MeSO_2$-C_6H_4	3,4,5-MeO-C_6H_2
14	2-naphthyl	3,4-MeO-C_6H_3	**35**	4-$MeSO_2$-C_6H_4	3-F-C_6H_4
15	C_6H_5	4-MeS-C_6H_4	**36**	4-$MeSO_2$-C_6H_4	3-Br-C_6H_4
16	C_6H_5	4-$MeSO_2$-C_6H_4	**37**	4-$MeSO_2$-C_6H_4	4-Br-C_6H_4
17	3,4-OCH_2O-C_6H_3	4-$MeSO_2$-C_6H_4	**38**	4-$MeSO_2$-C_6H_4	4-CF_3-C_6H_4
18	C_6H_5	4-$MeCONHSO_2$-C_6H_4	**39**	4-$MeSO_2$-C_6H_4	4-MeS-C_6H_4
19	4-$MeSO_2$-C_6H_4	C_6H_5	**40**	4-$MeSO_2$-C_6H_4	4-$MeSO_2$-C_6H_4
20	4-Cl-C_6H_4	4-MeS-C_6H_4	**41**	4-$MeSO_2$-C_6H_4	4-$MeCONHSO_2$-C_6H_4
21	4-Cl-C_6H_4	4-$MeSO_2$-C_6H_4	**42**	4-$MeSO_2$-C_6H_4	4-(4-MeS-C_6H_4)-C_6H_4

Table 2

Effect of 2,3-diarylpropenoic acids **1**–**42** on the inhibition of AKR1C1–AKR1C3.

Acid	Inhibition of AKR1C1[a] %	IC_{50} µM	Inhibition of AKR1C2[a] %	IC_{50} µM	Inhibition of AKR1C3[a] %	IC_{50} µM
1	90.1 ± 1.3	**7.9 ± 0.9**	47.5 ± 4.0		29.1 ± 2.8	
2	14.4 ± 8.1		20.6 ± 4.5		51.7 ± 4.3	**121.1 ± 0.3**
3	8.0 ± 0.2		3.2 ± 2.2		8.8 ± 2.0	
4	40.0 ± 14.8		27.0 ± 22.3		42.6 ± 2.3	
5	−5.2 ± 6.4		9.9 ± 1.1		10.3 ± 0.4	
6	7.8 ± 3.7		55.9 ± 3.1	**77.0 ± 0.3**	12.2 ± 2.4	
7	6.1 ± 0.1		0.6 ± 4.4		4.2 ± 0	
8	15.1 ± 1.1		4.3 ± 0.3		10.3 ± 0.4	
9	6.4 ± 8.3		13.8 ± 0.8		14.8 ± 3.5	
10	9.6 ± 8.6		15.9 ± 2.2		30.8 ± 2.6	
11	7.1 ± 1.7		4.2 ± 5.6		16.1 ± 4.6	
12	22.2 ± 6.8		9.4 ± 5.6		7.0 ± 0	
13	29.4 ± 6.8		77.8 ± 0.4	**24.2 ± 0.1**	59.7 ± 6.2	**127.8 ± 0.3**
14	9.7 ± 1.5		39.6 ± 9.5		78.3 ± 1.3	**38.7 ± 0.2**
15	87.0 ± 8.5	**12.3 ± 0.0**	59.1 ± 3.4	**41.2 ± 0.2**	92.8 ± 4.9	**30.2 ± 0.2**
16	77.6 ± 2.0	**30.8 ± 0.2**	61.4 ± 0.3	**34.4 ± 0.2**	52.3 ± 3.2	**139.2 ± 0.3**
17	45.2 ± 5.4		24.2 ± 9.4		35.8 ± 6.8	
18	97.8 ± 0.3	**8.7 ± 0.0**	87.3 ± 7.6	**25.2 ± 0.1**	34.8 ± 1.5	
19	26.3 ± 3.7		27.3 ± 3.5		55.5 ± 0.2	**69.8 ± 0.3**
20	88.1 ± 0.7	**6.6 ± 0.1**	75.2 ± 1.1	**27.3 ± 0.2**	86.0 ± 5.3	**8.3 ±0.0**
21	89.6 ± 0.6	**15.7 ± 0.1**	63.4 ± 7.4	**26.9 ± 0.2**	61.1 ± 3.2	**86.6 ± 0.3**
22	34.7 ± 16.2		24,3 ± 10,4		90,6 ± 3,3	**10.8 ± 0.0**
23	81.7 ± 10.8	**19.1 ± 0.1**	78.3 ± 3.0	**20.8 ± 0.1**	84.7 ± 0.3	**17.0 ± 0.1**
24	75.9 ± 2.5	**19.3 ± 0.1**	66.4 ± 0.0	**23.1 ± 0.1**	57.4 ± 0.4	**76.7 ± 0.3**
25	44.5 ± 1.9		43.0 ± 1.0		81.6 ± 0.4	**16.8 ± 0.1**
26	86.1 ± 7.2	**23.3 ± 0.1**	69.7 ± 3.6	**44.6 ± 0.2**	43.8 ± 1.2	
27	21.0 ± 0.2		9.2 ± 6.6		86.2 ± 0.0	**43.1 ± 0.2**
28	n.i.[b]		1.1 ± 14.9		92.7 ± 4.0	**13.4 ± 1.1**
29	n.i.		n.i.		89.1 ± 2.3	**13.6 ± 1.1**
30	n.i.		n.i.		71.2 ± 1.5	**36.9 ± 1.1**
31	n.i.		n.i.		39.9 ± 0.5	
32	n.i.		n.i.		43.8 ± 3.0	
33	46.5 ± 11.6		27.2 ± 9.8		71.8 ± 0.4	**33.1 ± 1.1**
34	n.i.		n.i.		5.7 ± 0.1	
35	15.4 ± 5.8		27.0 ± 2.8		78.3 ± 0.0	**38.9 ± 1.1**
36	34.8 ± 3.2		58.3 ± 4.2	**74.3 ± 1.1**	93.3 ± 1.8	**13.6 ± 1.1**
37	28.7 ± 13.4		19.2 ± 5.2		93.2 ± 0.4	**4.9 ± 1.1**
38	3.5 ± 4.7		18.4 ± 16.6		90.6 ± 1.5	**23.3 ± 1.1**
39	43.8 ± 13.1		14.4 ± 2.1		93.5 ± 0.5	**5.8 ± 0.1**
40	n.i.		n.i.		63.7 ± 1.3	**51.0 ± 1.1**
41	5.9 ± 8.8		10.6 ± 2.6		26.1 ± 5.5	
42	64.7 ± 3.8		57.4 ± 5.8		72.2 ± 8.1	

[a] The values represent % inhibition at 100 µM inhibitor.
[b] No inhibition.

Highlights

- A series of new 2,3-diarylpropenoic acids were prepared.
- The compounds were evaluated for their inhibition of aldo-keto reductases.
- Selective inhibitors of AKR1C3 were identified.
- Substituents on benzene rings play a crucial role in selective inhibition of AKR1C3.

Appendix A. Supporting information

2,3-Diarylpropenoic acids as selective non-steroidal inhibitors of type 5 17β-hydroxysteroid dehydrogenase (AKR1C3)

Martin Gazvoda, Nataša Beranič, Samo Turk, Bojan Burja, Marijan Kočevar, Tea Lanišnik Rižner, Stanislav Gobec, Slovenko Polanc

Table of contents

Applying a general procedure described in the Experimental protocols the following acids were prepared:

(2*E*)-3-(3,4-Dimetoxyphenyl)-2-(naphthalen-1-yl)prop-2-enoic acid (13). Reaction time: 16 h; temperature: 100 °C; yield 36%; mp 190.5–192.5 °C (EtOAc); IR (KBr) 2833, 1673, 1593, 1510, 1418, 1258, 1143, 1020 cm^{-1}; ^1H NMR (DMSO-d_6) δ 2.98 (3H, s), 3.59 (3H, s), 6.31 (1H, d, J = 1.2 Hz), 6.66 (1H, d, J = 8.4 Hz), 6.80 (1H, dd, J_1 = 1.2 Hz, J_2 = 8.4 Hz), 7.39−7.58 (4H, m), 7.81−7.83 (1H, m), 7.92−7.97 (2H, m), 8.15 (1H, s), 12.67 (1H, broad s); ^{13}C NMR (DMSO-d_6) δ 54.3, 55.4, 111.3, 112.4, 125.0, 125.1, 126.2, 126.3, 126.6, 127.0, 127.2, 127.9, 128.5, 128.8, 131.7, 133.6, 135.1, 140.9, 148.1, 150.1, 168.9; MS (ESI–) *m/z* 333 ([M – H]$^-$, 30); HRMS for $C_{21}H_{17}O_4$ ([M - H]$^-$): calcd 333.1127; found 333.1123. Anal. for $C_{21}H_{18}O_4$: calcd C, 75.43; H, 5.43; found C, 75.50; H, 5.33.

(2*E*)-3-[4-(Methylsulfanyl)phenyl]-2-phenylprop-2-enoic acid (15). Reaction time: 20 h; temperature: 100 °C; yield 62%; mp 165.0−168.0 °C (EtOAc/*n*-heptane); mp^{24} 167–169 ºC (*i*-PrOH); IR (KBr) 1673, 1590, 1493, 1422, 1286, 1267, 1095, 702 cm^{-1}; ^1H NMR ($CDCl_3$) δ 2.42 (3H, s), 6.95−7.02 (4H, m), 7.22−7.26 (2H, m), 7.35−7.42 (3H, m), 7.88 (1H, s); ^{13}C NMR ($CDCl_3$) δ 14.9, 125.2, 128.0, 128.8, 129.7, 130.58, 130.61, 131.2, 135.4, 141.3, 141.9, 173.1; MS (ESI–) *m*/*z* 269.1 ([M - H]$^-$, 100); Anal. for $C_{16}H_{14}O_2S$: calcd C, 71.08; H, 5.22; found C, 71.32; H, 5.08.

(2*E*)-2-[4-(Methylsulfonyl)phenyl]-3-phenylprop-2-enoic acid (19). Reaction time: 24 h; temperature: 130 °C; yield 49%; mp 228–230 ºC (EtOAc); mp^{25} 229–230 °C; IR 2971, 2901, 1667, 1611, 1595, 1448, 1422, 1273, 1142, 1089 cm^{-1}; ^1H NMR (DMSO-d_6) δ 3.26 (3H, s), 7.03−7.09 (2H, m), 7.21−7.31 (3H, m), 7.46 and 7.92 (4H, AA'XX', J = 8.4 Hz), 7.87 (1H, s), 12.92 (1H, broad s); ^{13}C NMR (DMSO-d_6) δ 43.5, 127.1, 128.5, 129.4, 130.2, 130.7, 131.9, 133.9, 139.9, 140.2, 141.9, 167.6; MS (ESI+) *m/z* 303 ([M + H]$^+$); HRMS for $C_{16}H_{15}O_4S$ ([M + H]$^+$): calcd 303.0686; found 303.0684; Anal. for $C_{16}H_{14}O_4S$: calcd C, 63.56; H, 4.67; found C, 63.28; H,4.71.

(2*E*)-2-(4-Chlorophenyl)-3-[4-(methylsulfanyl)phenyl]prop-2-enoic acid (20). Reaction time: 6 h; temperature: 100 °C; yield 55%; mp 180.4−182.7 °C (EtOAc/*n*-heptane); mp^{24} 185–187 ºC (toluene); IR (KBr) 1674, 1614, 1589, 1490, 1418, 1281, 1262, 1090 cm^{-1}; ^1H NMR (DMSO-d_6) δ 2.42 (3H, s), 7.00 (2H, d, J = 8.5 Hz), 7.10 (2H, d, J = 8.5 Hz), 7.20 (2H, d, J = 8.5 Hz), 7.45 (2H, d, J = 8.5 Hz), 7.74 (1H, s), 12.77 (1H, broad s); ^{13}C NMR (DMSO-d_6) δ 14.0, 125.1, 128.6, 130.3,

130.6, 131.0, 131.5, 132.3, 135.4, 139.1, 140.5, 168.0; MS (ESI–) *m*/*z* 303 ([M - H]$^-$, 38). Anal. for $C_{16}H_{13}ClO_2S$: calcd C, 63.05; H, 4.30; found C, 63.16; H, 4.25.

(2*E*)-3-(4-Methoxyphenyl)-2-[4-(methylsulfonyl)phenyl]prop-2-enoic acid (30). Reaction time: 22 h; temperature: 140 °C; yield 21%; mp 234–235 °C (EtOAc); IR 3025, 2938, 1666, 1597, 1566, 1511, 1408, 1312, 1174, 1146 cm^{-1}; ^{1}H NMR (DMSO-d_6) δ 3.27 (3H, s), 3.71 (3H, s), 6.81 (2H, d, J = 9.0 Hz), 7.00 (2H, d, J = 9.0 Hz), 7.47 (2H, d, J = 8.5 Hz), 7.81 (1H, s), 7.95 (2H, d, J = 8.5 Hz), 12.78 (1H, broad s); ^{13}C NMR (DMSO-d_6) δ 43.5, 55.2, 114.1, 126.2, 127.2, 129.2, 130.7, 132.1, 139.8, 139.9, 142.4, 160.2, 167.8; MS (ESI+) *m*/*z* 333 ([M + H]$^+$); HRMS for $C_{17}H_{17}O_5S$ ([M + H]$^+$): calcd 333.0791; found 333.0791. Anal. for $C_{17}H_{16}O_5S$: calcd C, 61.43; H, 4.85; found C, 61.26; H, 4.91.

(2*E*)-3-(4-Hydroxyphenyl)-2-[4-(methylsulfonyl)phenyl]prop-2-enoic acid (31). Reaction time: 19 h; temperature: 120 °C; yield 54% (column chromatography); mp 213–215 °C (*n*-hexane/EtOAc); mp[25] 219–220 °C; IR 3346, 2927, 1661, 1602, 1581, 1512, 1429, 1383, 1310, 1140 cm^{-1}; ^{1}H NMR (DMSO-d_6) δ 3.27 (3H, s), 6.60 (2H, d, J = 8.5 Hz), 6.87 (2H, d, J = 8.5 Hz), 7.44 (2H, d, J = 8.3 Hz), 7.73 (1H, s), 7.93 (2H, d, J = 8.3 Hz), 9.95 (1H, broad s) 12.72 (1H, broad s); ^{13}C NMR (DMSO-d_6) δ 43.5, 115.4, 124.6, 127.2, 130.8, 132.3, 139.7, 140.3, 142.6, 158.9, 168.0 (1 signal missing); MS (ESI+) *m*/*z* 319 ([M + H]$^+$); HRMS for $C_{16}H_{15}O_5S$ ([M + H]$^+$): calcd 319.0635; found 319.0634. Anal. for $C_{16}H_{14}O_5S$ x 0.1 H_2O: calcd C, 60.03; H, 4.47; found C, 59.93; H, 4.12.

(2*E*)-3-(3-Bromophenyl)-2-[4-(methylsulfonyl)phenyl]prop-2-enoic acid (36). Reaction time: 24 h; temperature: 120 °C; yield 73 %; mp 219–221 °C (EtOAc); IR 2972, 1672, 1596, 1559, 1477, 1424, 1287, 1264, 1143, 1090 cm^{-1}; ^{1}H NMR (DMSO-d_6) δ 3.25 (3H, s), 7.03 (1H, d), 7.17−7.22 (2H, m), 7.44−7.45 (1H, m), 7.47 (2H, d, J = 8.5 Hz), 7.84 (1H, s), 7.94 (2H, d, J = 8.5 Hz), 13.1 (1H, broad s); ^{13}C NMR (DMSO-d_6) δ 43.6, 121.6, 127.2, 129.0, 130.5, 130.7, 131.8, 132.6, 133.5, 136.4, 138.6, 140.1, 141.4, 167.3; MS (ESI+) *m*/*z* 380 ([M+H]$^+$); HRMS for $C_{16}H_{14}BrO_4S$ ([M + H]$^+$): calcd 380.9791; found 380.9787. Anal. for $C_{16}H_{13}BrO_4S$: calcd C, 50.41; H, 3.44; found C, 50.22; H, 3.20.

Applying the procedure described in the Experimental protocols for the oxidation of the methylthio moiety into methylsulfonyl group the following acid was prepared:

(2*E*)-2,3-Bis[4-(methylsulfonyl)phenyl]prop-2-enoic acid (40). Yield 85 %; mp 266–268 °C (EtOAc); IR 2988, 2901, 1683, 1622, 1593, 1409, 1311, 1275, 1149, 1067 cm^{-1}; ^{1}H NMR (DMSO-

d_6) δ 3.19 (3H, s), 3.27 (3H, s), 7.30 (2H, d, J = 8.5 Hz), 7.48 (2H, d), 7.78 (2H, d, J = 8.5 Hz), 7.93−7.96 (3H, m), 13.20 (1H, broad s); ^{13}C NMR (DMSO-d_6) δ 43.1, 43.5, 126.9, 127.2, 130.66, 130.73, 134.7, 138.3, 139.0, 140.2, 140.7, 140.9, 167.3; MS (ESI+) m/z 381 ([M + H]$^+$); Anal. for $C_{17}H_{16}O_6S_2$: calcd C, 53.67; H, 4.24; found C, 53.96; H, 4.52.

Predicted binding pose of the compound 1 (blue) in the AKR1C1 active site

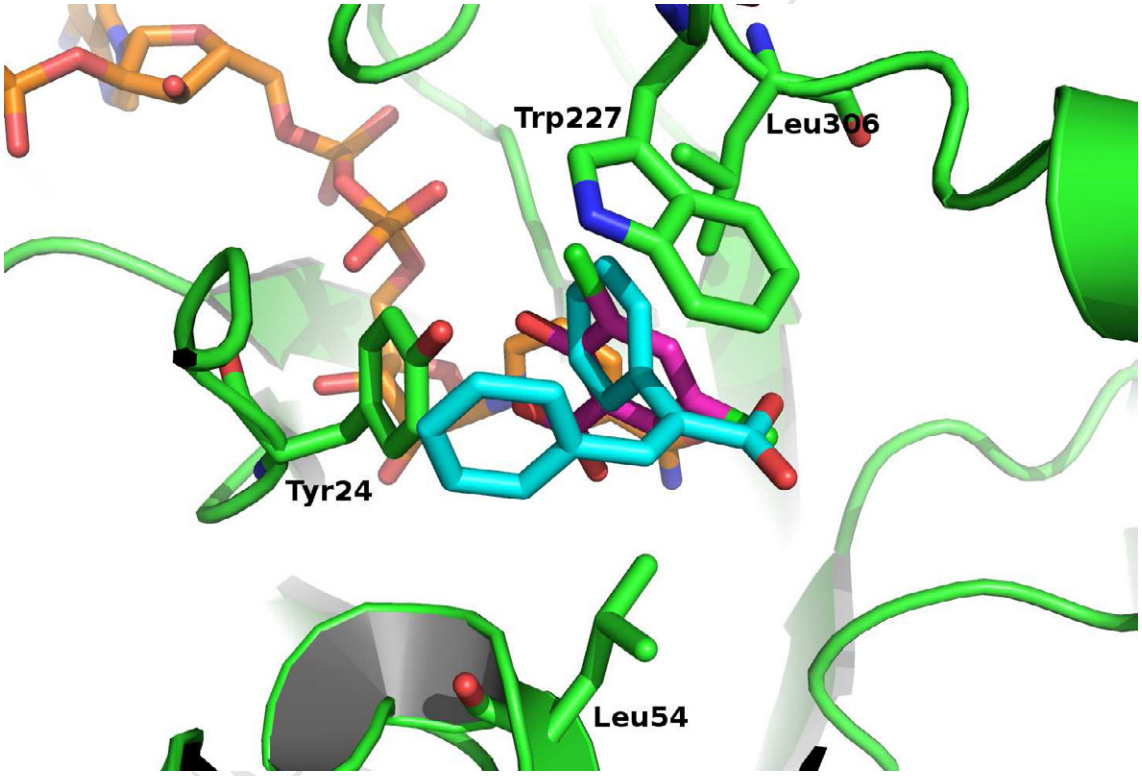

Fig. 1. Predicted binding pose of the compound **1** (blue) in the AKR1C1 active site (green). Only relevant amino acid residues are shown and labeled. Co-crystallized 3,5-dichlorosalicylic acid is shown as magenta sticks and cofactor as orange sticks.

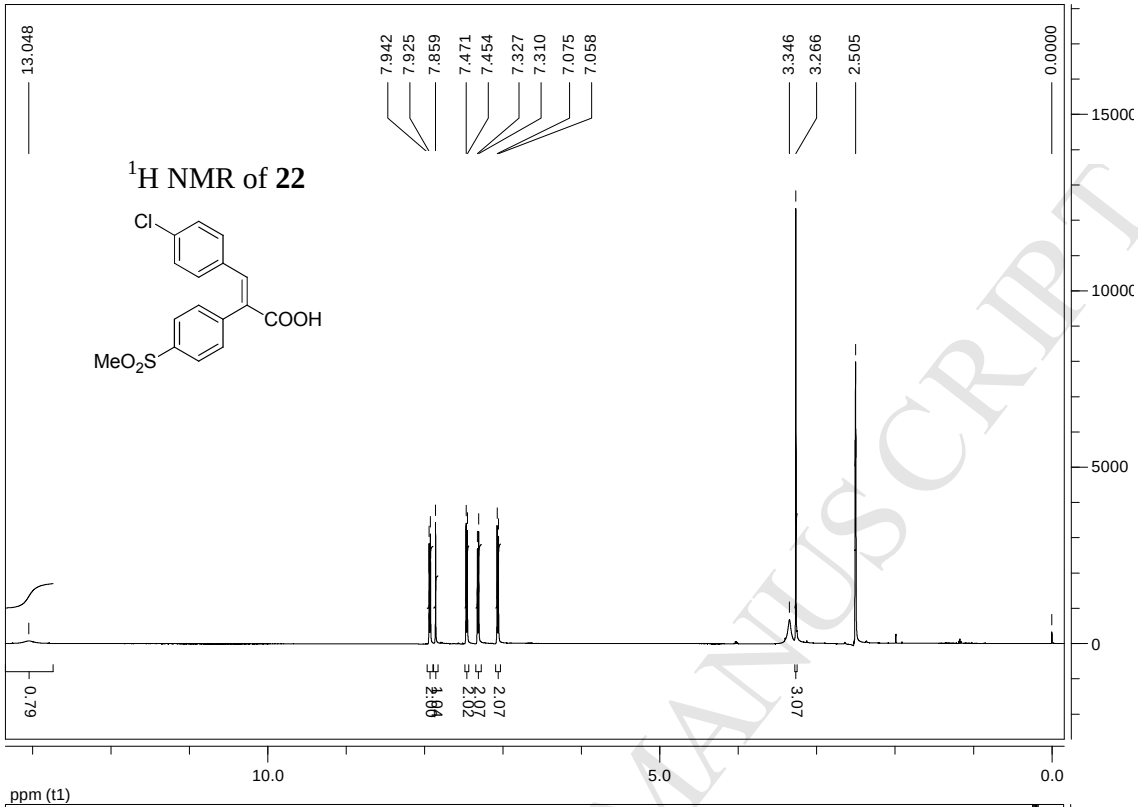

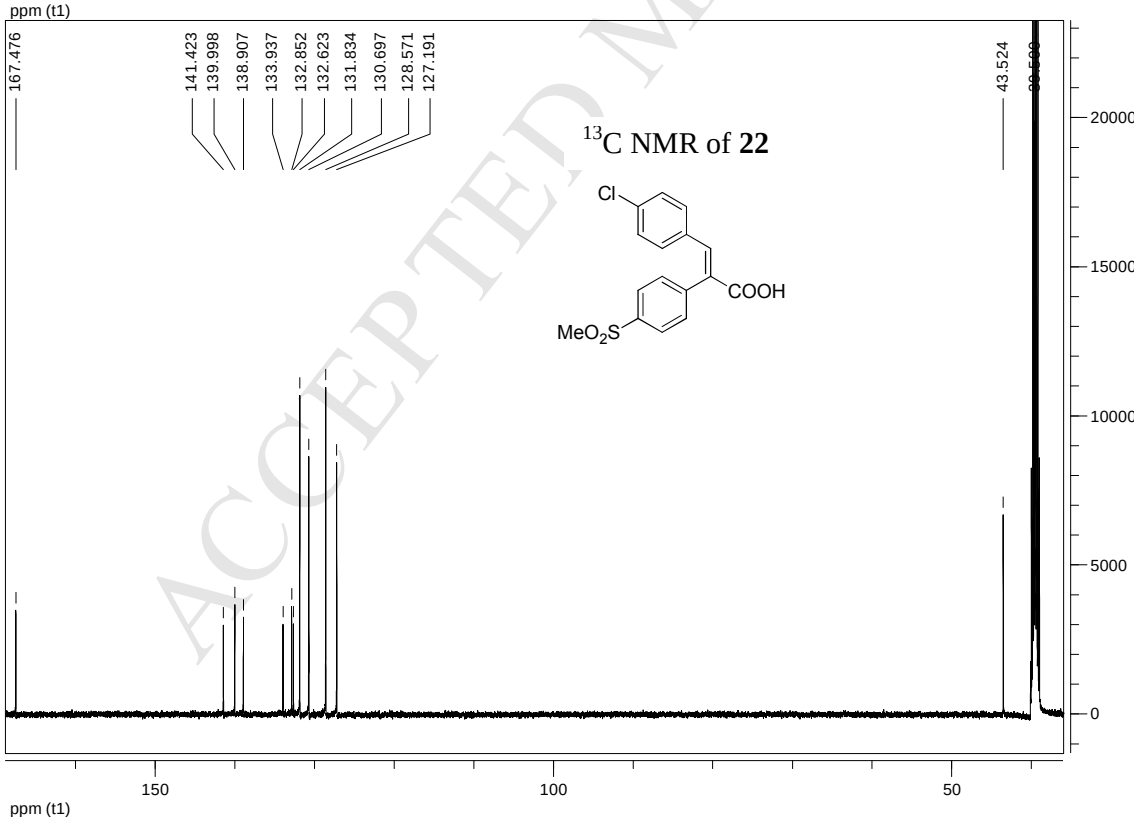

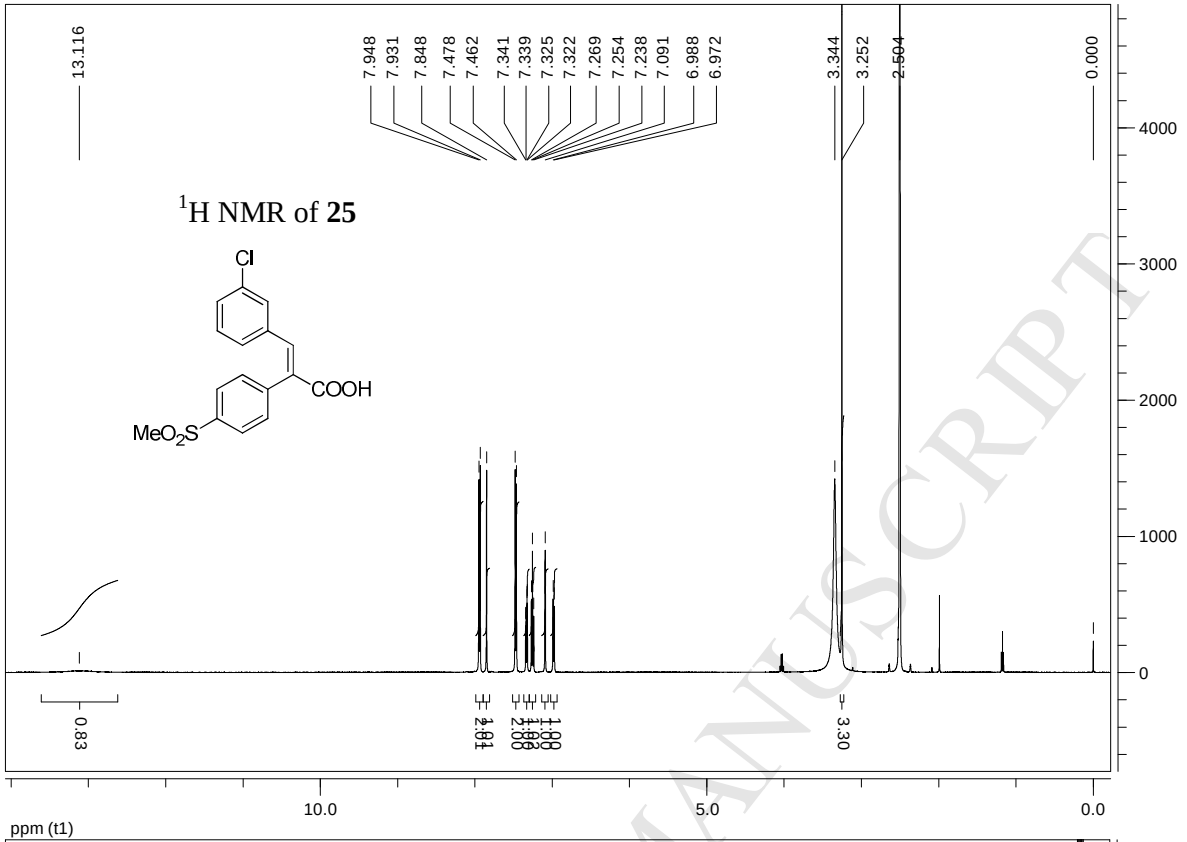

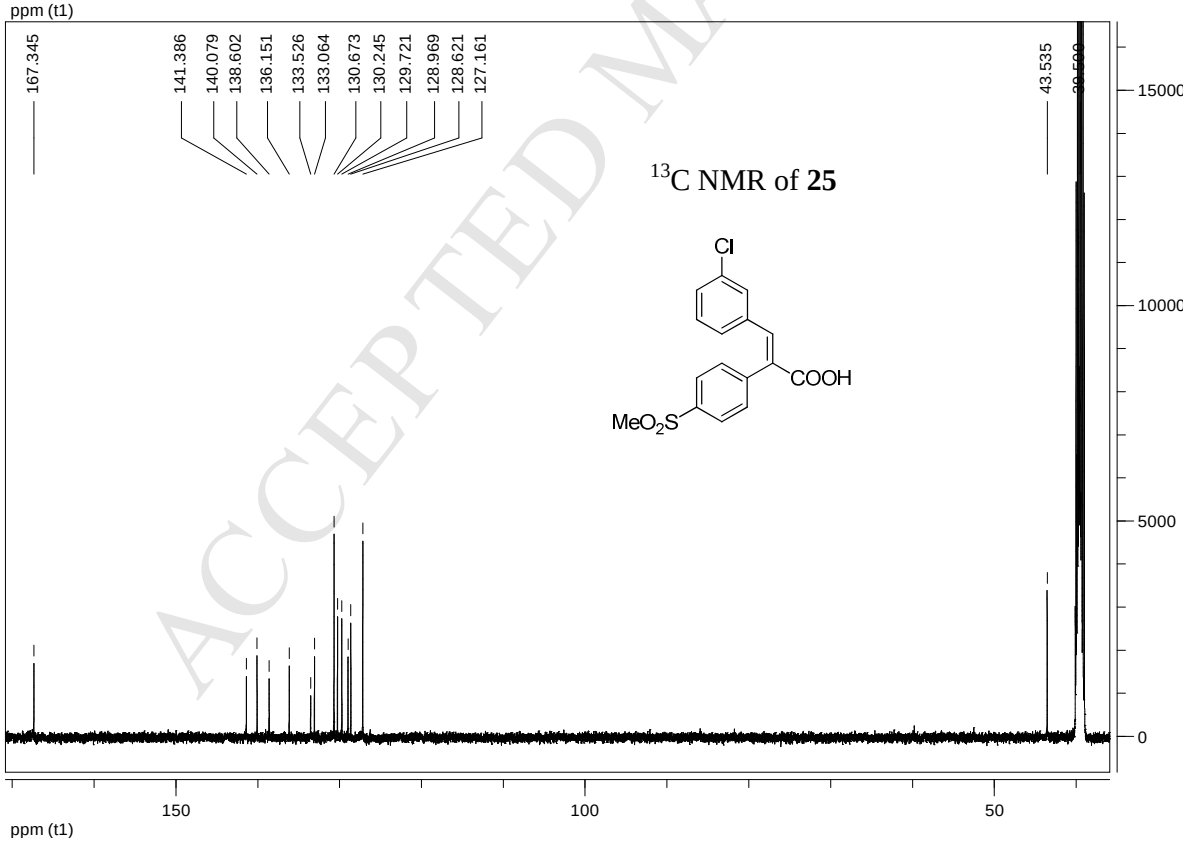

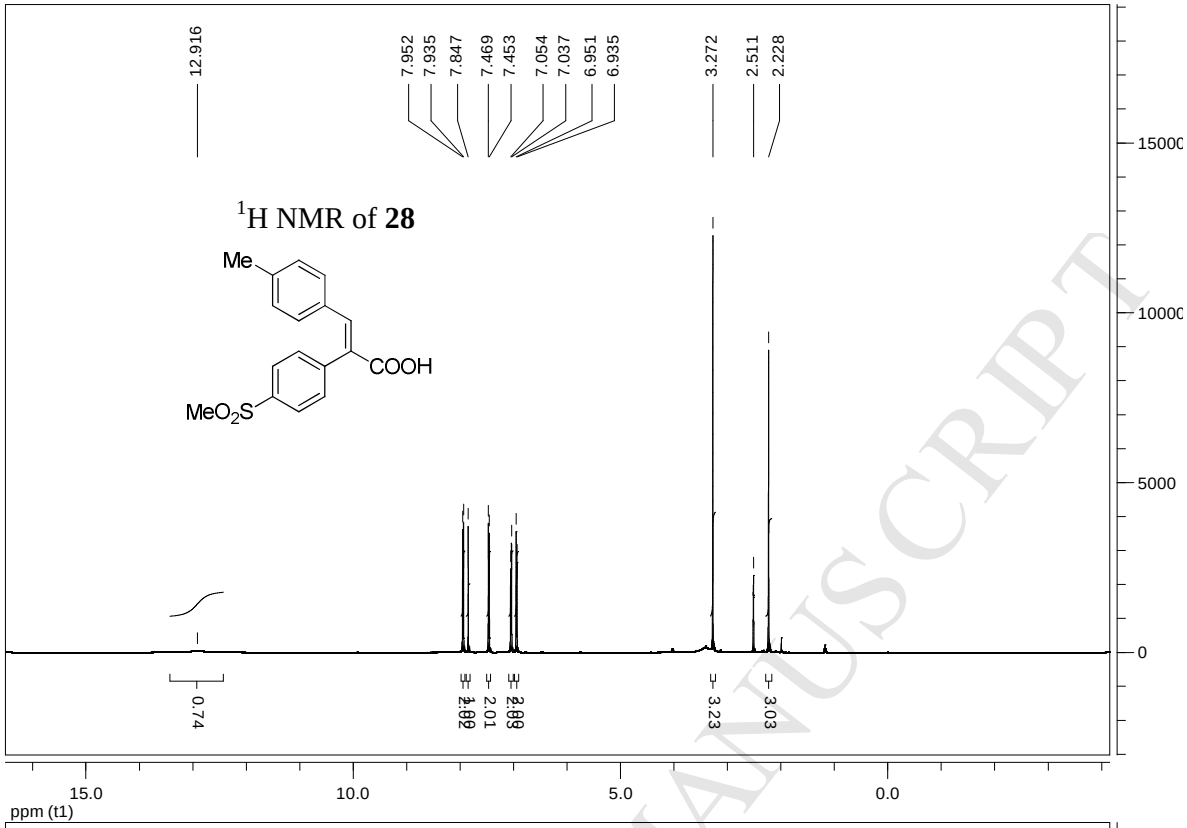

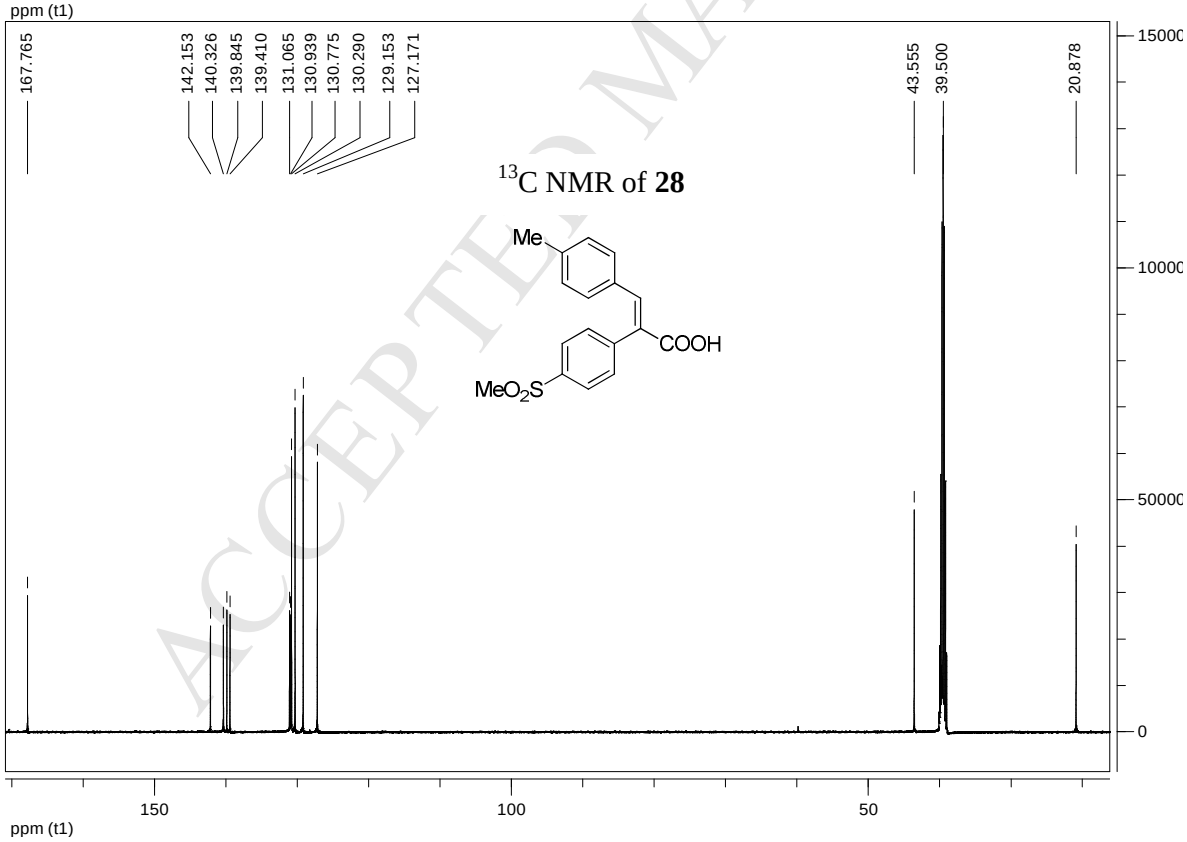

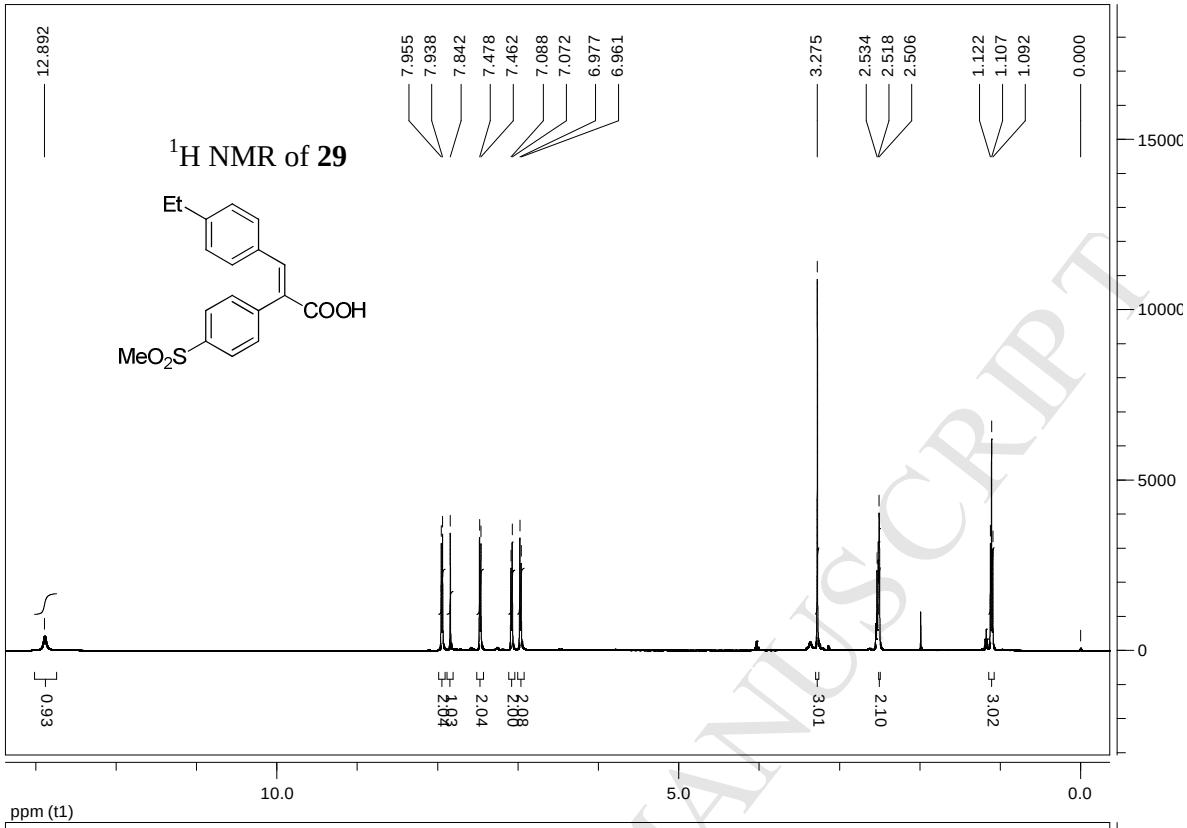

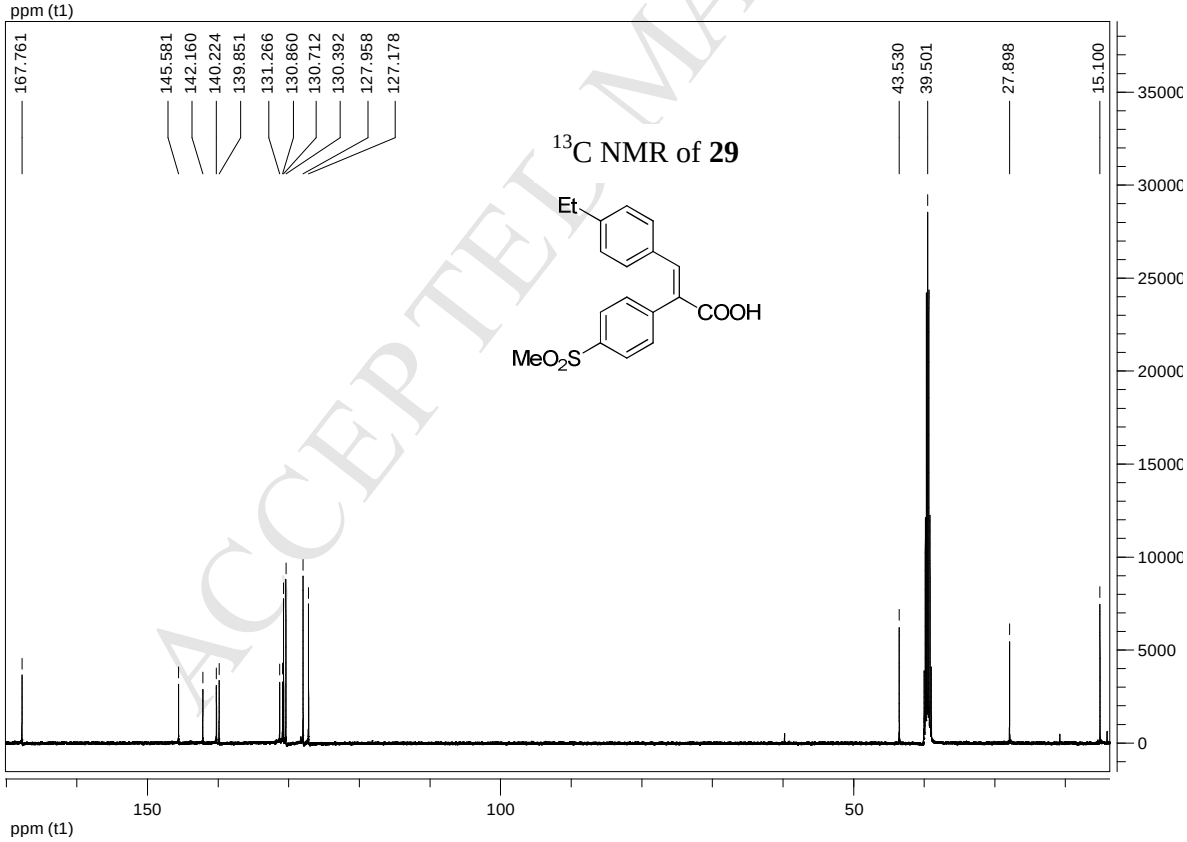

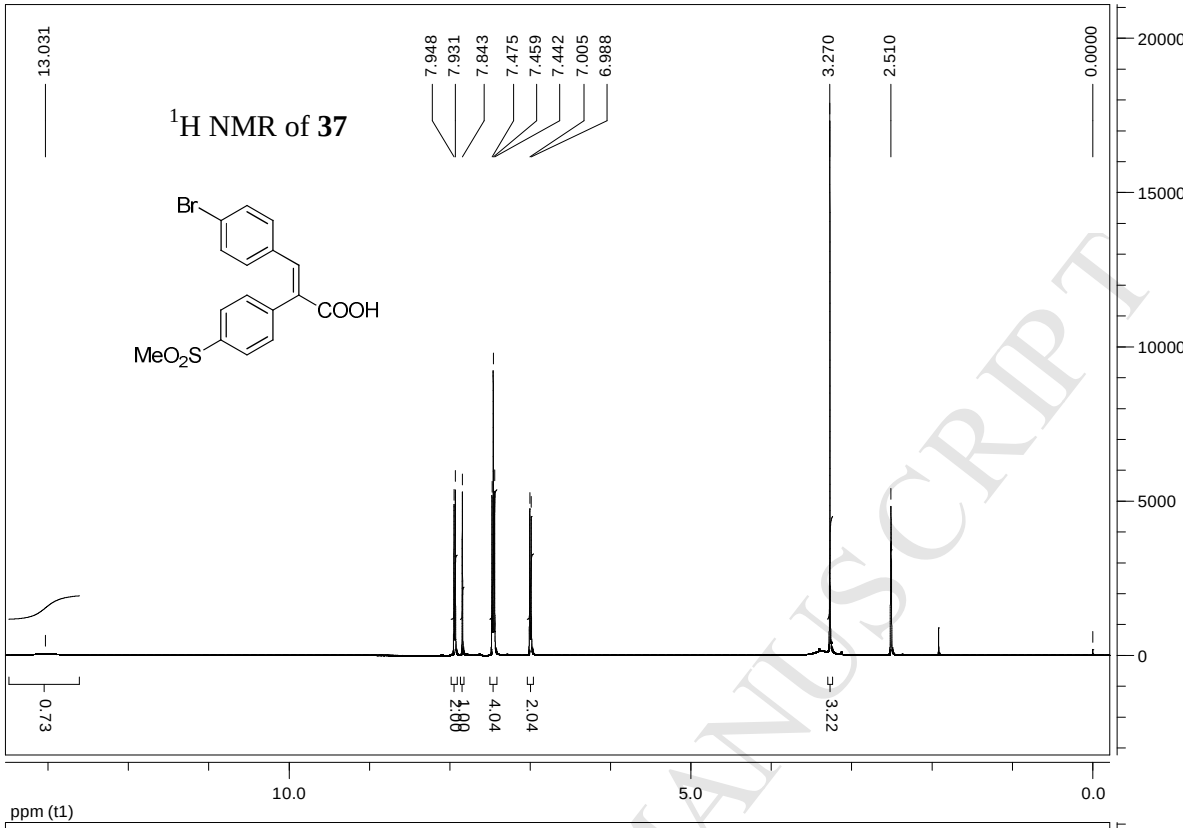

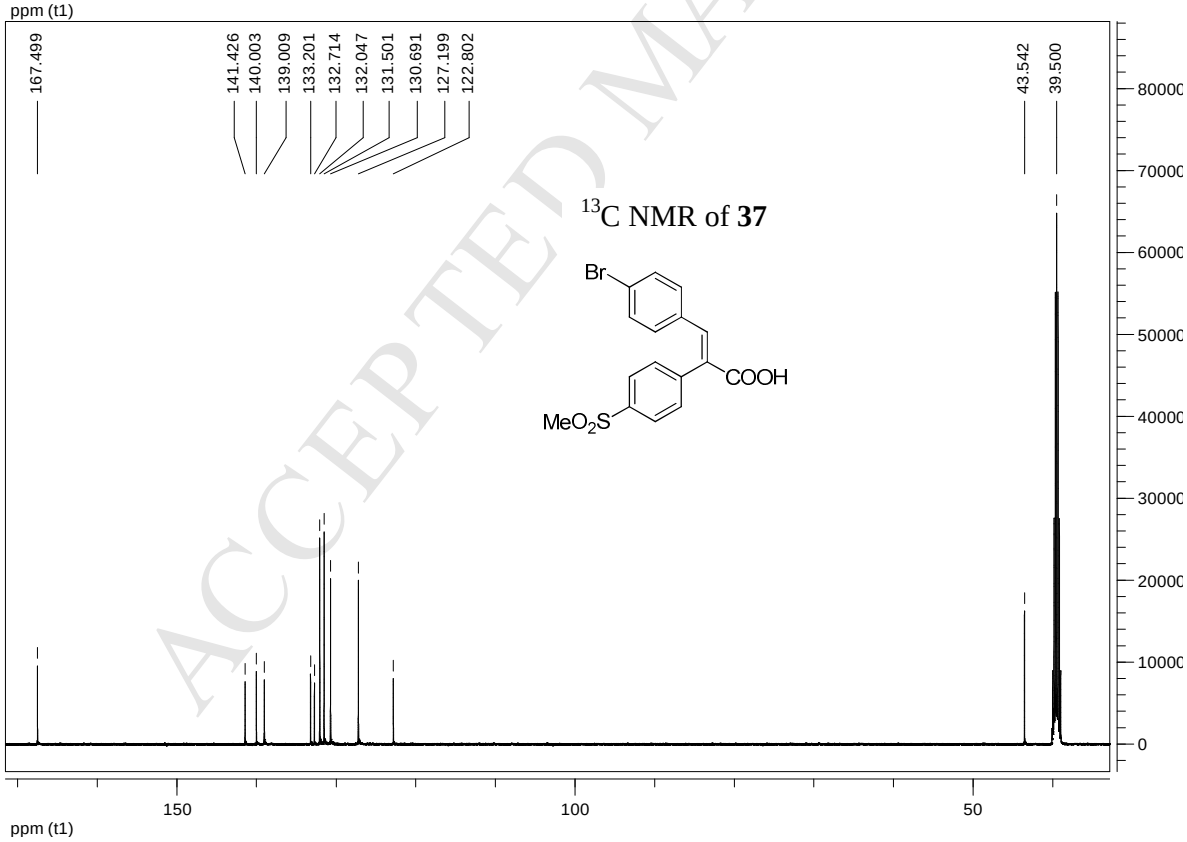

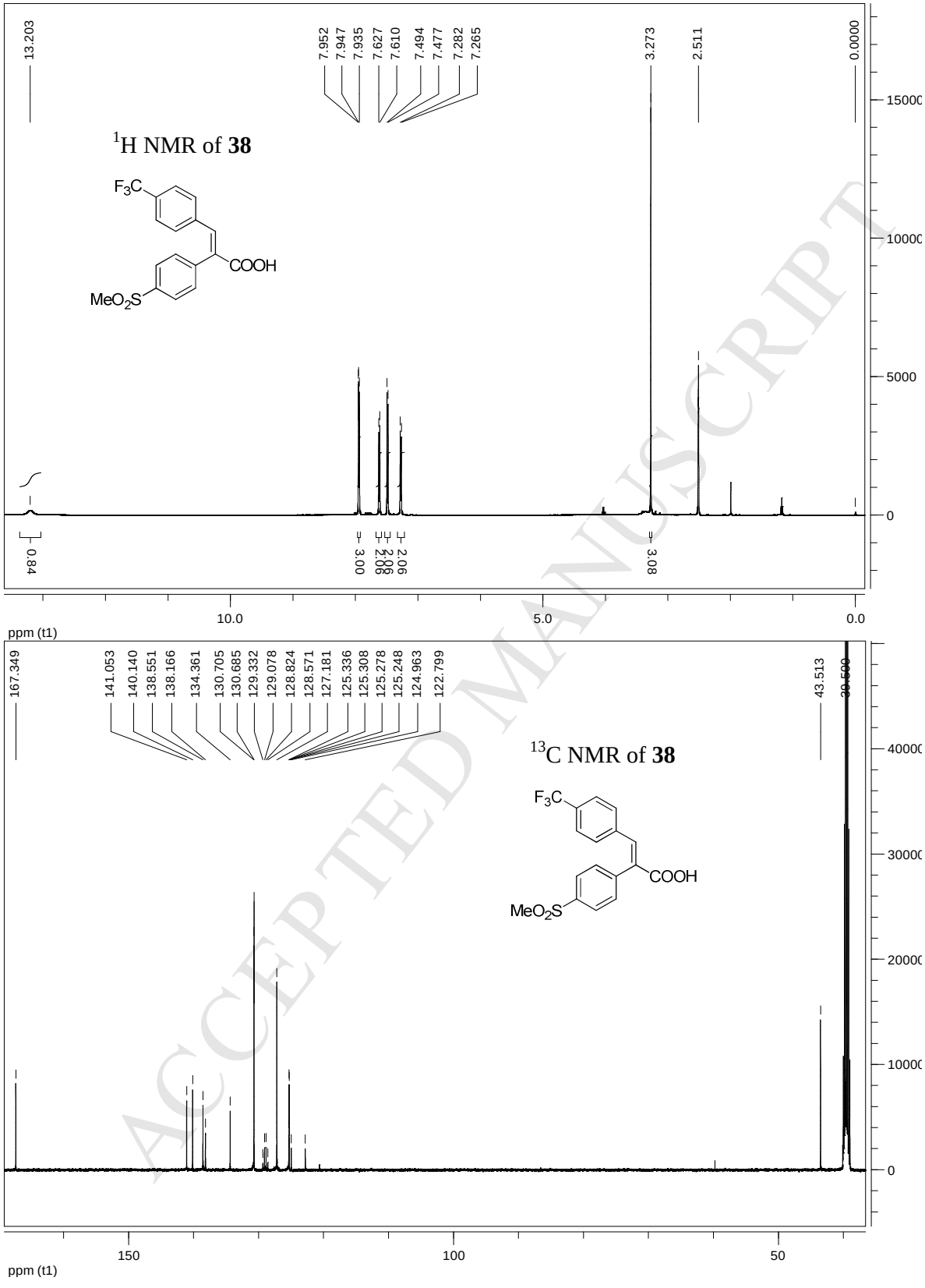

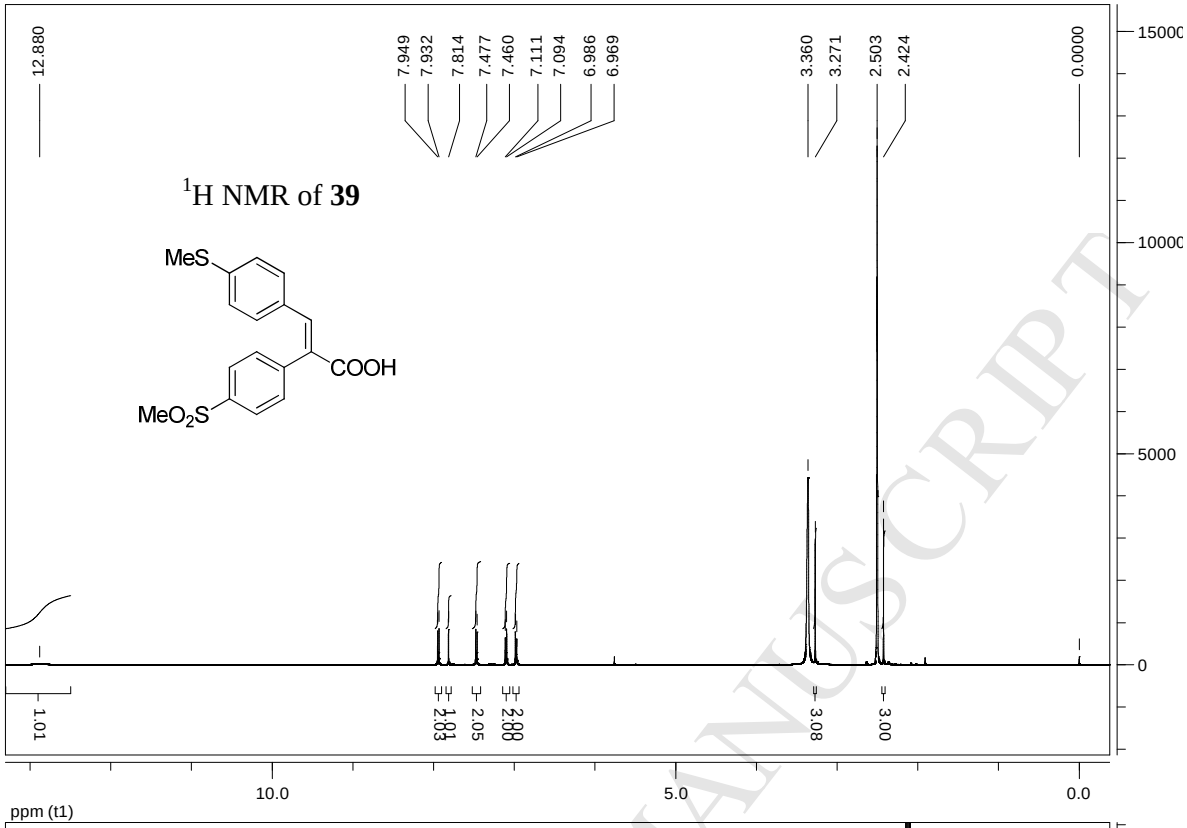

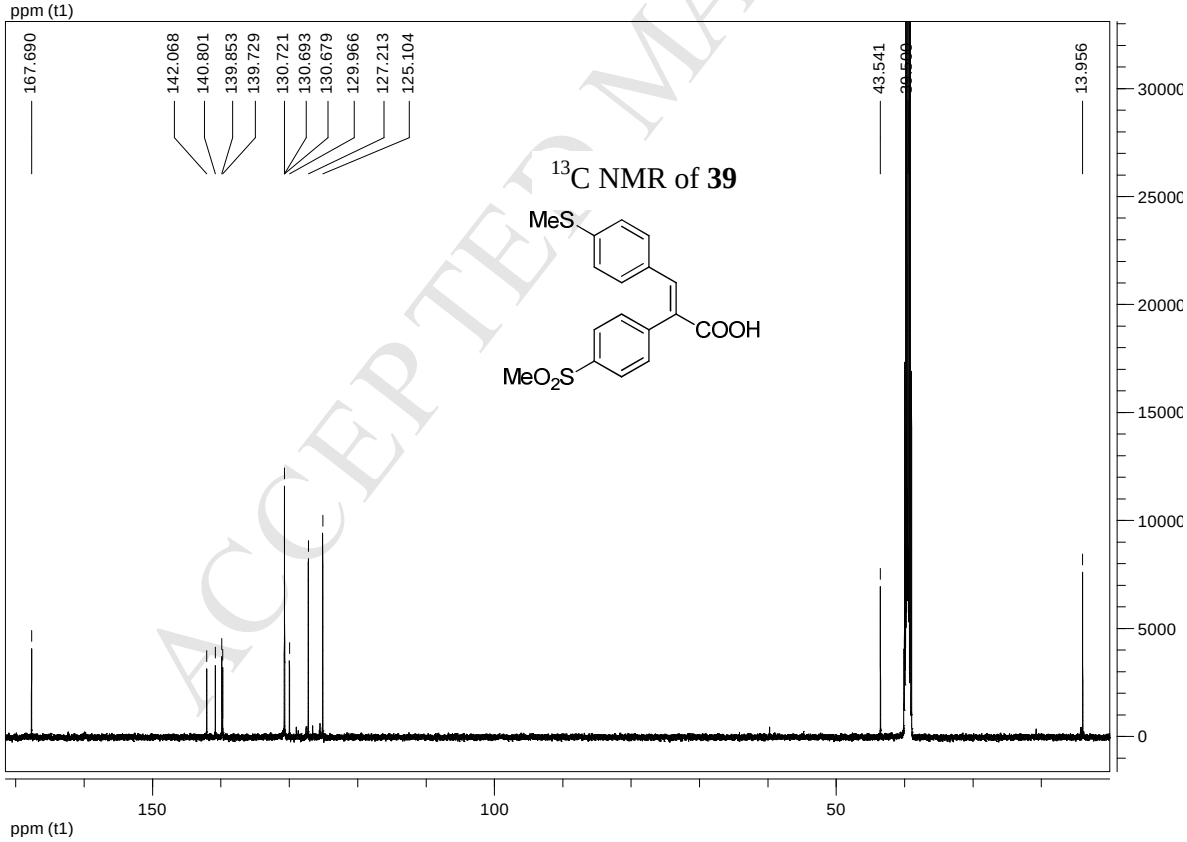

Purity of acids 1−42 determined by HPLC

A purity of each tested compound was checked by HPLC. The HPLC measurements were performed with an Agilent Technologies 1260 Infinity High Performance Autosampler and the data were processed by the ChemStation for LC 3D systems software. The absorbances at 250 nm, 260 nm and 210 nm were used for the UV detection. A SUPELCOSIL LC-18-DB HPLC column (5 µm particle size, 15 cm x 4.6 mm) was applied with an eluent $CH_3CN:H_2O$ = 60:40, with a flow rate of 1.0 mL/min or $CH_3CN:H_2O$ = 80:20 with a flow rate of 1.5 mL/min.

Acid **1**:

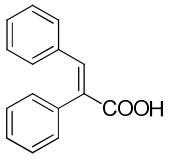

Injection volume: 20 µL; Eluent: $CH_3CN:H_2O$ = 60:40; Flow rate: 1.0 mL/min; Run time: 10 minutes;

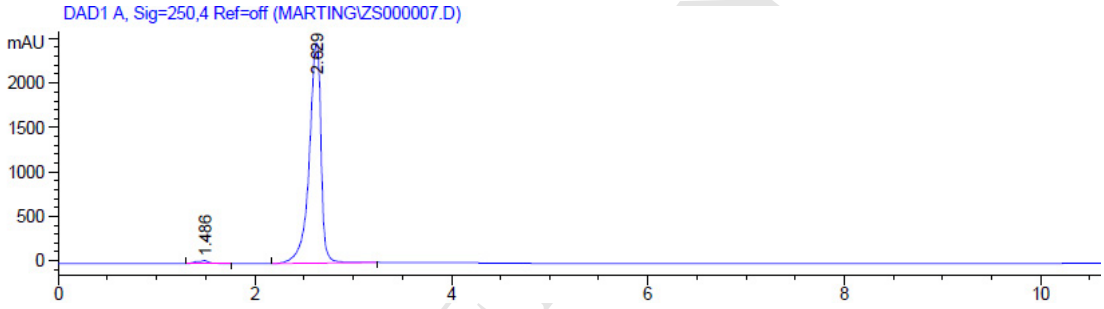

Signal 1: DAD1 A, Sig=250,4 Ref=off

Peak #	RetTime [min]	Type	Width [min]	Area [mAU*s]	Height [mAU]	Area %
1	1.486	BB	0.1252	290.95987	31.66351	1.3805
2	2.629	BB	0.1281	2.07860e4	2473.24243	98.6195
Totals :				2.10769e4	2504.90594	

Acid **2**:

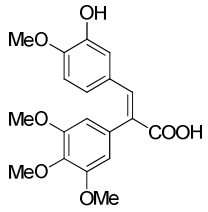

Injection volume: 20 μL; Eluent: $CH_3CN:H_2O$ = 60:40; Flow rate: 1.0 mL/min; Run time: 10 minutes;

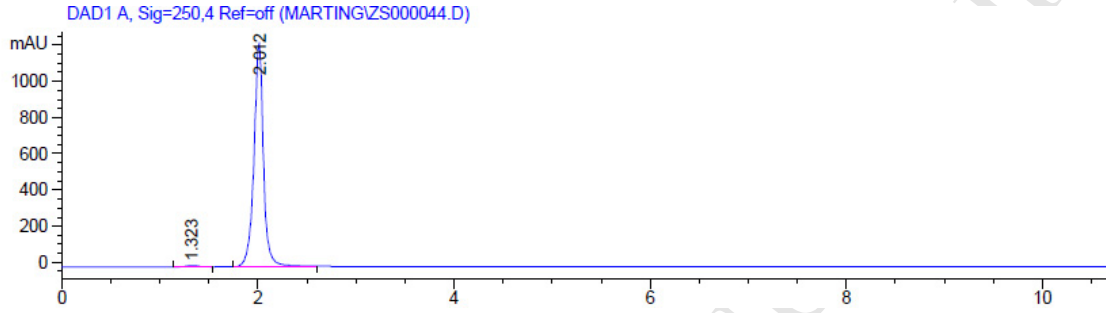

Signal 1: DAD1 A, Sig=250,4 Ref=off

Peak #	RetTime [min]	Type	Width [min]	Area [mAU*s]	Height [mAU]	Area %
1	1.323	BV	0.1241	62.92740	6.91976	0.7444
2	2.012	VB	0.1014	8390.16211	1233.55859	99.2556
Totals :				8453.08951	1240.47835	

Acid **3**: 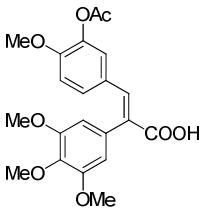

Injection volume: 20 μL; Eluent: $CH_3CN:H_2O$ = 60:40; Flow rate: 1.0 mL/min; Run time: 10 minutes;

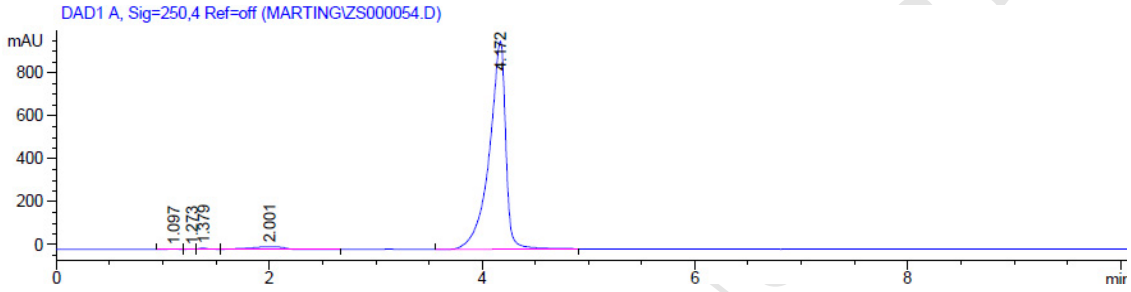

Signal 1: DAD1 A, Sig=250,4 Ref=off

Peak #	RetTime [min]	Type	Width [min]	Area [mAU*s]	Height [mAU]	Area %
1	1.097	BV	0.1130	10.49679	1.40698	0.0983
2	1.273	VV	0.0637	10.86171	2.54747	0.1017
3	1.379	VV	0.0807	36.87602	6.64705	0.3454
4	2.001	VB	0.2887	264.13330	11.46931	2.4743
5	4.172	BB	0.1550	1.03529e4	966.44574	96.9802
Totals :				1.06752e4	988.51655	

Acid **4**:

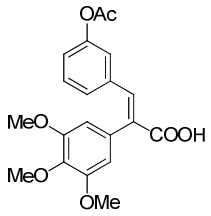

Injection volume: 20 μL; Eluent: $CH_3CN:H_2O$ = 60:40; Flow rate: 1.0 mL/min; Run time: 10 minutes;

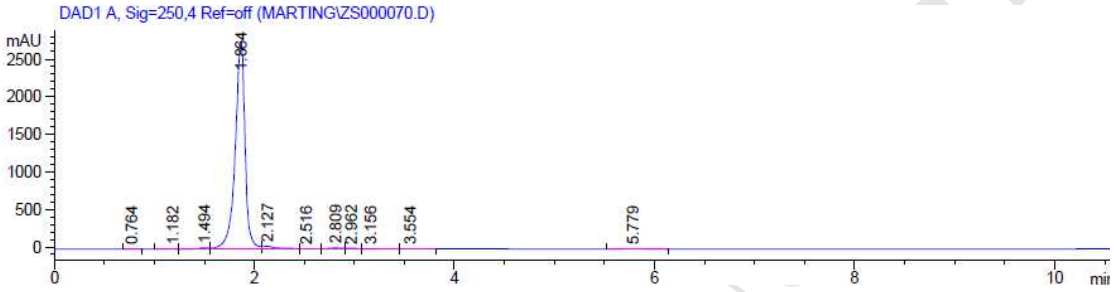

Signal 1: DAD1 A, Sig=250,4 Ref=off

Peak #	RetTime [min]	Type	Width [min]	Area [mAU*s]	Height [mAU]	Area %
1	0.764	BB	0.0635	8.79783	2.07160	0.0443
2	1.182	BV	0.0655	18.47845	4.18784	0.0930
3	1.494	VV	0.0962	124.85480	18.63762	0.6282
4	1.864	VV	0.1039	1.89198e4	2764.31226	95.1906
5	2.127	VV	0.1407	377.15109	35.86217	1.8975
6	2.516	VV	0.1625	80.95168	7.02188	0.4073
7	2.809	VV	0.1391	139.42810	14.64727	0.7015
8	2.962	VV	0.1200	66.65894	8.10102	0.3354
9	3.156	VB	0.1726	72.91757	5.88503	0.3669
10	3.554	BB	0.1965	24.69491	1.73070	0.1242
11	5.779	BB	0.2037	41.97354	3.18591	0.2112
Totals :				1.98757e4	2865.64330	

Acid **5**: 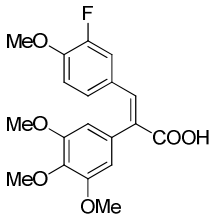

Injection volume: 20 μL; Eluent: $CH_3CN:H_2O$ = 60:40; Flow rate: 1 mL/min; Run time: 10 minutes;

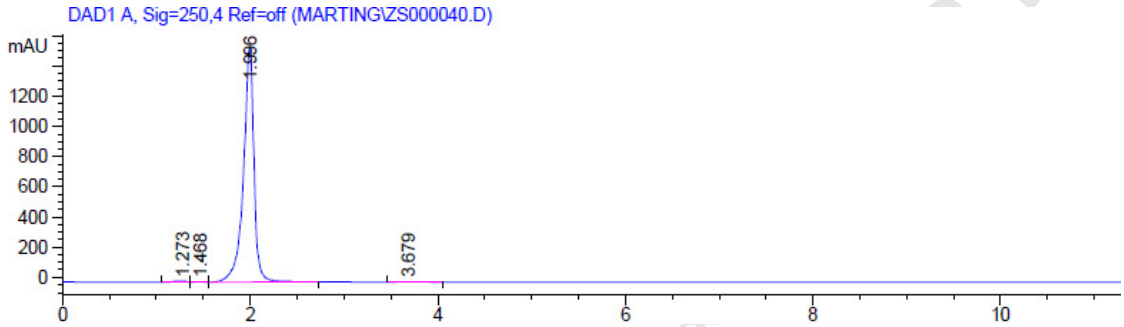

Signal 1: DAD1 A, Sig=250,4 Ref=off

Peak #	RetTime [min]	Type	Width [min]	Area [mAU*s]	Height [mAU]	Area %
1	1.273	VV	0.1248	69.99376	7.64469	0.5653
2	1.468	VV	0.1116	13.65792	1.70167	0.1103
3	1.996	VB	0.1157	1.22561e4	1559.98694	98.9928
4	3.679	BB	0.2122	41.04433	2.88096	0.3315
Totals :				1.23808e4	1572.21425	

Acid **6**:

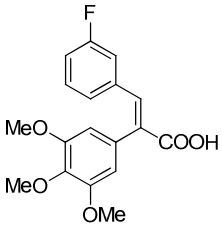

Injection volume: 20 μL; Eluent: $CH_3CN:H_2O$ = 60:40; Flow rate: 1.0 mL/min; Run time: 10 minutes;

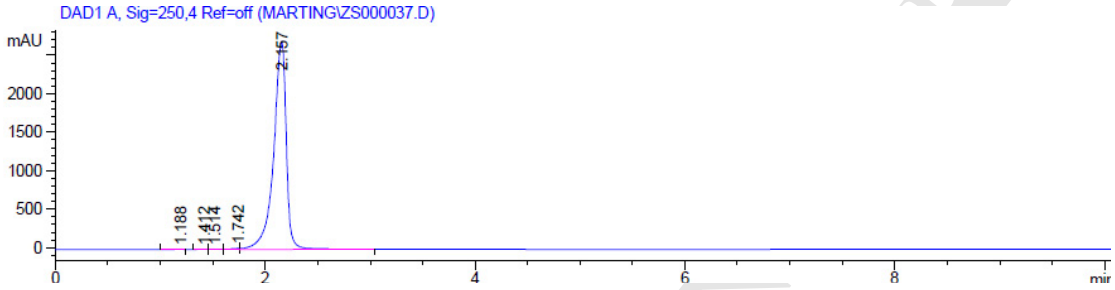

Signal 1: DAD1 A, Sig=250,4 Ref=off

Peak #	RetTime [min]	Type	Width [min]	Area [mAU*s]	Height [mAU]	Area %
1	1.188	BV	0.0608	30.99111	7.40456	0.1357
2	1.412	VV	0.0784	31.32307	5.85782	0.1371
3	1.514	VV	0.1096	40.66700	5.41776	0.1780
4	1.742	VV	0.0875	83.60449	13.64804	0.3660
5	2.157	VB	0.1255	2.26543e4	2711.30420	99.1831
Totals :				2.28409e4	2743.63238	

Acid **7**:

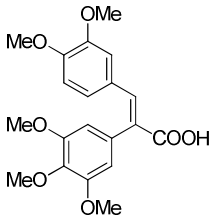

Injection volume: 20 μL; Eluent: $CH_3CN:H_2O$ = 60:40; Flow rate: 1.0 mL/min; Run time: 10 minutes;

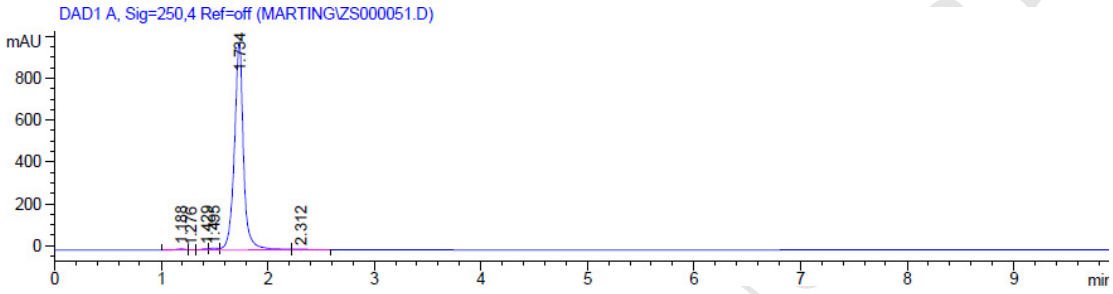

Signal 1: DAD1 A, Sig=250,4 Ref=off

Peak #	RetTime [min]	Type	Width [min]	Area [mAU*s]	Height [mAU]	Area %
1	1.188	BV	0.0890	31.48886	5.48057	0.5178
2	1.276	VV	0.0519	7.28952	2.13008	0.1199
3	1.429	VV	0.0577	27.80760	7.09872	0.4573
4	1.495	VV	0.0790	43.63830	8.07783	0.7176
5	1.734	VV	0.0878	5937.51514	992.97858	97.6328
6	2.312	VB	0.1412	33.73643	3.35698	0.5547
Totals :				6081.47584	1019.12276	

Acid **8**:

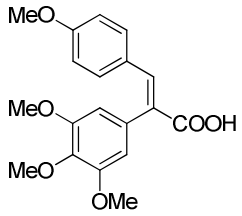

Injection volume: 20 μL; Eluent: $CH_3CN:H_2O$ = 60:40; Flow rate: 1.0 mL/min; Run time: 10 minutes;

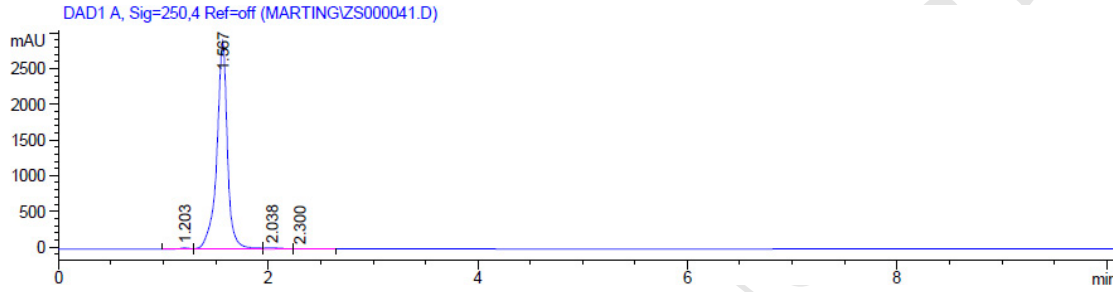

Signal 1: DAD1 A, Sig=250,4 Ref=off

Peak #	RetTime [min]	Type	Width [min]	Area [mAU*s]	Height [mAU]	Area %
1	1.203	BV	0.0807	101.15851	17.70278	0.4826
2	1.567	VV	0.1046	2.06139e4	2910.02417	98.3388
3	2.038	VV	0.1413	191.24721	19.02917	0.9123
4	2.300	VB	0.1791	55.81504	4.25445	0.2663
Totals :				2.09622e4	2951.01057	

Acid **9**:

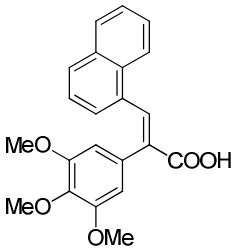

Injection volume: 20 μL; Eluent: $CH_3CN:H_2O$ = 60:40; Flow rate: 1.0 mL/min; Run time: 10 minutes;

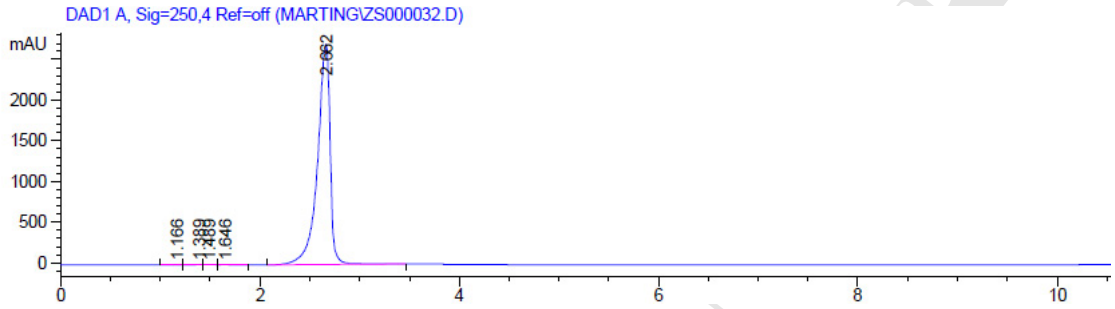

Signal 1: DAD1 A, Sig=250,4 Ref=off

Peak #	RetTime [min]	Type	Width [min]	Area [mAU*s]	Height [mAU]	Area %
1	1.166	BV	0.0685	8.79301	1.81711	0.0364
2	1.389	VV	0.0733	19.89313	3.91278	0.0825
3	1.489	VV	0.0977	38.32263	5.75447	0.1589
4	1.646	VB	0.1241	26.56158	3.03633	0.1101
5	2.662	BB	0.1335	2.40306e4	2707.99438	99.6121
Totals :				2.41242e4	2722.51507	

Acid **10**:

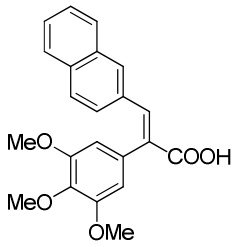

Injection volume: 20 μL; Eluent: $CH_3CN:H_2O$ = 60:40; Flow rate: 1.0 mL/min; Run time: 10 minutes;

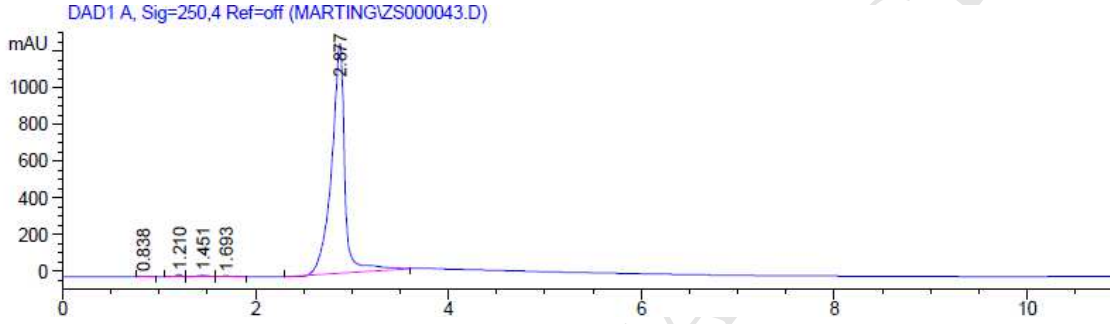

Signal 1: DAD1 A, Sig=250,4 Ref=off

Peak #	RetTime [min]	Type	Width [min]	Area [mAU*s]	Height [mAU]	Area %
1	0.838	BB	0.0740	9.37613	2.02443	0.0775
2	1.210	VV	0.0609	48.47398	12.06451	0.4007
3	1.451	VV	0.1365	60.00398	7.10669	0.4961
4	1.693	VB	0.1006	31.69940	4.47796	0.2621
5	2.877	BB	0.1375	1.19465e4	1249.67114	98.7636
Totals :				1.20961e4	1275.34474	

Acid **11**:

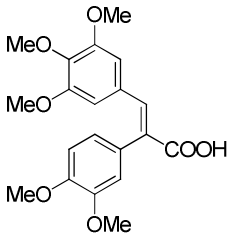

Injection volume: 20 μL; Eluent: $CH_3CN:H_2O$ = 60:40; Flow rate: 1.0 mL/min; Run time: 10 minutes;

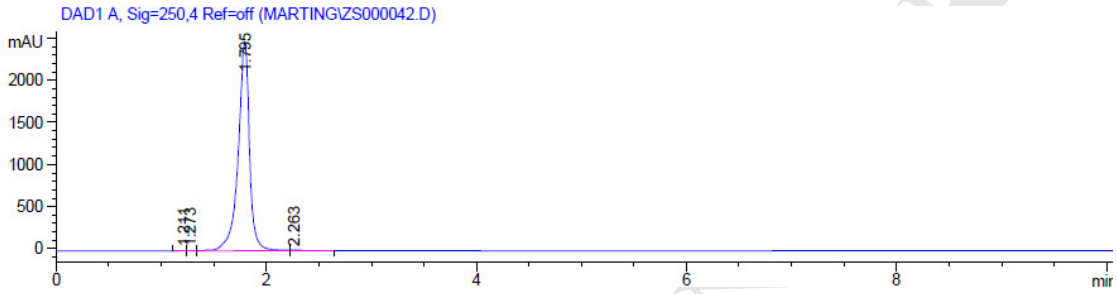

Signal 1: DAD1 A, Sig=250,4 Ref=off

Peak #	RetTime [min]	Type	Width [min]	Area [mAU*s]	Height [mAU]	Area %
1	1.211	BV	0.0621	24.33888	5.90599	0.1285
2	1.273	VV	0.0745	28.26418	5.45154	0.1492
3	1.795	VV	0.1125	1.88134e4	2479.70874	99.2959
4	2.263	VB	0.1478	80.79733	7.37801	0.4264
Totals :				1.89468e4	2498.44428	

Acid **12**:

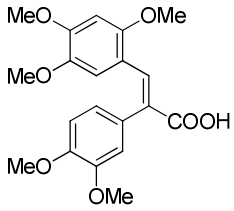

Injection volume: 20 μL; Eluent: $CH_3CN:H_2O$ = 60:40; Flow rate: 1.0 mL/min; Run time: 10 minutes;

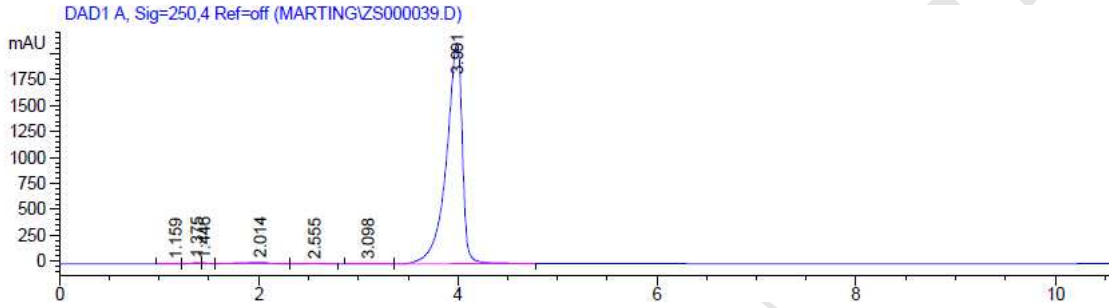

Signal 1: DAD1 A, Sig=250,4 Ref=off

Peak #	RetTime [min]	Type	Width [min]	Area [mAU*s]	Height [mAU]	Area %
1	1.159	BV	0.1158	11.65776	1.33606	0.0482
2	1.375	VV	0.0824	69.46424	12.21263	0.2870
3	1.446	VV	0.0655	37.49666	8.48671	0.1549
4	2.014	VV	0.2679	305.57709	15.37611	1.2626
5	2.555	VB	0.1607	31.46740	2.80905	0.1300
6	3.098	BV	0.1912	15.85656	1.27403	0.0655
7	3.991	VB	0.1664	2.37298e4	2123.12549	98.0517
Totals :				2.42013e4	2164.62008	

Acid **13**:

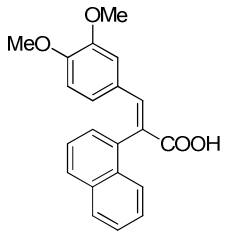

Injection volume: 20 μL; Eluent: $CH_3CN:H_2O$ = 60:40; Flow rate: 1.0 mL/min; Run time: 10 minutes;

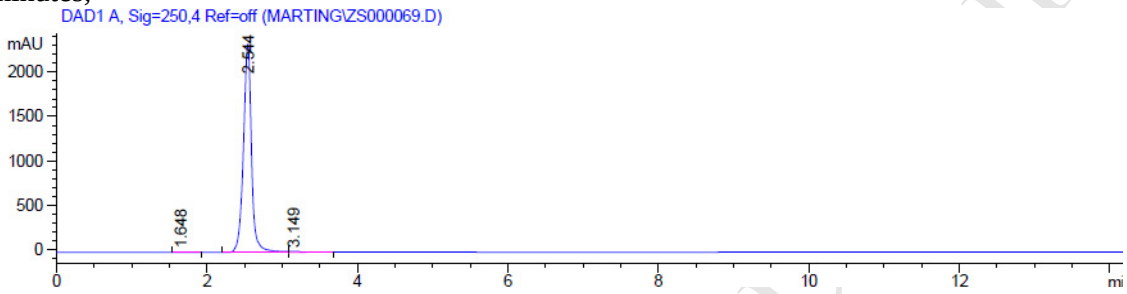

Signal 1: DAD1 A, Sig=250,4 Ref=off

Peak #	RetTime [min]	Type	Width [min]	Area [mAU*s]	Height [mAU]	Area %
1	1.648	VB	0.1231	12.00586	1.35792	0.0668
2	2.544	BV	0.1147	1.78365e4	2345.78271	99.2516
3	3.149	VB	0.2146	122.48573	7.65635	0.6816
Totals :				1.79710e4	2354.79699	

Acid **14**:

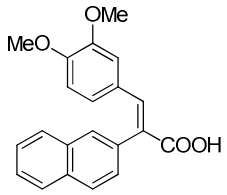

Injection volume: 20 μL; Eluent: $CH_3CN:H_2O$ = 60:40; Flow rate: 1.0 mL/min; Run time: 10 minutes;

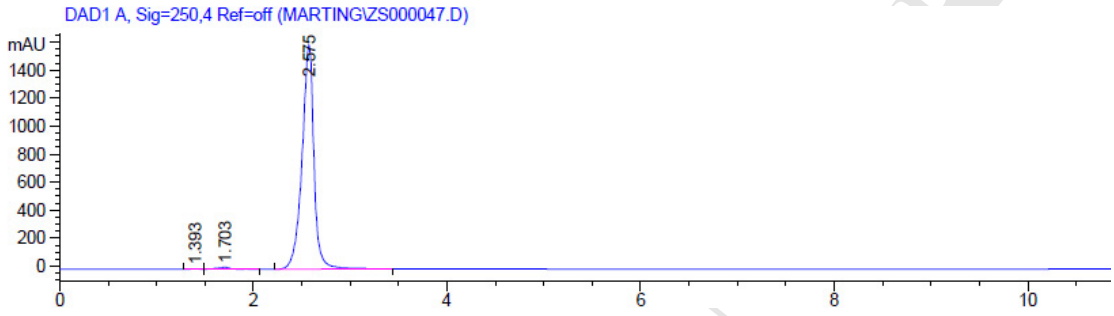

Signal 1: DAD1 A, Sig=250,4 Ref=off

Peak #	RetTime [min]	Type	Width [min]	Area [mAU*s]	Height [mAU]	Area %
1	1.393	BV	0.0858	19.72658	3.29923	0.1418
2	1.703	VB	0.1493	133.19397	13.02580	0.9577
3	2.575	BB	0.1283	1.37548e4	1600.66443	98.9005
Totals :				1.39077e4	1616.98946	

Acid **15**:

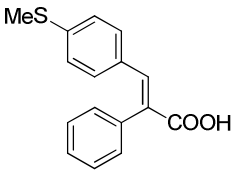

Injection volume: 20 μL; Eluent: $CH_3CN:H_2O$ = 60:40; Flow rate: 1.0 mL/min; Run time: 10 minutes;

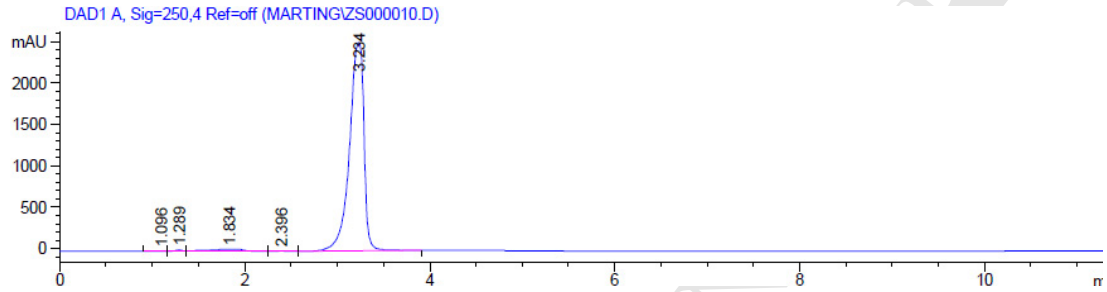

Signal 1: DAD1 A, Sig=250,4 Ref=off

Peak #	RetTime [min]	Type	Width [min]	Area [mAU*s]	Height [mAU]	Area %
1	1.096	BV	0.1389	17.90719	1.88448	0.0637
2	1.289	VV	0.0798	80.60739	15.22711	0.2868
3	1.834	VV	0.3134	610.63336	24.11922	2.1729
4	2.396	VV	0.1208	15.37680	1.97566	0.0547
5	3.234	VB	0.1670	2.73781e4	2515.29565	97.4219
Totals :				2.81026e4	2558.50213	

Acid **16**:

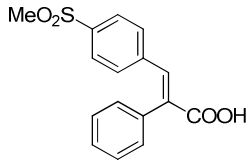

Injection volume: 20 μL; Eluent: $CH_3CN:H_2O$ = 60:40; Flow rate: 1.0 mL/min; Run time: 10 minutes;

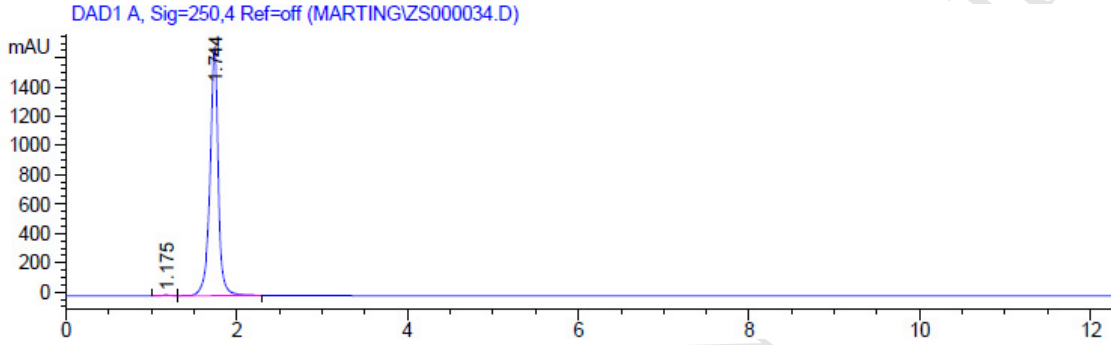

Signal 1: DAD1 A, Sig=250,4 Ref=off

Peak #	RetTime [min]	Type	Width [min]	Area [mAU*s]	Height [mAU]	Area %
1	1.175	BV	0.0812	33.42977	6.17320	0.2894
2	1.744	VB	0.0990	1.15177e4	1700.10254	99.7106
Totals :				1.15511e4	1706.27574	

Acid **17**:

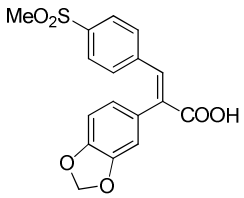

Injection volume: 20 μL; Eluent: $CH_3CN:H_2O$ = 60:40; Flow rate: 1.0 mL/min; Run time: 10 minutes;

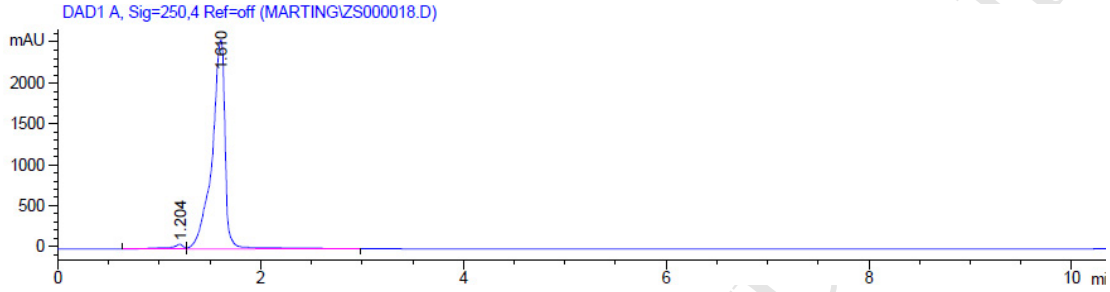

Signal 1: DAD1 A, Sig=250,4 Ref=off

Peak #	RetTime [min]	Type	Width [min]	Area [mAU*s]	Height [mAU]	Area %
1	1.204	BV	0.1260	528.86438	56.09927	2.2356
2	1.610	VB	0.1338	2.31276e4	2551.34180	97.7644
Totals :				2.36565e4	2607.44106	

Acid **18**: 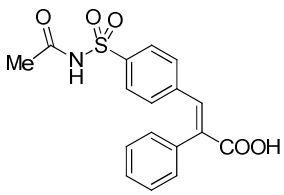

Injection volume: 20 μL; Eluent: $CH_3CN:H_2O$ = 80:20; Flow rate: 1.5 mL/min; Run time: 10 minutes;

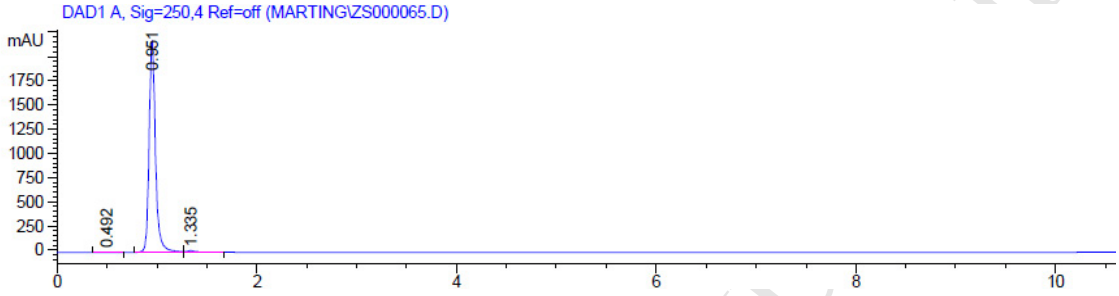

Signal 1: DAD1 A, Sig=250,4 Ref=off

Peak #	RetTime [min]	Type	Width [min]	Area [mAU*s]	Height [mAU]	Area %
1	0.492	BB	0.1014	11.20597	1.73281	0.1124
2	0.951	VV	0.0682	9822.73438	2195.45728	98.5357
3	1.335	VB	0.1074	134.76776	17.20043	1.3519
Totals :				9968.70810	2214.39052	

Acid **19**:

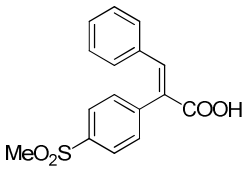

Injection volume: 20 µL; Eluent: $CH_3CN:H_2O$ = 60:40; Flow rate: 1.0 mL/min; Run time: 10 minutes;

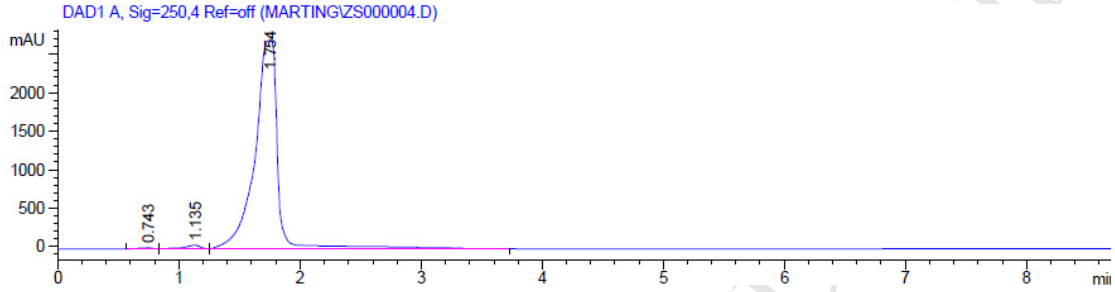

Signal 1: DAD1 A, Sig=250,4 Ref=off

Peak #	RetTime [min]	Type	Width [min]	Area [mAU*s]	Height [mAU]	Area %
1	0.743	BV	0.1026	130.89302	17.23842	0.3577
2	1.135	VV	0.1300	482.35974	50.24570	1.3181
3	1.754	VB	0.1968	3.59817e4	2711.53174	98.3242
Totals :				3.65950e4	2779.01586	

Acid **20**:

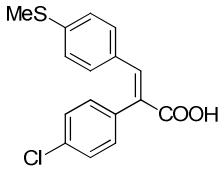

Injection volume: 20 μL; Eluent: $CH_3CN:H_2O$ = 60:40; Flow rate: 1.0 mL/min; Run time: 10 minutes;

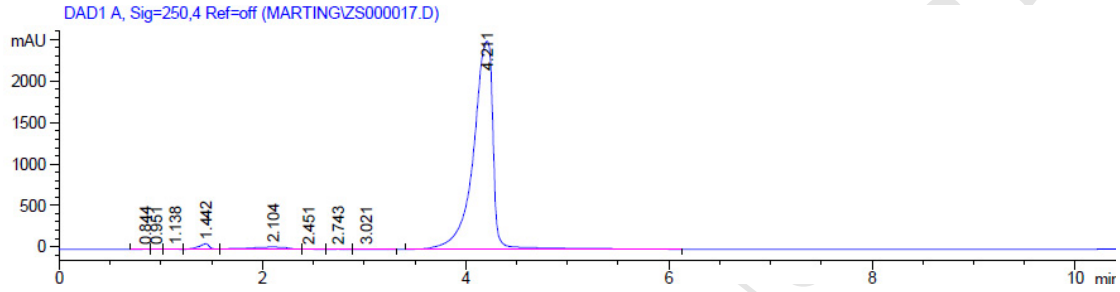

Signal 1: DAD1 A, Sig=250,4 Ref=off

Peak #	RetTime [min]	Type	Width [min]	Area [mAU*s]	Height [mAU]	Area %
1	0.844	BV	0.0564	21.50703	5.92053	0.0606
2	0.951	VV	0.0935	22.70934	3.51072	0.0640
3	1.138	VV	0.1094	44.62593	5.57644	0.1257
4	1.442	VV	0.1079	513.52405	68.13187	1.4466
5	2.104	VV	0.3406	753.22632	27.24002	2.1219
6	2.451	VV	0.1397	30.56843	3.08369	0.0861
7	2.743	VV	0.1525	23.05767	2.19626	0.0650
8	3.021	VB	0.1946	26.29200	1.95895	0.0741
9	4.211	BB	0.2045	3.40627e4	2506.89941	95.9561
Totals :				3.54982e4	2624.51788	

Acid **21**:

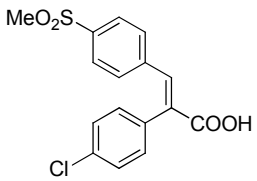

Injection volume: 20 μL; Eluent: $CH_3CN:H_2O$ = 60:40; Flow rate: 1.0 mL/min; Run time: 10 minutes;

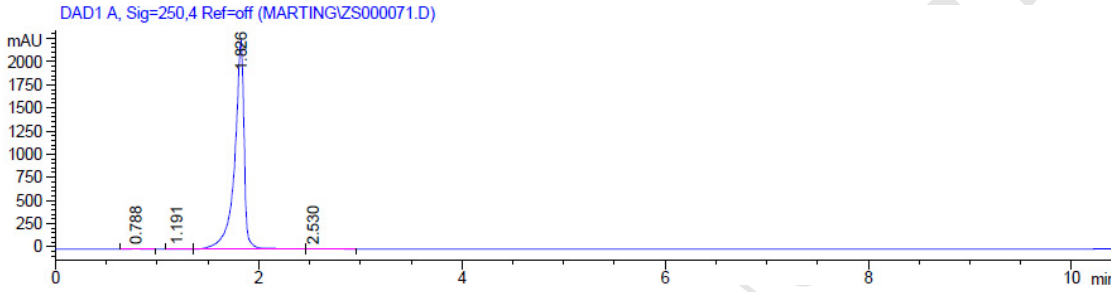

Signal 1: DAD1 A, Sig=250,4 Ref=off

Peak #	RetTime [min]	Type	Width [min]	Area [mAU*s]	Height [mAU]	Area %
1	0.788	BB	0.0982	29.55809	4.19636	0.1995
2	1.191	VV	0.0992	7.68496	1.02825	0.0519
3	1.826	VB	0.0946	1.47256e4	2244.23730	99.3819
4	2.530	BB	0.2093	54.34188	3.49621	0.3667
Totals :				1.48172e4	2252.95812	

Acid **22**:

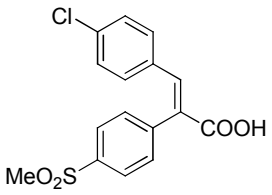

Injection volume: 20 μL; Eluent: $CH_3CN:H_2O$ = 60:40; Flow rate: 1.0 mL/min; Run time: 10 minutes;

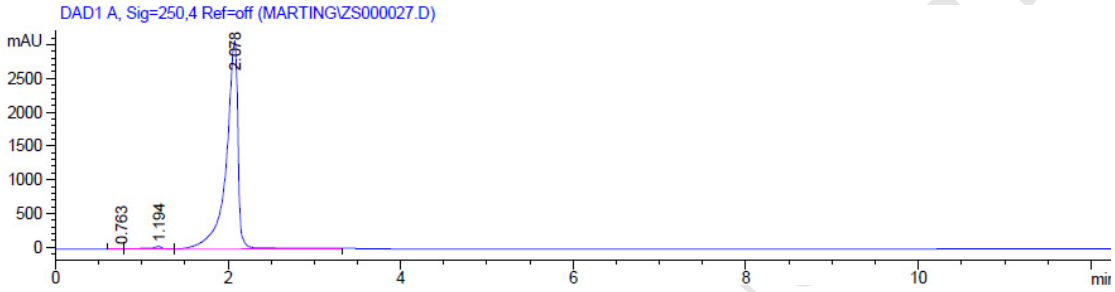

Signal 1: DAD1 A, Sig=250,4 Ref=off

Peak #	RetTime [min]	Type	Width [min]	Area [mAU*s]	Height [mAU]	Area %
1	0.763	BV	0.0677	8.20078	1.71758	0.0273
2	1.194	VV	0.1363	379.45554	38.06166	1.2621
3	2.078	VB	0.1407	2.96785e4	3072.45068	98.7107
Totals :				3.00661e4	3112.22992	

Acid **23**:

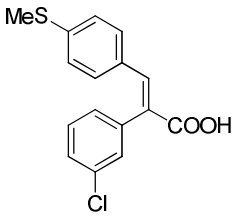

Injection volume: 20 μL; Eluent: $CH_3CN:H_2O$ = 60:40; Flow rate: 1.0 mL/min; Run time: 10 minutes;

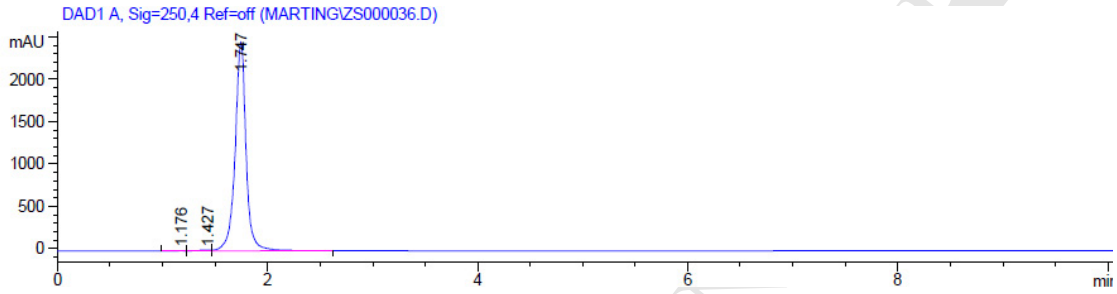

Signal 1: DAD1 A, Sig=250,4 Ref=off

Peak #	RetTime [min]	Type	Width [min]	Area [mAU*s]	Height [mAU]	Area %
1	1.176	BV	0.0679	11.82875	2.47034	0.0657
2	1.427	VV	0.1175	103.56159	12.65694	0.5754
3	1.747	VB	0.1069	1.78838e4	2457.19629	99.3589
Totals :				1.79992e4	2472.32357	

Acid **24**:

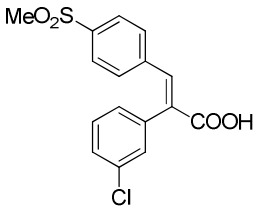

Injection volume: 20 μL; Eluent: $CH_3CN:H_2O$ = 60:40; Flow rate: 1.0 mL/min; Run time: 10 minutes;

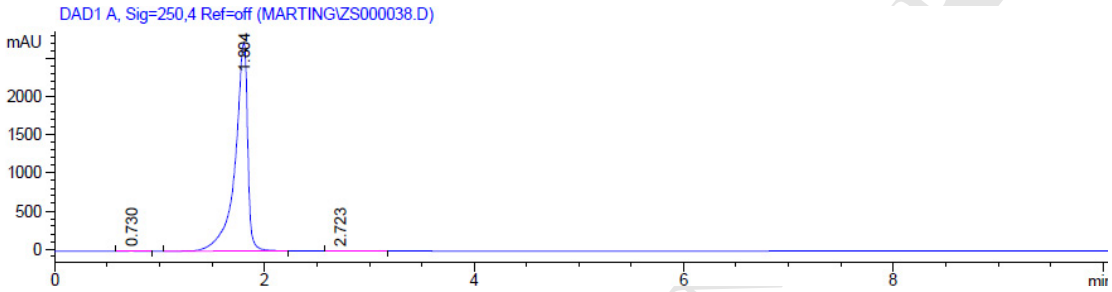

Signal 1: DAD1 A, Sig=250,4 Ref=off

Peak #	RetTime [min]	Type	Width [min]	Area [mAU*s]	Height [mAU]	Area %
1	0.730	BB	0.0951	22.62497	3.25497	0.0986
2	1.804	VB	0.1236	2.29083e4	2738.59839	99.8669
3	2.723	BB	0.1185	7.89540	1.11638	0.0344
Totals :				2.29388e4	2742.96974	

Acid **25**:

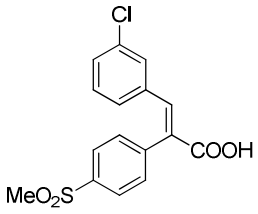

Injection volume: 20 µL; Eluent: $CH_3CN:H_2O$ = 80:20; Flow rate: 1.5 mL/min; Run time: 10 minutes;

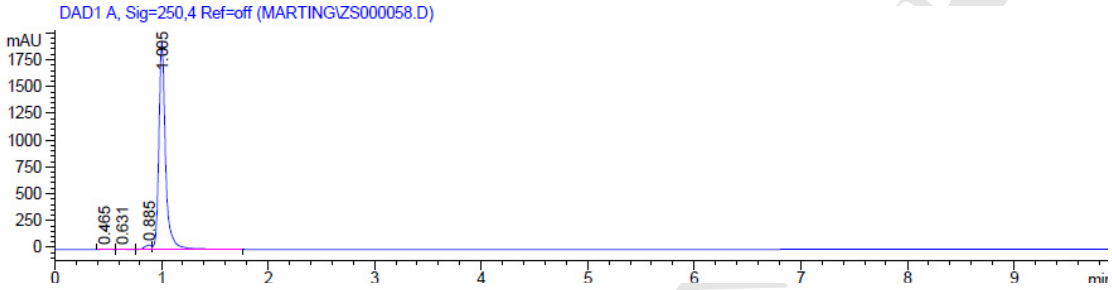

Signal 1: DAD1 A, Sig=250,4 Ref=off

Peak #	RetTime [min]	Type	Width [min]	Area [mAU*s]	Height [mAU]	Area %
1	0.465	BV	0.0790	26.31185	4.87575	0.2997
2	0.631	VV	0.0717	22.10410	4.63387	0.2517
3	0.885	VV	0.0692	184.50603	42.01119	2.1013
4	1.005	VB	0.0672	8547.77344	1946.53931	97.3473
Totals :				8780.69542	1998.06011	

Acid **26**:

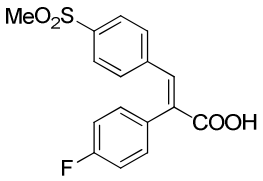

Injection volume: 20 μL; Eluent: $CH_3CN:H_2O$ = 60:40; Flow rate: 1.0 mL/min; Run time: 10 minutes;

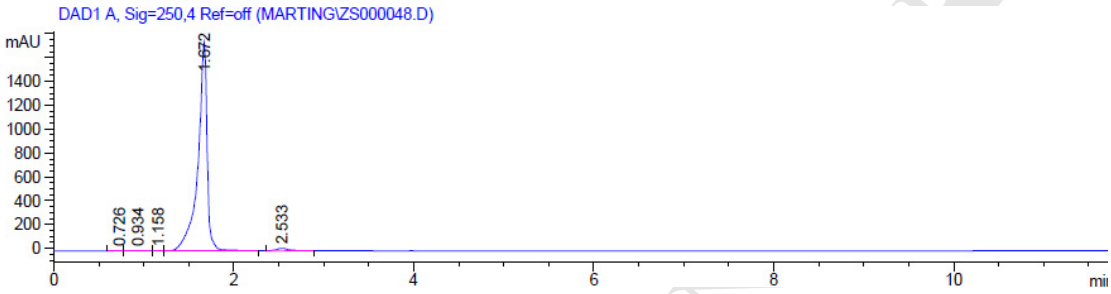

Signal 1: DAD1 A, Sig=250,4 Ref=off

Peak #	RetTime [min]	Type	Width [min]	Area [mAU*s]	Height [mAU]	Area %
1	0.726	BV	0.0853	22.69932	3.82232	0.1773
2	0.934	VV	0.2021	64.58668	4.23152	0.5044
3	1.158	VV	0.0813	17.75757	3.17161	0.1387
4	1.672	VB	0.1014	1.24955e4	1748.19495	97.5822
5	2.533	BB	0.1569	204.56467	19.11172	1.5975
Totals :				1.28051e4	1778.53211	

Acid **27**:

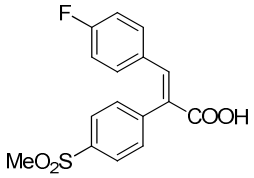

Injection volume: 20 µL; Eluent: $CH_3CN:H_2O$ = 80:20; Flow rate: 1.5 mL/min; Run time: 10 minutes;

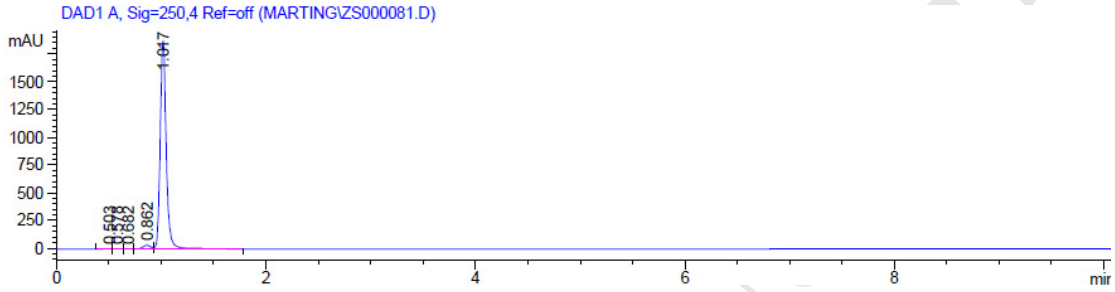

Signal 1: DAD1 A, Sig=250,4 Ref=off

Peak #	RetTime [min]	Type	Width [min]	Area [mAU*s]	Height [mAU]	Area %
1	0.503	BV	0.0801	12.31536	2.47426	0.1591
2	0.578	VV	0.0688	17.99948	3.83443	0.2326
3	0.682	VV	0.0679	9.05155	1.95813	0.1170
4	0.862	VV	0.0782	177.02937	34.30334	2.2876
5	1.017	VB	0.0625	7522.28564	1885.69958	97.2037
Totals :				7738.68141	1928.26974	

Acid **28**:

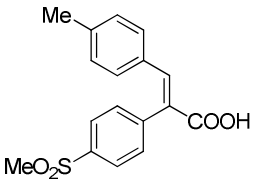

Injection volume: 20 μL; Eluent: $CH_3CN:H_2O$ = 60:40; Flow rate: 1.0 mL/min; Run time: 10 minutes;

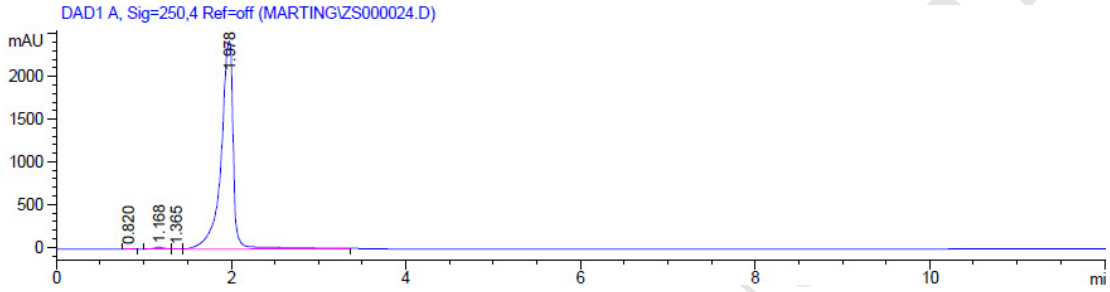

Signal 1: DAD1 A, Sig=250,4 Ref=off

Peak #	RetTime [min]	Type	Width [min]	Area [mAU*s]	Height [mAU]	Area %
1	0.820	BB	0.0555	11.32088	3.03392	0.0473
2	1.168	BV	0.0949	159.70201	23.01826	0.6667
3	1.365	VV	0.0905	13.14723	2.24031	0.0549
4	1.978	VB	0.1460	2.37707e4	2432.41333	99.2312
Totals :				2.39548e4	2460.70582	

Acid **29**:

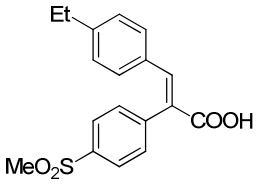

Injection volume: 20 µL; Eluent: $CH_3CN:H_2O$ = 60:40; Flow rate: 1.0 mL/min; Run time: 10 minutes;

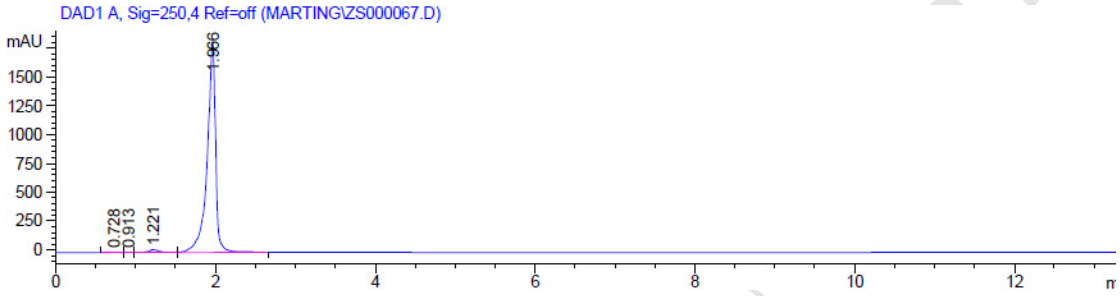

Signal 1: DAD1 A, Sig=250,4 Ref=off

Peak #	RetTime [min]	Type	Width [min]	Area [mAU*s]	Height [mAU]	Area %
1	0.728	BV	0.1191	22.86541	2.53797	0.1674
2	0.913	VV	0.0796	10.22548	1.81841	0.0749
3	1.221	VV	0.1363	224.03180	22.87101	1.6400
4	1.966	VB	0.1056	1.34030e4	1826.13403	98.1177
Totals :				1.36601e4	1853.36142	

Acid **30**:

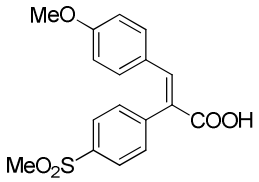

Injection volume: 20 μL; Eluent: $CH_3CN:H_2O$ = 60:40; Flow rate: 1.0 mL/min; Run time: 10 minutes;

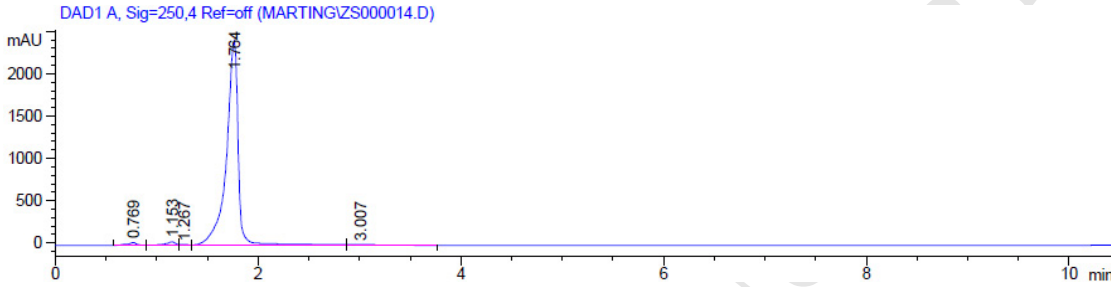

Signal 1: DAD1 A, Sig=250,4 Ref=off

Peak #	RetTime [min]	Type	Width [min]	Area [mAU*s]	Height [mAU]	Area %
1	0.769	BV	0.0999	245.14107	33.27809	1.1686
2	1.153	VV	0.1081	335.49460	42.51787	1.5993
3	1.267	VV	0.0865	64.89405	11.39256	0.3094
4	1.764	VV	0.1224	2.00465e4	2425.52710	95.5619
5	3.007	VB	0.3438	285.47015	10.68165	1.3608
Totals :				2.09775e4	2523.39727	

Acid **31**:

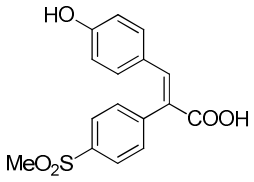

Injection volume: 20 μL; Eluent: $CH_3CN:H_2O$ = 80:20; Flow rate: 1.5 mL/min; Run time: 10 minutes;

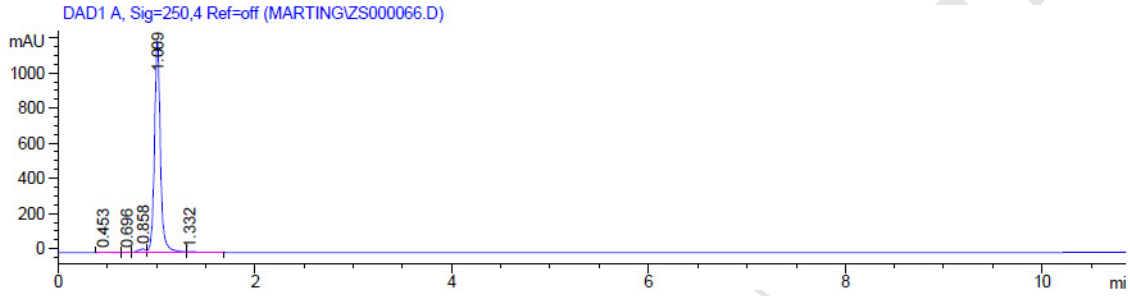

Signal 1: DAD1 A, Sig=250,4 Ref=off

Peak #	RetTime [min]	Type	Width [min]	Area [mAU*s]	Height [mAU]	Area %
1	0.453	BB	0.0974	23.05219	3.14875	0.4341
2	0.696	BV	0.0753	7.46322	1.37522	0.1405
3	0.858	VV	0.0706	103.21199	20.56252	1.9436
4	1.009	VV	0.0655	5124.88330	1207.27100	96.5061
5	1.332	VB	0.1316	51.81536	5.23149	0.9757
Totals :				5310.42607	1237.58898	

Acid **32**:

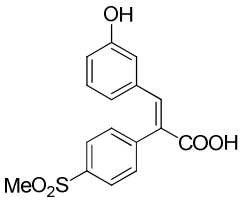

Injection volume: 20 μL; Eluent: $CH_3CN:H_2O$ = 60:40; Flow rate: 1.0 mL/min; Run time: 10 minutes;

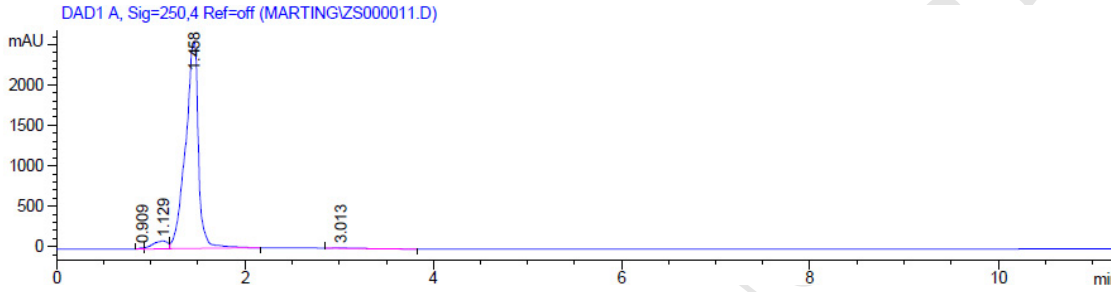

Signal 1: DAD1 A, Sig=250,4 Ref=off

Peak #	RetTime [min]	Type	Width [min]	Area [mAU*s]	Height [mAU]	Area %
1	0.909	BV	0.0425	47.67751	18.24652	0.1852
2	1.129	VV	0.1527	1065.52319	96.59529	4.1390
3	1.458	VB	0.1400	2.45963e4	2561.23975	95.5427
4	3.013	BB	0.1201	34.26773	4.64091	0.1331
Totals :				2.57438e4	2680.72246	

Acid **33**:

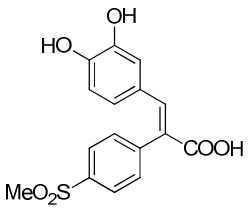

Injection volume: 20 μL; Eluent: $CH_3CN:H_2O$ = 60:40; Flow rate: 1.0 mL/min; Run time: 10 minutes;

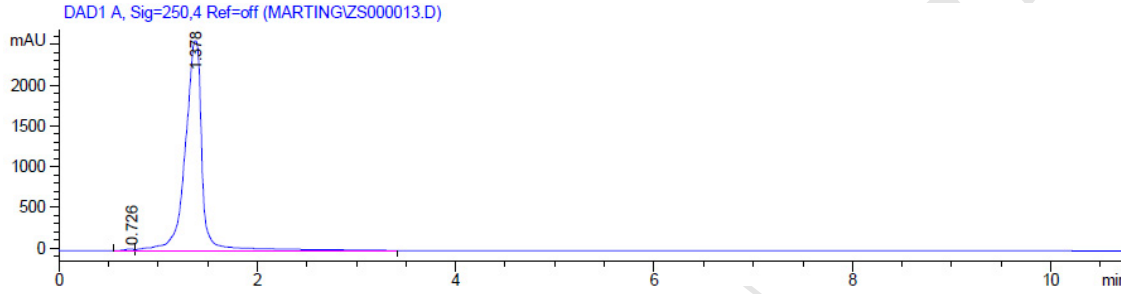

Signal 1: DAD1 A, Sig=250,4 Ref=off

Peak #	RetTime [min]	Type	Width [min]	Area [mAU*s]	Height [mAU]	Area %
1	0.726	BV	0.0891	112.50421	16.59386	0.3659
2	1.378	VB	0.1707	3.06351e4	2577.07178	99.6341
Totals :				3.07476e4	2593.66563	

Acid **34**:

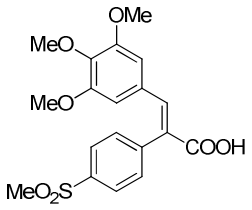

Injection volume: 20 μL; Eluent: $CH_3CN:H_2O$ = 60:40; Flow rate: 1.0 mL/min; Run time: 10 minutes;

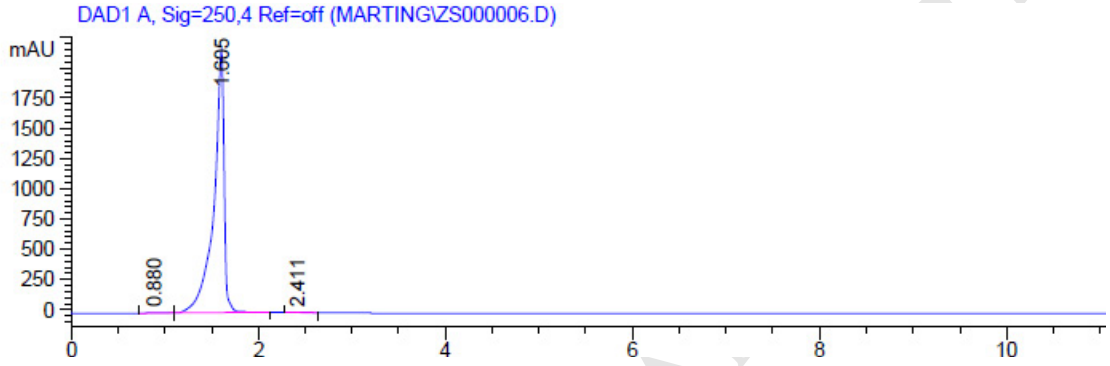

Signal 1: DAD1 A, Sig=250,4 Ref=off

Peak #	RetTime [min]	Type	Width [min]	Area [mAU*s]	Height [mAU]	Area %
1	0.880	BV	0.1534	61.99350	6.16054	0.3664
2	1.605	VB	0.1084	1.68393e4	2172.75659	99.5222
3	2.411	BB	0.1222	18.85623	2.28572	0.1114
Totals :				1.69202e4	2181.20286	

Acid **35**:

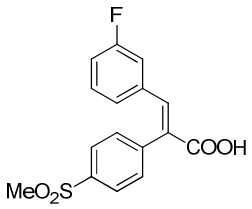

Injection volume: 20 μL; Eluent: CH_3CN:H_2O = 60:40; Flow rate: 1.0 mL/min; Run time: 10 minutes;

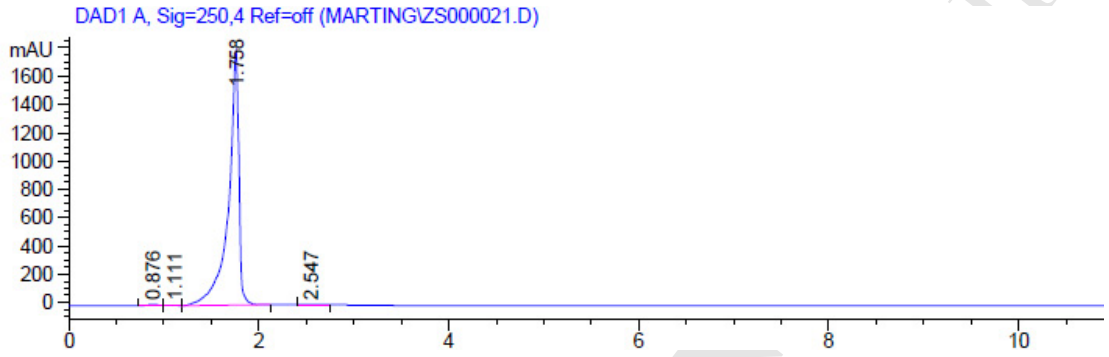

Signal 1: DAD1 A, Sig=250,4 Ref=off

Peak #	RetTime [min]	Type	Width [min]	Area [mAU*s]	Height [mAU]	Area %
1	0.876	BV	0.1213	67.80187	8.12850	0.4898
2	1.111	VV	0.0877	33.50153	5.30237	0.2420
3	1.758	VB	0.1048	1.37202e4	1803.41064	99.1211
4	2.547	BB	0.1300	20.34628	2.28352	0.1470
Totals :				1.38418e4	1819.12505	

Acid **36**:

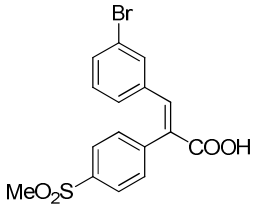

Injection volume: 20 μL; Eluent: $CH_3CN:H_2O$ = 60:40; Flow rate: 1.0 mL/min; Run time: 10 minutes;

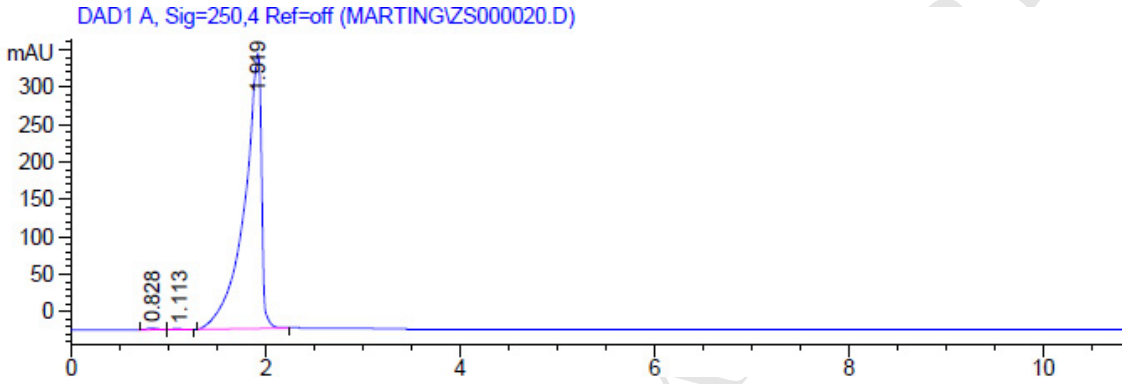

Signal 1: DAD1 A, Sig=250,4 Ref=off

Peak #	RetTime [min]	Type	Width [min]	Area [mAU*s]	Height [mAU]	Area %
1	0.828	BV	0.1038	19.11580	2.60016	0.4266
2	1.113	VB	0.0880	7.81407	1.23271	0.1744
3	1.919	BB	0.1654	4454.55469	367.63260	99.3991
Totals :				4481.48456	371.46547	

Acid **37**:

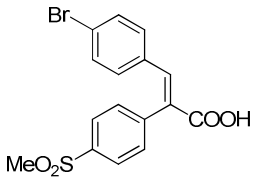

Injection volume: 20 µL; Eluent: $CH_3CN:H_2O$ = 80:20; Flow rate: 1.5 mL/min; Run time: 10 minutes;

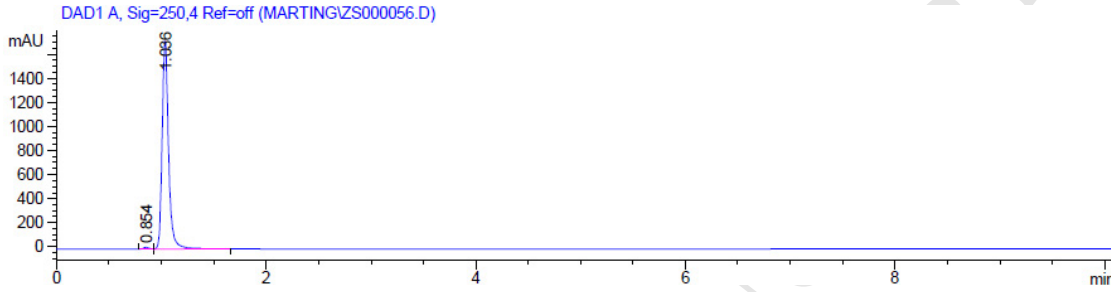

Signal 1: DAD1 A, Sig=250,4 Ref=off

Peak #	RetTime [min]	Type	Width [min]	Area [mAU*s]	Height [mAU]	Area %
1	0.854	BV	0.0593	59.61741	15.35952	0.8007
2	1.036	VB	0.0655	7386.23926	1739.38953	99.1993
Totals :				7445.85667	1754.74905	

Acid **38**:

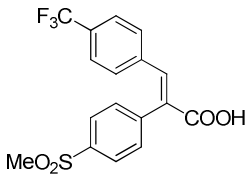

Injection volume: 20 μL; Eluent: $CH_3CN:H_2O$ = 60:40; Flow rate: 1.0 mL/min; Run time: 10 minutes;

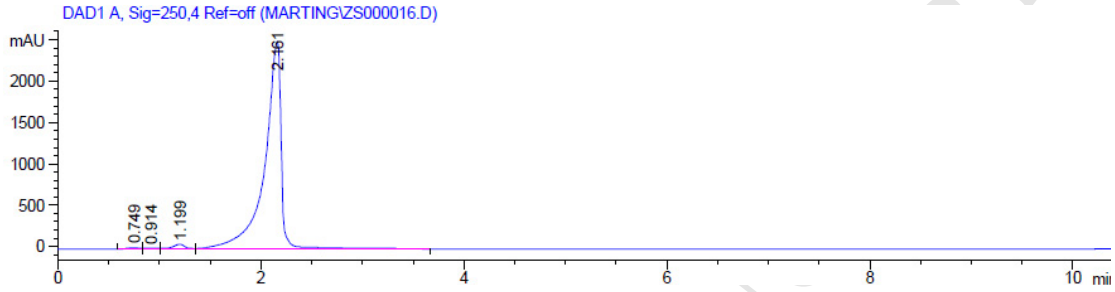

Signal 1: DAD1 A, Sig=250,4 Ref=off

Peak #	RetTime [min]	Type	Width [min]	Area [mAU*s]	Height [mAU]	Area %
1	0.749	BV	0.1062	148.18922	19.17753	0.5024
2	0.914	VV	0.1411	99.58707	10.27574	0.3376
3	1.199	VV	0.1343	510.98929	57.17010	1.7322
4	2.161	VB	0.1617	2.87401e4	2508.14990	97.4278
Totals :				2.94988e4	2594.77327	

Acid **39**:

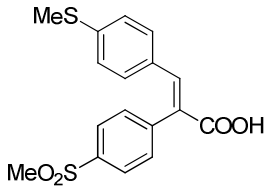

Injection volume: 20 µL; Eluent: $CH_3CN:H_2O$ = 80:20; Flow rate: 1.5 mL/min; Run time: 10 minutes;

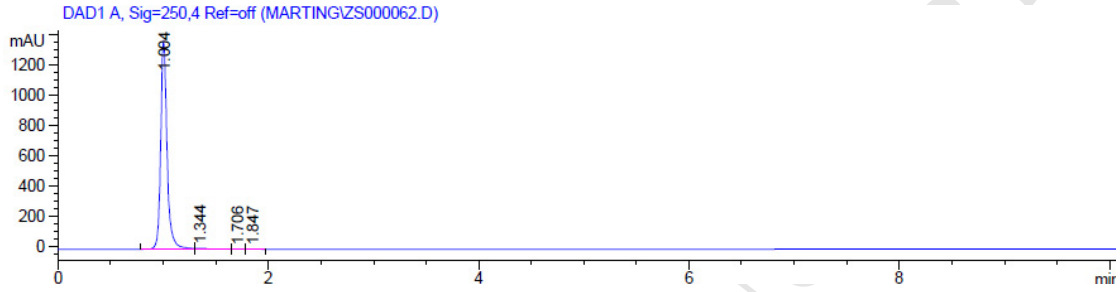

Signal 1: DAD1 A, Sig=250,4 Ref=off

Peak #	RetTime [min]	Type	Width [min]	Area [mAU*s]	Height [mAU]	Area %
1	1.004	BV	0.0655	5878.83154	1384.33582	98.6218
2	1.344	VB	0.1229	65.90869	7.19091	1.1057
3	1.706	BV	0.0868	6.51858	1.07353	0.1094
4	1.847	VB	0.0809	9.72588	1.80471	0.1632
Totals :				5960.98469	1394.40497	

Acid **40**:

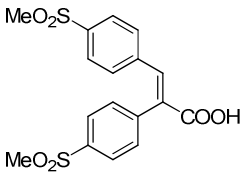

Injection volume: 20 µL; Eluent: $CH_3CN:H_2O$ = 80:20; Flow rate: 1.5 mL/min; Run time: 10 minutes;

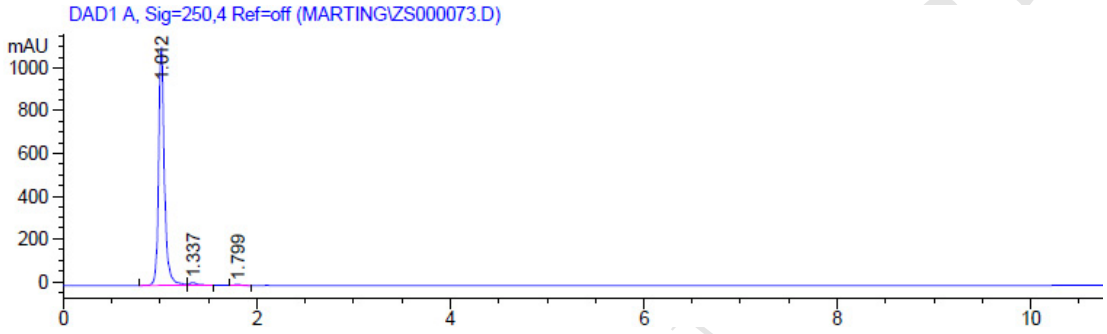

Signal 1: DAD1 A, Sig=250,4 Ref=off

Peak #	RetTime [min]	Type	Width [min]	Area [mAU*s]	Height [mAU]	Area %
1	1.012	BV	0.0629	4685.00781	1117.69604	98.1790
2	1.337	VB	0.0877	73.22070	11.91837	1.5344
3	1.799	BB	0.0761	13.67798	2.84629	0.2866
Totals :				4771.90649	1132.46071	

Acid **41**:

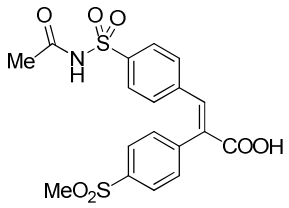

Injection volume: 20 μL; Eluent: $CH_3CN:H_2O$ = 80:20; Flow rate: 1.5 mL/min; Run time: 10 minutes;

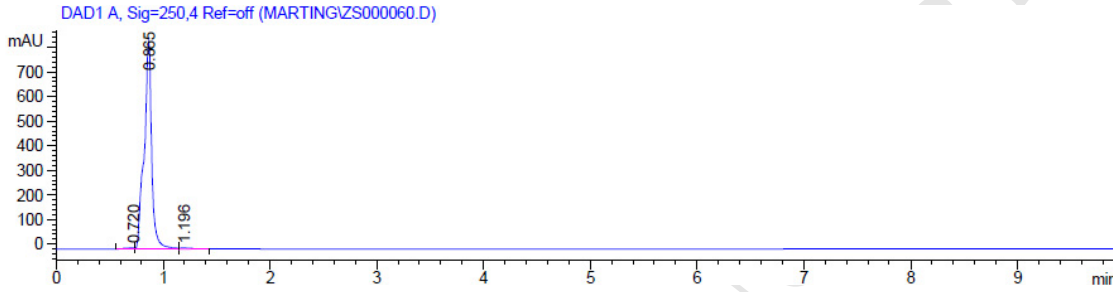

Signal 1: DAD1 A, Sig=250,4 Ref=off

Peak #	RetTime [min]	Type	Width [min]	Area [mAU*s]	Height [mAU]	Area %
1	0.720	VV	0.0882	33.64045	5.53393	0.7870
2	0.865	VV	0.0719	4203.66064	847.74023	98.3485
3	1.196	VB	0.1124	36.94837	4.47115	0.8644
Totals :				4274.24947	857.74531	

Acid **42**:

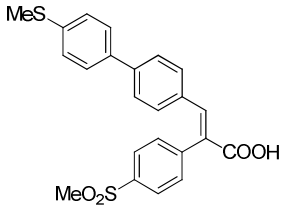

Injection volume: 20 μL; Eluent: $CH_3CN:H_2O$ = 60:40; Flow rate: 1.0 mL/min; Run time: 10 minutes;

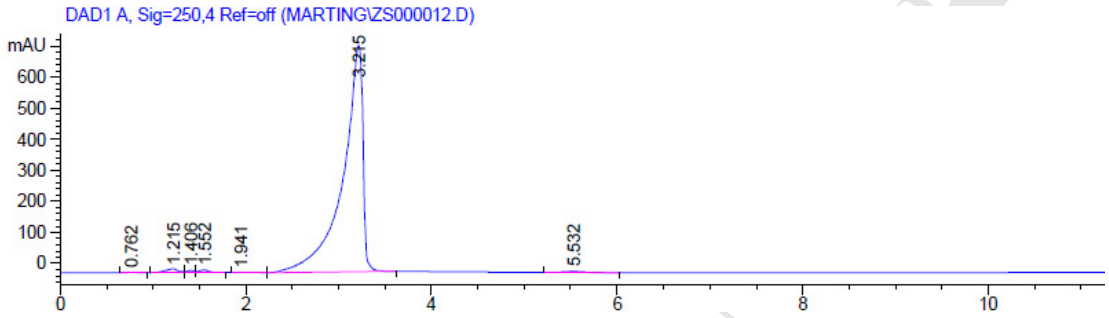

Signal 1: DAD1 A, Sig=250,4 Ref=off

Peak #	RetTime [min]	Type	Width [min]	Area [mAU*s]	Height [mAU]	Area %
1	0.762	BB	0.0935	11.91182	1.70601	0.1064
2	1.215	BV	0.1470	122.50547	11.80780	1.0946
3	1.406	VV	0.0805	40.70861	7.36750	0.3638
4	1.552	VB	0.1230	68.96523	7.97008	0.6162
5	1.941	BV	0.1524	16.95156	1.49396	0.1515
6	3.215	VB	0.2022	1.08720e4	728.29901	97.1471
7	5.532	BB	0.2419	58.23187	3.65438	0.5203
Totals :				1.11913e4	762.29874	